UNIVERSITY OF CAPE TOWN

MASTER'S DISSERTATION

Reps for JIMWLK: Applications of representation theory to a novel approach to the JIMWLK equation

Author:
Jonathan RAYNER

Supervisor:
Assoc. Prof. Heribert WEIGERT

A dissertation submitted in fulfillment of the requirements for the degree of Master of Science

in

Theoretical Physics

Department of Physics, Faculty of Science

University of Cape Town

Abstract

Department of Physics,
Faculty of Science

Master of Science

Reps for JIMWLK: Applications of representation theory to a novel approach to the JIMWLK equation

by Jonathan RAYNER

In recent work, R. Moerman and H. Weigert have introduced a truncation scheme for the Balitsky hierarchy, arguing that this is the most general possible method for obtaining finite N_c approximate solutions to the JIMWLK equation, while ensuring that these solutions obey several key properties that are known to be true of any exact solution to JIMWLK [1]. To carry out this truncation, it becomes necessary to systematically construct an orthogonal basis for the space of color singlets with purely adjoint indices. The primary contribution of this dissertation is to construct a basis that makes significant strides towards this goal, using irreducible representations of the permutation group S_k and recently-developed Hermitian Young projection operators [2–4]. Our method directly produces the basis for these singlets, avoiding the need to construct a basis for all multiplets and project out the singlets, as is common in other approaches. In our basis, orthogonality holds both between elements associated with non-isomorphic and isomorphic representations, with the exception of representations that are identical (and not just isomorphic). In working through the robust mathematical framework that describes this construction, we show that failures of orthogonality are a direct result of these basis elements being associated with identical induced representations arising from derangements with differing cycle structure, which suggests a possible strategy for constructing a fully-orthogonal basis in future research. We also prove that this basis always consists of elements that are real or purely imaginary and show how to determine these properties at the level of representations using characters and Frobenius reciprocity. We then shift gears to prove a small number of analytic properties of the images of commonly-used Wilson line operators. Explicitly, we provide a proof that hasn't existed in the literature previously that the image of the dipole operator in the complex plane is the hypocycloid with N_c-cusps and we prove that all Wilson line operators that appear in the amplitude matrix used in the JIMWLK evolution of two quark-antiquark pairs are bounded by the unit circle.

Acknowledgements

Foremost, I would like to thank my supervisor, Heribert Weigert. My thanks are in acknowledgment of Heribert's insight in directing the topics of this research, his willingness to commit innumerable hours to his students, and what I feel was exactly the right amount of patience in allowing me to explore off the beaten track, while reigning me in when necessary. I first met Heribert at the end of my first year at university and he has supervised several of my projects since, meaning that he has played a critical role in my development as a student and researcher, with this work being the culmination of many years of his guidance.

The work presented in this dissertation benefited greatly from collaboration with other students in our research team. Judith Alcock-Zeilinger dedicated many hours of her time to allowing me to bounce questions and ideas off of her (particularly relating to the projection operators that she created with Heribert, representation theory, and guidance in writing this dissertation) and gave us a series of lectures on Birdtracks. Robert Moerman answered endless questions on the truncation that he and Heribert have created, and on the physics of the CGC more broadly. Daniel Adamiak spent large amounts of time confirming many of the solutions to the mathematical puzzles that are resolved in this dissertation (as well as many more that do not appear, because they were incorrect). Luke Lippstreu was an excellent source of information on quantum field theory in general.

Then of course I must thank my mother. She was the first person to inspire my love and respect for mathematics, science, and the pursuit of knowledge. Despite being unfairly denied many opportunities in her life, she chose to channel these disadvantages into advantages that she gave me, providing unconditional support to me throughout my life wherever possible and making many sacrifices.

There are several other miscellaneous people to whom I owe my gratitude. William Grunow consistently engaged with me in extremely helpful conversations about this work, despite not being in our research team. Dela Gwala provided enormous amounts of emotional support over the last few years. Tim Wolff-Piggott and Jason Fourie did the same, and helped me in countless other ways in my personal life while I was writing this dissertation, as well as assisted in proofreading. Nandi Rayner helped me out of a few jams, especially when I ran out of money a few months before the end of this research. The other members of our office (Lizelle Niit, Robert Hambrock, and Nicole Moodley) all have helped me in my personal life, contributed to aesthetic decisions about this dissertation, and I'm grateful for how extremely fun they are to have as colleagues. Andy Buffler's leadership as head of department has made the Physics Department at the University of Cape Town a truly special place, and I am grateful for our many private conversations over the years and his assistance.

This work was funded by a fellowship from the Harry Crossley Foundation and supplementary funding from the Department of Physics, University of Cape Town.

Contents

This work is dedicated to the next generation of young people everywhere around the world.

Following the words of Carl Sagan, may science continue to be our candle in the dark.

Chapter 1

Introduction

"Pick a flower on Earth and you move the farthest star."

Paul Dirac

1.1 Background: The Color Glass Condensate and the JIMWLK equation

In any high energy scattering event involving hadronic matter, effective parton size in nuclei increases with decreasing x_{bj}. Simultaneously, the occupation number of gluons in the nuclei increases with increasing energy of the collision event, eventually significantly exceeding the occupation number of quarks. At sufficiently high energy and low x_{bj}, a new state of matter is believed to form as the number and effective size of gluons becomes so large that gluon occupation *saturates* [5–7] (see Figure 1.1). The effective theory of this state of matter is known as the *Color Glass Condensate* (CGC) [8–12]. The reference to a spin glass refers to the fact that quantum effects in the dense medium of gluons appear "frozen" on the time scales that a probe interacts with the medium. The choice to think of the CGC as a condensate refers to the high occupation number of gluons. Since internal quantum effects in the CGC are invisible to a probe interacting with the medium, these scattering events are modelled as a particle interacting with a collection of strong classical sources (which are taken to be independent of one another). Additional quantum-mechanical effects from the probe-target interaction are described in this model by the JIMWLK renormalization group equation. This renormalization group equation arises due to the form of *factorization* that has been described: that the interactions can be treated as a quantum mechanical probe interacting with a classical target, where as energies increase, additional gluon emissions can be included in the classical sources that form the target.

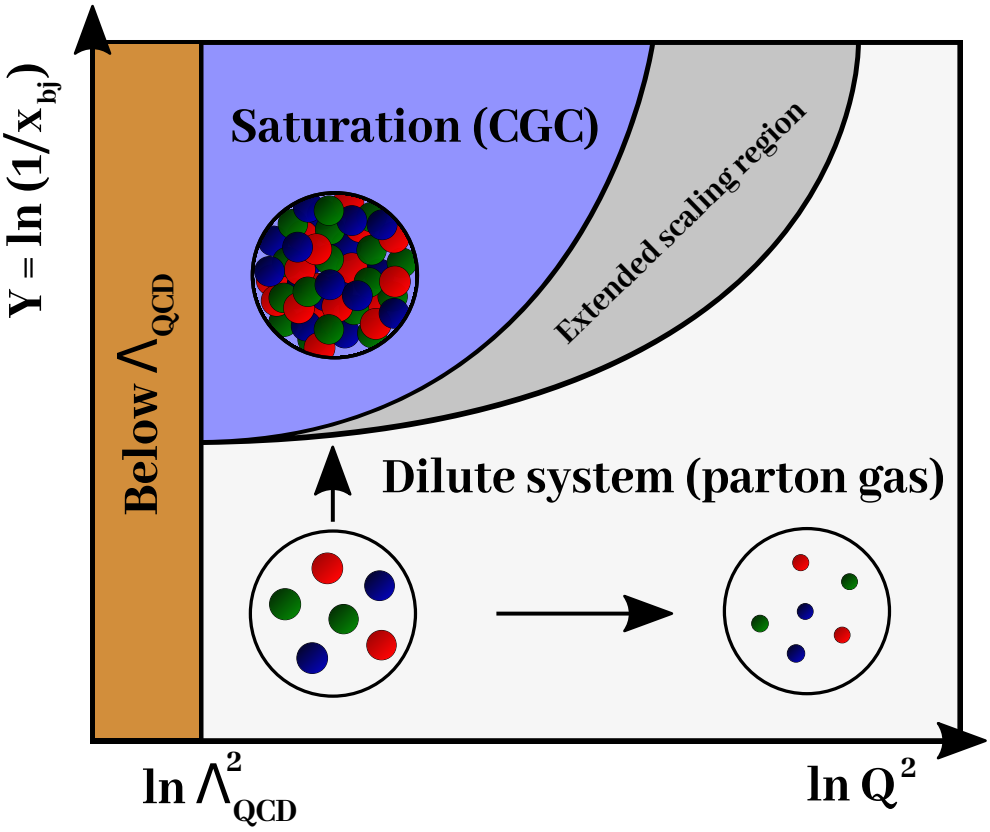

FIGURE 1.1: QCD phase diagram. Colored dots represent the partons in the target, whose effect size visible to a probe increases with decreases in Q^2. As x_{bj} decreases at fixed Q^2, the number of partons increases until at sufficiently small x_{bj}, the target can no longer be considered dilute and a new state of matter forms (the CGC). In the extended scaling region, the evolution equations of the CGC and the parton gas agree in the appropriate limits (see [13] and [10, Sec. 3.7] for details).

The JIMWLK equation introduces a serious challenge in calculations. Calculating the correlation function of any probe in the presence of the CGC requires solving an infinite hierarchy of coupled functional differential equations, generated by JIMWLK evolution. Standard practice in the literature is to instead work with the BK-equation [14–18], which is a truncated form of this hierarchy that can be obtained by taking the limit where the number of colors approaches infinity, $N_c \to \infty$ [12, Sec. 4.4]. However, it is known that the BK equation is unable to probe some aspects of JIMWLK evolution, such as the expected difference in cross sections for exclusive and inclusive vector meson production [19], and so a finite N_c truncation scheme becomes desirable.

1.2 Purpose of this dissertation

R. Moerman and H. Weigert have introduced a novel parameterisation scheme that allows one to truncate the infinite hierarchy generated by JIMWLK at finite N_c, while preserving critical properties of JIMWLK evolution: group theoretic constraints and independent evolution of symmetric and antisymmetric components when JIMWLK evolution of correlators is organised as a matrix equation. The lowest-order truncations possible with this scheme (which can be thought of as a Gaussian ansatz for color sources in the CGC weight function and corrections thereafter) were first applied in [19–21]. In this dissertation we summarise the full scheme (Section 2.3), which is presented in detail in [1].

In order to carry out R. Moerman and H. Weigert's truncation scheme, it becomes necessary to construct an appropriate basis for the space of color singlets with an arbitrary number of adjoint indices and no fundamental indices (we use the notation $\mathcal{S}(A^{\otimes k})$ to refer to this space). A major contribution of this dissertation is to describe a systematic method for constructing this basis (Chapters 3 and 4). This approach will also likely prove useful in other contexts, because these algebraic objects are ubiquitous in the study of QCD, as the confinement hypothesis requires that all free particles be organised as color singlets.

Two common approaches to constructing a basis for this space already exist in the literature. One chooses either work with the *trace basis* [22] or to decompose the k-fold tensor product of the adjoint representation $A^{\otimes k}$ into irreducible representations, then select only the space of singlets $\mathcal{S}(A^{\otimes k})$, forming a basis consisting of a single element from each singlet. In the former case, the trace basis is undesirable in that it is not orthogonal and elements of this basis become linearly independent for low values of N_c. In the latter case, we show that we can improve upon this approach by presenting a method to directly decompose $\mathcal{S}(A^{\otimes k})$ into irreducible representations using the permutation symmetries of $\mathcal{S}(A^{\otimes k})$ and the theory of *induced representations*, circumventing the need to decompose $A^{\otimes k}$ (Chapter 4). This method has been used elsewhere in work on QCD scattering amplitudes [23], but has not yet been applied in the CGC context.

We then aim to form an orthogonal basis for $\mathcal{S}(A^{\otimes k})$ by projecting the trace basis with a set of orthogonal projection operators [2–4] corresponding to the needed irreducible representations in the decomposition (Section 3.3). This automatically encodes symmetry features of these representations and sheds light on the N_c-dependence of the basis. However, it turns out that this basis fails to be orthogonal whenever multiple basis elements are created by a single projection operator, in a manner that we'll show is explained by the imprinting of the cycle structure of S_k onto the trace basis (Section 4.3). Gram-Schmidt orthogonalisation gets us out of this difficulty in these cases, with it being an open research question as to how to resolve this systematically at the level of the representations.

We will see that the same method that allows us to generate this basis will also allow us to determine a priori which elements of this distinguished basis are real or purely imaginary. Furthermore, we prove that every element is always real or purely imaginary (Section 4.5), which is a necessary prerequisite for certain results discovered by R. Moerman in related work on the real and imaginary parts of matrices of CGC correlators [1].

Diverging from the discussion of approximate solutions to the JIMWLK equation, we find considerable interest in establishing some exact properties of CGC correlators. Specifically, we focus on deriving analytic bounds for the images of Wilson line operators that appear in CGC correlators in the simplest practical applications. We present two significant results that have not appeared elsewhere in the literature: a complete proof that the image of the dipole operator (the normalised trace of a $SU(N_c)$ matrix) in the complex plane is the hypocycloid with N_c cusps (Section 5.1) and a set of proofs that establish that every four-point Wilson line operator that arises in the JIMWLK evolution of two quark-antiquark pairs is bounded by the unit circle (Section 5.2). Furthermore, we provide basic numerical evidence for further conjectures about the nature of the images of these operators.

Altogether, this dissertation explicitly develops and works through a key component of a novel approach to the evolution of CGC correlators at finite N_c, provides firm mathematical resolutions of several open questions surrounding this truncation scheme and CGC correlators more broadly, and opens the way for several new well-defined research questions.

Chapter 2

A novel parameterisation of JIMWLK evolution

"Everyone generalises from one example. At least, I do."

Vlad Taltos (Issola, Steven Brust)

In this chapter we describe the obstacles that are encountered in calculating the JIMWLK evolution of CGC correlators and introduce a novel method for working around these difficulties. In particular, we will see that for any CGC correlator, the JIMWLK equation generates an infinite hierarchy of coupled nonlinear functional differential equations that is unsolvable by known techniques and thus approximate solutions are employed (Section 2.1). The standard approach in the literature to resolving this problem is to take the large N_c limit or to employ numerical methods. We describe the limitations of employing either strategy (Section 2.2). We then conclude the chapter by working through a new parameterisation scheme that is developed in detail in parallel work [1] and is argued to be the most general way of obtaining analytic evolution of CGC correlators through reparameterisation, while preserving certain properties of JIMWLK that are violated by the large N_c limit (Section 2.3).

We will see that this new paramerisation scheme critically relies on a special set of algebraic objects, which we refer to as the *adjoint color structures*. The study of these adjoint color structures forms a significant part of the contribution of this dissertation (Chapters 3 and 4), with the new parameterisation scheme introduced in this chapter serving as the primary motivation for this work.

2.1 The Problem: JIMWLK generates an infinite hierarchy of coupled differential equations

We introduce the JIMWLK equation and demonstrate that it generates a (currently) unsolvable infinite hierarchy of coupled differential equations involving CGC correlators. The leading order (in Y, leading log in $1/x_{bj}$) JIMWLK equation is

$$\frac{d}{dY}Z_Y[U] = -H_{\text{JIMWLK}}Z_Y[U] \tag{2.1}$$

$Z_Y[U]$ is the CGC weight function that allows us to calculate the expectation value of operators in the CGC regime:

$$\langle\hat{O}\rangle_Y := \int \mathcal{D}[U]\,\mathcal{O}[U]Z_Y[U] \tag{2.2}$$

where $\mathcal{D}[U]$ is a functional Haar measure on $SU(N_c)$. Objects here are parameterised in terms of *Wilson lines* $U_{\boldsymbol{x}} \in SU(N_c)$, which describe the scattering amplitude of (anti-)quarks with the target at transverse coordinate $\boldsymbol{x}$ in the eikonal approximation (which means that the transverse coordinates are assumed to be fixed during the collision [24, Sec. 2.2]). The JIMWLK Hamiltonian is given by

$$H_{\text{JIMWLK}} := -\frac{\alpha_s}{2\pi^2}\int\limits_{\boldsymbol{xzy}} \mathcal{K}_{\boldsymbol{xzy}}\big(i\nabla^a_{\boldsymbol{x}}i\nabla^a_{\boldsymbol{y}} + i\bar{\nabla}^a_{\boldsymbol{x}}i\bar{\nabla}^a_{\boldsymbol{y}} + \widetilde{U}^{ab}_{\boldsymbol{z}}(i\bar{\nabla}^a_{\boldsymbol{x}}i\nabla^b_{\boldsymbol{y}} + i\nabla^a_{\boldsymbol{x}}i\bar{\nabla}^b_{\boldsymbol{y}})\big) \tag{2.3}$$

where $\widetilde{U}^{ab}_{\boldsymbol{z}}$ is a Wilson line in the adjoint representation, the JIMWLK kernel is defined as

$$\mathcal{K}_{\boldsymbol{xzy}} := \frac{(\boldsymbol{x}-\boldsymbol{z})\cdot(\boldsymbol{z}-\boldsymbol{y})}{(\boldsymbol{x}-\boldsymbol{z})^2(\boldsymbol{z}-\boldsymbol{y})^2} \tag{2.4}$$

(notice that $\mathcal{K}_{\boldsymbol{xzy}}$ is symmetric in $\boldsymbol{x}$ and $\boldsymbol{y}$ - we will need this later) and the operators

$$i\nabla^a_{\boldsymbol{x}} := [U_{\boldsymbol{x}}t^a]_{ij}\frac{\delta}{\delta U_{\boldsymbol{x},ij}}, \quad i\bar{\nabla}^a_{\boldsymbol{x}} := -[t^aU_{\boldsymbol{x}}]_{ij}\frac{\delta}{\delta U_{\boldsymbol{x},ij}} \tag{2.5}$$

are the left and right invariant vector fields on $SU(N_c)$.[1] The space of left (respectively: right) invariant vector fields is isomorphic to the tangent space at the identity, which is of course the Lie Algebra (once equipped with the naturally-inherited Lie bracket from the vector fields). Then one checks that the vector fields in Equation (2.5) obey the Lie algebra commutation relations

$$[i\nabla^a_{\boldsymbol{x}}, i\nabla^b_{\boldsymbol{y}}] = if^{abc}i\nabla^c_{\boldsymbol{x}}\delta^{(2)}(\boldsymbol{x}-\boldsymbol{y}), \qquad [i\bar{\nabla}^a_{\boldsymbol{x}}, i\bar{\nabla}^b_{\boldsymbol{y}}] = if^{abc}i\bar{\nabla}^c_{\boldsymbol{x}}\delta^{(2)}(\boldsymbol{x}-\boldsymbol{y}), \tag{2.6a}$$

$$0 = [i\bar{\nabla}^a_{\boldsymbol{x}}, i\nabla^b_{\boldsymbol{y}}] \tag{2.6b}$$

[1] Note: for the action of these operators on $U_x^\dagger$, $U_x^\dagger$ is treated as dependent on U_x through $U_xU_x^\dagger = \mathbb{1}$. If we wish to treat U_x and $U_x^\dagger$ as independent degrees of freedom, then we must add a term to the vector field that includes a derivative w.r.t. $U_x^\dagger$, deriving this term from the unitarity condition.

where the δ functions appear because $U_{\boldsymbol{x}}$ and $U_{\boldsymbol{y}}$ truly live on different group manifolds when $\boldsymbol{x} \neq \boldsymbol{y}$ and so we can only form the commutator of elements in their respective Lie algebras when $\boldsymbol{x} = \boldsymbol{y}$.

The JIMWLK equation results in an evolution equation for the rapidity dependence of CGC correlators. To see this, differentiate Equation (2.2) w.r.t. Y, noting that the only rapidity dependence on the RHS lies in the CGC weight function:

$$\frac{d}{dY}\langle\hat{O}\rangle_Y = \int \mathcal{D}[U]\,\mathcal{O}[U]\frac{dZ_Y[U]}{dY} \tag{2.7a}$$

$$= -\int \mathcal{D}[U]\,\mathcal{O}[U] H Z_Y[U] \tag{2.7b}$$

Integrating by parts twice with the assumption of vanishing boundary terms gives

$$= -\int \mathcal{D}[U]\,H(\mathcal{O}[U]) Z_Y[U] \tag{2.7c}$$

which is written compactly as

$$\frac{d}{dY}\langle\hat{O}\rangle_Y = -\langle H_{\text{JIMWLK}}\hat{O}\rangle_Y \tag{2.7d}$$

Despite its elegant form

$$\frac{d}{dY}\langle\hat{O}\rangle_Y = -\langle H_{\text{JIMWLK}}\hat{O}\rangle_Y \tag{2.8}$$

cannot be solved exactly for CGC operators of interest using currently-known methods. The critical obstacle is that for a given n-point Wilson line correlator, Equation (2.8) results in a differential equation that depends on both the n-point correlator and the $n+1$-point correlator. To determine the evolution of the $n+1$-point correlator, we again must use Equation (2.8), which generates another functional differential equation that depends on the $n+1$-point correlator and $n+2$-point correlator, and so on. In other words, Equation (2.8) is not a *closed* equation, in the sense that for any Wilson line correlator, it generates an infinite set of coupled differential equations. In the next two subsections we work through the action of the JIMWLK Hamiltonian on the simplest possible CGC correlators to see this explicitly, but let's first describe the physical interpretation of the generation of this infinite hierarchy of coupled equations.

The physical picture for JIMWLK evolution is intuitive. As we shall see shortly, the terms in the JIMWLK Hamiltonian

$$i\nabla^a_{\boldsymbol{x}} i\nabla^a_{\boldsymbol{y}} + i\bar{\nabla}^a_{\boldsymbol{x}} i\bar{\nabla}^a_{\boldsymbol{y}} \tag{2.9}$$

correspond to the situation where a (anti-)quark emits and reabsorbs a gluon either before or after passing through the target and this gluon does not interact with the target.

On the other hand, the terms

$$\widetilde{U}^{ab}_{\boldsymbol{z}}(i\bar{\nabla}^a_{\boldsymbol{x}} i\nabla^b_{\boldsymbol{y}} + i\nabla^a_{\boldsymbol{x}} i\bar{\nabla}^b_{\boldsymbol{y}}) \tag{2.10}$$

in the JIMWLK Hamiltonian correspond to the situation where the quark emits a gluon, which then is reabsorbed after interacting with the background field of the target (Figure 2.1a), evidenced by the insertion of a gluon via the adjoint Wilson line. The terms in Equation (2.10) are responsible for generating the aforementioned infinite hierarchy of coupled differential equations, because of course the gluon can itself emit and reabsorb a gluon that interacts with the background field of the target (Figure 2.1b), explaining why the 3-point function in turn depends on the 4-point function. In the next subsections we work through some examples to illustrate the generation of this infinite hierarchy explicitly.

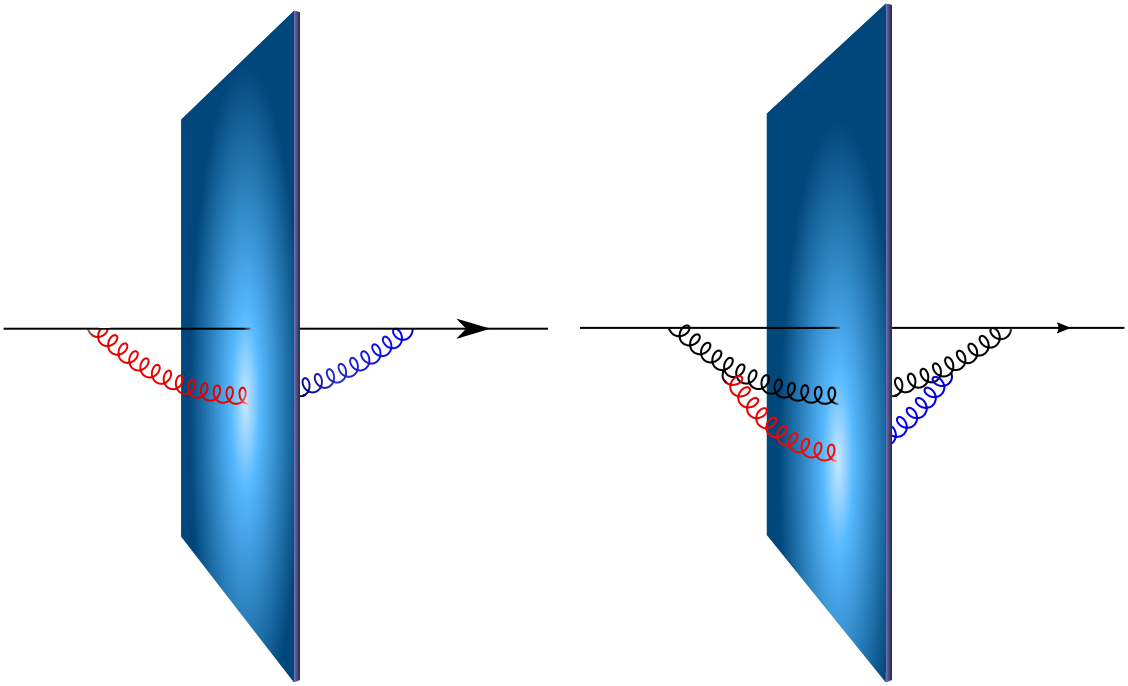

(A) Quark emits a gluon, which interacts with the target background field.

(B) Gluon that interacts with the target emits and reabsorbs a gluon that also interacts with the target.

FIGURE 2.1: A stylised depiction of the physics captured by the JIMWLK equation. An incoming quark (black directioned line) interacts with the Lorentz-contracted target (depicted as a blue plane) through the emission and reabsorption of gluons.

2.1.1 Dipole correlator evolution depends on the 3-point function

Consider the case when a photon splits into a $q\bar{q}$ pair, which then interacts with the target through the emission and reabsorption of gluons. Then to calculate the Y-dependence of $\langle \mathrm{tr}(U_{\boldsymbol{x}}U_{\boldsymbol{y}}^\dagger)/N_c\rangle_Y$ (which is commonly referred to as the *dipole correlator*), we derive its evolution using the JIMWLK Hamiltonian:

$$\frac{d}{dY}\left\langle \frac{\mathrm{tr}(U_{\boldsymbol{x}}U_{\boldsymbol{y}}^\dagger)}{N_c}\right\rangle_Y = -\left\langle H_{\text{JIMWLK}}\frac{\mathrm{tr}(U_{\boldsymbol{x}}U_{\boldsymbol{y}}^\dagger)}{N_c}\right\rangle_Y \tag{2.11}$$

The terms inside the CGC average that do not include the adjoint Wilson line $U_{\boldsymbol{z}}^{ab}$ are proportional to

$$\int_{\boldsymbol{uzv}} \mathcal{K}_{\boldsymbol{uzv}}\left(i\nabla_{\boldsymbol{u}}^a i\nabla_{\boldsymbol{v}}^a + i\bar{\nabla}_{\boldsymbol{u}}^a i\bar{\nabla}_{\boldsymbol{v}}^a\right)\mathrm{tr}(U_{\boldsymbol{x}}U_{\boldsymbol{y}}^\dagger) \tag{2.12a}$$

which we can rewrite as

$$= \int_{\boldsymbol{uzv}} \mathcal{K}_{\boldsymbol{uzv}}\left(i\nabla_{\boldsymbol{u}}^a i\nabla_{\boldsymbol{v}}^a \mathrm{tr}(U_{\boldsymbol{x}}U_{\boldsymbol{y}}^\dagger) + i\bar{\nabla}_{\boldsymbol{u}}^a i\bar{\nabla}_{\boldsymbol{v}}^a \mathrm{tr}((U_{\boldsymbol{y}}U_{\boldsymbol{x}}^\dagger)^\dagger)\right) \tag{2.12b}$$

Since $i\nabla_{\boldsymbol{x}}^a U_{\boldsymbol{y}} = i\bar{\nabla}_{\boldsymbol{x}}^a U_{\boldsymbol{y}}^\dagger$ (and similarly for the anti-fundamental Wilson lines), and noting that the trace commutes with the derivative, we have

$$= \int_{\boldsymbol{uzv}} \mathcal{K}_{\boldsymbol{uzv}}\,\mathrm{tr}\left(i\nabla_{\boldsymbol{u}}^a i\nabla_{\boldsymbol{v}}^a(U_{\boldsymbol{x}}U_{\boldsymbol{y}}^\dagger) + (\boldsymbol{x}\leftrightarrow\boldsymbol{y})\right) \tag{2.12c}$$

$$= \int_{\boldsymbol{uzv}} \mathcal{K}_{\boldsymbol{uzv}}\,\mathrm{tr}\left(i\nabla_{\boldsymbol{u}}^a i\nabla_{\boldsymbol{v}}^a(U_{\boldsymbol{x}})U_{\boldsymbol{y}}^\dagger + U_{\boldsymbol{x}}i\nabla_{\boldsymbol{u}}^a i\nabla_{\boldsymbol{v}}^a(U_{\boldsymbol{y}}^\dagger) + 2i\nabla_{\boldsymbol{u}}^a(U_{\boldsymbol{x}})i\nabla_{\boldsymbol{v}}^a(U_{\boldsymbol{y}}^\dagger) + (\boldsymbol{x}\leftrightarrow\boldsymbol{y})\right) \tag{2.12d}$$

where we have used the fact that $\mathcal{K}_{\boldsymbol{uzv}}$ is symmetric in $\boldsymbol{u}$ and $\boldsymbol{v}$. Then we have

$$= \int_{\boldsymbol{uzv}} \mathcal{K}_{\boldsymbol{uzv}}\,\mathrm{tr}\left(i\nabla_{\boldsymbol{u}}^a i\nabla_{\boldsymbol{v}}^a(U_{\boldsymbol{x}})U_{\boldsymbol{y}}^\dagger + U_{\boldsymbol{x}}i\nabla_{\boldsymbol{u}}^a i\nabla_{\boldsymbol{v}}^a(U_{\boldsymbol{y}}^\dagger) + 2i\nabla_{\boldsymbol{u}}^a(U_{\boldsymbol{x}})i\nabla_{\boldsymbol{v}}^a(U_{\boldsymbol{y}}^\dagger) + (\boldsymbol{x}\leftrightarrow\boldsymbol{y})\right) \tag{2.12e}$$

$$= C_F\int_{\boldsymbol{z}}(\mathcal{K}_{\boldsymbol{xzx}} + \mathcal{K}_{\boldsymbol{yzy}} - 2\mathcal{K}_{\boldsymbol{xzy}})\left(\mathrm{tr}(U_{\boldsymbol{x}}U_{\boldsymbol{y}}^\dagger) + (\boldsymbol{x}\leftrightarrow\boldsymbol{y})\right) \tag{2.12f}$$

$$= 2\,C_F\int_{\boldsymbol{z}}(\mathcal{K}_{\boldsymbol{xzx}} + \mathcal{K}_{\boldsymbol{yzy}} - 2\mathcal{K}_{\boldsymbol{xzy}})\,\mathrm{tr}(U_{\boldsymbol{x}}U_{\boldsymbol{y}}^\dagger) \tag{2.12g}$$

where we have again used that $\mathcal{K}_{\boldsymbol{xzy}}$ is symmetric in its first and last variables and the $\mathfrak{su}(N_c)$ Casimir is given by $C_F\mathbb{1} := t^a t^a = (N_c^2-1)/(2N_c)\mathbb{1}$.

The terms that contain the adjoint Wilson line $U^{ab}_{\boldsymbol{z}}$ inside the average on the RHS of eq. (2.11) are proportional to

$$\int_{\boldsymbol{uzv}} \mathcal{K}_{\boldsymbol{uzv}}\, \widetilde{U}^{ab}_{\boldsymbol{z}} (i\bar{\nabla}^a_{\boldsymbol{u}} i\nabla^b_{\boldsymbol{v}} + i\nabla^a_{\boldsymbol{u}} i\bar{\nabla}^b_{\boldsymbol{v}}) \operatorname{tr}(U_{\boldsymbol{x}} U^\dagger_{\boldsymbol{y}}) \tag{2.13a}$$

Because the left and right invariant vector fields commute, we have

$$= \int_{\boldsymbol{uzv}} \mathcal{K}_{\boldsymbol{uzv}}\, \widetilde{U}^{ab}_{\boldsymbol{z}} \operatorname{tr}\left(i\bar{\nabla}^a_{\boldsymbol{u}} i\nabla^b_{\boldsymbol{v}} (U_{\boldsymbol{x}} U^\dagger_{\boldsymbol{y}}) + (\boldsymbol{a} \leftrightarrow \boldsymbol{b}, \boldsymbol{u} \leftrightarrow \boldsymbol{v}) \right) \tag{2.13b}$$

$$= \int_{\boldsymbol{uzv}} \mathcal{K}_{\boldsymbol{uzv}}\, \widetilde{U}^{ab}_{\boldsymbol{z}} \operatorname{tr}\Big(i\bar{\nabla}^a_{\boldsymbol{u}} i\nabla^b_{\boldsymbol{v}} (U_{\boldsymbol{x}}) U^\dagger_{\boldsymbol{y}} + U_{\boldsymbol{x}} i\bar{\nabla}^a_{\boldsymbol{u}} i\nabla^b_{\boldsymbol{v}} (U^\dagger_{\boldsymbol{y}}) \tag{2.13c}$$

$$+ i\bar{\nabla}^a_{\boldsymbol{u}} (U_{\boldsymbol{x}}) i\nabla^b_{\boldsymbol{v}} (U^\dagger_{\boldsymbol{y}}) + i\bar{\nabla}^b_{\boldsymbol{v}} (U_{\boldsymbol{x}}) i\nabla^a_{\boldsymbol{u}} (U^\dagger_{\boldsymbol{y}}) + (\boldsymbol{a} \leftrightarrow \boldsymbol{b}, \boldsymbol{u} \leftrightarrow \boldsymbol{v}) \Big) \tag{2.13d}$$

$$= \int_{\boldsymbol{z}} (-\mathcal{K}_{\boldsymbol{xzx}} - \mathcal{K}_{\boldsymbol{yzy}} + 2\mathcal{K}_{\boldsymbol{xzy}})\, \widetilde{U}^{ab}_{\boldsymbol{z}} 2 \operatorname{tr}(t^a U_{\boldsymbol{x}} t^b U^\dagger_{\boldsymbol{y}}) \tag{2.13e}$$

$$\frac{d}{dY} \left\langle \frac{\operatorname{tr}(U_{\boldsymbol{x}} U^\dagger_{\boldsymbol{y}})}{N_c} \right\rangle_Y = \frac{\alpha_s}{\pi^2} \Bigg(- C_F \left\langle \int_{\boldsymbol{z}} \widetilde{\mathcal{K}}_{\boldsymbol{xzy}} \frac{\operatorname{tr}(U_{\boldsymbol{x}} U^\dagger_{\boldsymbol{y}})}{N_c} \right\rangle_Y + \left\langle \int_{\boldsymbol{z}} \widetilde{\mathcal{K}}_{\boldsymbol{xzy}} \frac{\widetilde{U}^{ab}_{\boldsymbol{z}} \operatorname{tr}(t^a U_{\boldsymbol{x}} t^b U^\dagger_{\boldsymbol{y}})}{N_c} \right\rangle_Y \Bigg) \tag{2.14a}$$

with

$$\widetilde{\mathcal{K}}_{\boldsymbol{xzy}} := -\mathcal{K}_{\boldsymbol{xzx}} - \mathcal{K}_{\boldsymbol{yzy}} + 2\mathcal{K}_{\boldsymbol{xzy}} \tag{2.14b}$$

Equation (2.14) was found in [14,16]. As we've cautioned against earlier, the RHS of the evolution equation for the dipole operator depends on both the average of the dipole operator itself, as well as the 3-point function $\widetilde{U}^{ab}_{\boldsymbol{z}} \operatorname{tr}(t^a U_{\boldsymbol{x}} t^b U^\dagger_{\boldsymbol{y}})/N_c$. The 3-point function must be determined from an evolution equation which in turn couples it to the 4-point function and so on, ad infinitum.

2.1.2 The evolution of higher correlators is naturally organised as a matrix equation

As was noted in [19, Sec. 4], a critical additional subtlety comes into the discussion when we consider the JIMWLK evolution of correlators involving more than two quarks. The evolution of these objects can be organised as a matrix of correlators, rather than individual correlators themselves. This formulation places constraints on the types of approximation schemes that are admissible, as will be elaborated on in Section 2.3.

The simplest example where the need for such a matrix treatment appears is when we consider 2 quark-antiquark pairs. The JIMWLK evolution of this system is given by

$$\frac{d}{dY}\left\langle \frac{\operatorname{tr}(U_{\boldsymbol{x_1}}U^\dagger_{\boldsymbol{x_2}})\operatorname{tr}(U_{\boldsymbol{x_3}}U^\dagger_{\boldsymbol{x_4}})}{N_c^2}\right\rangle_Y = -\left\langle H_{\text{JIMWLK}}\frac{\operatorname{tr}(U_{\boldsymbol{x_1}}U^\dagger_{\boldsymbol{x_2}})\operatorname{tr}(U_{\boldsymbol{x_3}}U^\dagger_{\boldsymbol{x_4}})}{N_c^2}\right\rangle_Y \tag{2.15}$$

The action of the JIMWLK Hamiltonian (ignoring factors of $1/N_c$ and suppressing the subscript label on H for the moment) gives

$$H\Big(\operatorname{tr}(U_{\boldsymbol{x_1}}U^\dagger_{\boldsymbol{x_2}})\operatorname{tr}(U_{\boldsymbol{x_3}}U^\dagger_{\boldsymbol{x_4}})\Big) = H\Big(\operatorname{tr}(U_{\boldsymbol{x_1}}U^\dagger_{\boldsymbol{x_2}})\Big)\operatorname{tr}(U_{\boldsymbol{x_3}}U^\dagger_{\boldsymbol{x_4}}) \tag{2.16a}$$

$$+\operatorname{tr}(U_{\boldsymbol{x_1}}U^\dagger_{\boldsymbol{x_2}})H\Big(\operatorname{tr}(U_{\boldsymbol{x_3}}U^\dagger_{\boldsymbol{x_4}})\Big) + \text{cross terms} \tag{2.16b}$$

The cross terms alluded to above cause the action of the JIMWLK Hamiltonian on the 4-point function to depend not only on the 4-point function itself and a 5-point function, but also on other inequivalent 4 point functions. To see that the cross terms introduce a dependence on the 5-point function, consider one such cross term that arises:

$$-\frac{\alpha_s}{2\pi^2}\int_{\boldsymbol{uzv}}\mathcal{K}_{\boldsymbol{uzv}}i\nabla^a_{\boldsymbol{u}}\Big(\operatorname{tr}(U_{\boldsymbol{x_1}}U^\dagger_{\boldsymbol{x_2}})\Big)i\nabla^a_{\boldsymbol{v}}\Big(\operatorname{tr}(U_{\boldsymbol{x_3}}U^\dagger_{\boldsymbol{x_4}})\Big) \tag{2.17a}$$

$$=-\frac{\alpha_s}{2\pi^2}\int_{\boldsymbol{z}}\widetilde{\mathcal{K}}_{\boldsymbol{x_1x_2zx_3x_4}}\operatorname{tr}(U_{\boldsymbol{x_1}}t^aU^\dagger_{\boldsymbol{x_2}})\operatorname{tr}(U_{\boldsymbol{x_3}}t^aU^\dagger_{\boldsymbol{x_4}}) \tag{2.17b}$$

where

$$\widetilde{\mathcal{K}}_{\boldsymbol{x_1x_2zx_3x_4}} := \mathcal{K}_{\boldsymbol{x_1zx_3}} - \mathcal{K}_{\boldsymbol{x_1zx_4}} - \mathcal{K}_{\boldsymbol{x_2zx_3}} + \mathcal{K}_{\boldsymbol{x_2zx_4}} \tag{2.17c}$$

We can use the Fierz identity $T^a_{ij}T^a_{kl} = \frac{1}{2}(\delta_{il}\delta_{jk} - \frac{1}{N_c}\delta_{ij}\delta_{kl})$ to obtain

$$=-\frac{\alpha_s}{4\pi^2}\int_{\boldsymbol{z}}\widetilde{\mathcal{K}}_{\boldsymbol{x_1x_2zx_3x_4}}\Big(\operatorname{tr}(U_{\boldsymbol{x_1}}U^\dagger_{\boldsymbol{x_4}}U_{\boldsymbol{x_3}}U^\dagger_{\boldsymbol{x_2}}) - \frac{1}{N_c}\operatorname{tr}(U_{\boldsymbol{x_1}}U^\dagger_{\boldsymbol{x_2}})\operatorname{tr}(U_{\boldsymbol{x_3}}U^\dagger_{\boldsymbol{x_4}})\Big) \tag{2.17d}$$

which explicitly shows that the cross term produces a 4-point function term that is inequivalent to the original $(q\bar{q})^2$ 4-point function, as well as a term involving the original $(q\bar{q})^2$ 4-point function.

This result is consistent with our previous understanding of the physical meaning of the $i\nabla^a_{\boldsymbol{u}} i\nabla^a_{\boldsymbol{v}}$ operator in the JIMWLK Hamiltonian: the cross term above that this operator generates corresponds to the case when one of the $q\bar{q}$ pairs emits a gluon which is absorbed by the other $q\bar{q}$ pair, *without* interacting with the background field of the target nucleus. This is a new possibility over and above the self-energy and gluon exchange corrections that a single $q\bar{q}$ pair can experience. One can check that the other cross terms have the same interpretation: they generate all the possible ways that one $q\bar{q}$ pair can emit a gluon that is absorbed by the other $q\bar{q}$ pair, including the cases where the gluon does and does not interact with the background field of the target nucleus (cross terms involving $\widetilde{U}^{ab}_{\boldsymbol{z}}$ are interacting, the rest are non-interacting).

A simple way to organise this information was given in [19, Sec. 4]. The key observation is that we can cast the evolution equations in matrix form by considering the JIMWLK equation applied component-wise to a matrix of n-point correlators that mix under the action of the JIMWLK Hamiltonian. The component-wise action of the right-invariant vector fields in the JIMWLK Hamiltonian on this matrix of correlators produces a matrix of coefficients multiplying the matrix of correlators on the left, while the left-invariant vector fields multiply the matrix of correlators by a matrix of coefficients on the right (we will see this explicitly in Section 2.3). We call this matrix of n-point correlators the *amplitude matrix*. Altogether, we have:

$$\frac{d}{dY}\mathcal{A}(Y) = -\{\mathcal{M}, \mathcal{A}(Y)\} + \text{a matrix of 5-point correlators} \tag{2.18a}$$

$$\mathcal{A}(Y) := \begin{pmatrix} \left\langle \frac{\operatorname{tr}(U_{\boldsymbol{x_1}} U^\dagger_{\boldsymbol{x_2}}) \operatorname{tr}(U_{\boldsymbol{x_3}} U^\dagger_{\boldsymbol{x_4}})}{N_c^2} \right\rangle_Y & \left\langle \frac{\operatorname{tr}(U_{\boldsymbol{x_1}} t^a U^\dagger_{\boldsymbol{x_2}}) \operatorname{tr}(U_{\boldsymbol{x_3}} t^a U^\dagger_{\boldsymbol{x_4}})}{N_c\sqrt{d_A/4}} \right\rangle_Y \\ \left\langle \frac{\operatorname{tr}(U_{\boldsymbol{x_1}} U^\dagger_{\boldsymbol{x_2}} t^b) \operatorname{tr}(U_{\boldsymbol{x_3}} U^\dagger_{\boldsymbol{x_4}} t^b)}{N_c\sqrt{d_A/4}} \right\rangle_Y & \left\langle \frac{\operatorname{tr}(U_{\boldsymbol{x_1}} t^a U^\dagger_{\boldsymbol{x_2}} t^b) \operatorname{tr}(U_{\boldsymbol{x_3}} t^a U^\dagger_{\boldsymbol{x_4}} t^b)}{d_A/4} \right\rangle_Y \end{pmatrix} \tag{2.18b}$$

where $d_A := N_c^2 - 1$ is the dimension of the adjoint representation and $\mathcal{M}$ is some rapidity-independent matrix to be determined from the JIMWLK equation. Notice that in the limit $\boldsymbol{x_3} \to \boldsymbol{x_4}$, using the Fierz identity gives us

$$\mathcal{A}(Y) \xrightarrow{\boldsymbol{x_3}\to\boldsymbol{x_4}} \begin{pmatrix} \left\langle \frac{\operatorname{tr}(U_{\boldsymbol{x_1}} U^\dagger_{\boldsymbol{x_2}})}{N_c} \right\rangle_Y & 0 \\ 0 & \left\langle \frac{\widetilde{U}^{ab}_{\boldsymbol{z}} \operatorname{tr}(t^a U_{\boldsymbol{x_1}} t^b U^\dagger_{\boldsymbol{x_2}})}{C_F N_c} \right\rangle_Y \end{pmatrix} \tag{2.19a}$$

and so $\mathcal{A}(Y)$ for two quark-antiquark pairs contains all of the evolution information of the JIMWLK evolution of the dipole (eq. (2.14)), if we take the appropriate coincidence limits. We expect this behaviour to generalise: that is, we expect the evolution of the amplitude matrix of higher n-point correlators to always encode the evolution equations of lower n-point correlators in the appropriate coincidence limits [1].

From now on we will work with the amplitude matrix formulation, thinking of the JIMWLK evolution of the dipole operator given earlier as a special 1 x 1 case of this setup. As we will see in Section 2.3, this formulation both simplifies and constrains the way that we can think about finding approximate solutions to the JIMWLK equation.

Now that we've seen that JIMWLK generates an infinite hierarchy of coupled differential equations in both the dipole and the $(q\bar{q})^2$ cases, we discuss in the next section some existing approaches to dealing with this problem and their limitations. We discuss our approach to resolving these difficulties in Section 2.3.

2.2 A brief summary: some existing approximate solutions to the JIMWLK equation and their limitations

We have seen in Section 2.1 that using JIMWLK to analytically determine the rapidity dependence of CGC correlators is currently intractable. The two common approaches to handling this difficulty are to turn to numerical solutions, or to take the large N_c limit. However, both of these approaches have their limitations, which was the motivation for developing the method that will be introduced in the next section.

In the case of numerical simulations, one recognises that the JIMWLK evolution of the CGC weight function (eq. (2.1)) can be viewed as a Fokker-Planck equation, which can then be recast as a Langevin equation to considerably increase numerical efficiency [25]. Then one calculates observables directly using numerical implementations of the path integral (eq. (2.2)), all while avoiding the large N_c limit. In this sense, JIMWLK evolution at leading log order in x_{bj} is a solved problem. However, this approach is limited in that the Fokker-Planck argument relies on the observation that the evolution equation for the CGC weight function at this order is only linear and quadratic in source terms [25]. At NLLO, higher order source terms appear in this evolution equation and so we can no longer obtain a Langevin description of the evolution. Thus developing new analytic methods (or numerical methods) is critical for calculations beyond LLO in x_{bj}.

In the case of the large N_c limit, what this approximation buys us is most easily explained using the example of JIMWLK evolution of the dipole correlator. We saw in Equation (2.14) that this evolution is given by

$$\frac{d}{dY}\left\langle \frac{\mathrm{tr}(U_{\boldsymbol{x}}U_{\boldsymbol{y}}^\dagger)}{N_c}\right\rangle_Y = \frac{\alpha_s}{\pi^2}\left(- C_F\left\langle \int_{\boldsymbol{z}} \widetilde{\mathcal{K}}_{\boldsymbol{xzy}} \frac{\mathrm{tr}(U_{\boldsymbol{x}}U_{\boldsymbol{y}}^\dagger)}{N_c}\right\rangle_Y + \left\langle \int_{\boldsymbol{z}} \widetilde{\mathcal{K}}_{\boldsymbol{xzy}} \frac{\widetilde{U}_{\boldsymbol{z}}^{ab}\,\mathrm{tr}(t^a U_{\boldsymbol{x}} t^b U_{\boldsymbol{y}}^\dagger)}{N_c}\right\rangle_Y\right) \tag{2.20a}$$

with

$$\widetilde{\mathcal{K}}_{\boldsymbol{xzy}} := -\mathcal{K}_{\boldsymbol{xzx}} - \mathcal{K}_{\boldsymbol{yzy}} + 2\mathcal{K}_{\boldsymbol{xzy}} \tag{2.20b}$$

We can rewrite this equation in a form that makes the effect of the N_c limit more clear. Let's define the dipole operator

$$\hat{S}_{\boldsymbol{xy}} := \frac{\mathrm{tr}(U_{\boldsymbol{x}}U_{\boldsymbol{y}}^\dagger)}{N_c} \tag{2.21a}$$

Then we have the Fierz identity

$$\widetilde{U}^{ab}_{\boldsymbol{z}} \operatorname{tr}(t^a U_{\boldsymbol{x}} t^b U^\dagger_{\boldsymbol{y}}) = \frac{1}{2}(N_c^2 \hat{S}_{\boldsymbol{xz}} \hat{S}_{\boldsymbol{zy}} - \hat{S}_{\boldsymbol{xy}}) \tag{2.21b}$$

and using $C_F = (N_c^2 - 1)/2N_c$ we obtain

$$\frac{d}{dY}\langle \hat{S}_{\boldsymbol{xy}} \rangle_Y = \frac{\alpha_s N_c}{2\pi^2} \int_{\boldsymbol{z}} \widetilde{\mathcal{K}}_{\boldsymbol{xzy}} \langle \hat{S}_{\boldsymbol{xz}} \hat{S}_{\boldsymbol{zy}} - \hat{S}_{\boldsymbol{xy}} \rangle_Y \tag{2.21c}$$

The key result (although not necessarily immediately obvious) is that in the large N_c limit, the average factorizes as

$$\frac{d}{dY}\langle \hat{S}_{\boldsymbol{xy}} \rangle_Y = \frac{\alpha_s N_c}{2\pi^2} \int_{\boldsymbol{z}} \widetilde{\mathcal{K}}_{\boldsymbol{xzy}} \langle \hat{S}_{\boldsymbol{xz}} \rangle_Y \langle \hat{S}_{\boldsymbol{zy}} \rangle_Y - \langle \hat{S}_{\boldsymbol{xy}} \rangle_Y \tag{2.22}$$

which results in a closed equation for the dipole operator, known as the Balitsky-Kovchegov (BK) equation [14–18]. A derivation of this result can be found in [12, Sec. 4.4].

The large N_c approximation/BK equation has worked suprisingly well in applications [20, 26]. However, it also has its limitations, for example in that it predicts no difference between inclusive and exclusive vector meson production cross sections when we expect this difference to be nonzero [19]. In addition to this, in taking the large N_c limit we naively introduce errors of order $1/N_c^2$ into the evolution equations [20]. $1/N_c^2$ is not necessarily large compared to experimental errors, but the key observation is that this error is at the level of the functional differential equation, whereas the error that results from this in the solution of the equation can be considerably larger. One can see this by noticing that when numerically implementing BK evolution, the $1/N_c^2$ error is present at each step in the numerical evolution, which means that the error can in principle grow much larger with correlator evolution. Thus it becomes desirable to find an alternative analytic method for studying JIMWLK at finite N_c.

In [19, 20] a finite N_c truncation was was introduced as inspired by the previous ideas of [27, eq. 2.15]. This new truncation was shown to be equivalent to using a Gaussian distribution as the ansatz for the CGC wave function in terms of target color sources [19, App. B] and is known in the literature as the *Gaussian truncation*. However, despite some successes, the Gaussian truncation is known to be limited in some ways, for example in that it predicts exact Casimir scaling in the dipole evolution, which is known to be violated in QCD [20, Sec. 4.1]. Thus, effort has been made to generalise this strategy to systematically include additional degrees of freedom to capture these and other effects. The following section introduces the result of this program, introducing a fully general result as devised by R. Moerman and H. Weigert in [1]. Some critical mathematical details of this method are delayed to Chapter 3 and comprise the primary contribution of this dissertation to this research.

2.3 A novel parameterisation gives us a finite N_c truncation that respects coincidence limits

Generalizing previous work [19–21], R. Moerman and H. Weigert have a devised a parameterisation scheme that is argued to be the most general parameterization of JIMWLK evolution that has the following properties:

Properties of R. Moerman and H. Weigert's truncation scheme [1]

- Valid for any finite value of N_c
- N_c explicitly kept as a parameter and so any results can be compared with the large N_c limit at any time
- Independent evolution of symmetric and antisymmetric parts of any amplitude matrix, known to be needed for any solution to the amplitude matrix formulation of JIMWLK
- Obeys a set of group-theoretic coincidence limits known to be imposed by full JIMWLK evolution

The full presentation of this method will appear in parallel work [1], while the purpose of this section is to briefly summarise the method, in order to provide context for the later sections of this dissertation.

We briefly elaborate on why the above properties are desirable. First, as mentioned in the previous section, the large N_c limit renders certain correlators inaccessible and so a finite N_c truncation scheme becomes desirable. Second, keeping N_c as a parameter wherever possible allows us to seamlessly compare with results obtained previously in the large N_c limit. Third, we know that in the amplitude matrix formulation, the JIMWLK Hamiltonian acts component-wise and so therefore the JIMWLK equation evolves symmetric and antisymmetric parts of the matrix of correlators independently. Thus, any reparameterisation should also do the same.

As for the desirability of preserving coincidence limits, observe that for any Wilson line correlator, each possible combination of limits where two transverse coordinates are made to coincide will result in a group-theoretic constraint on the correlator. The simplest possible example is

$$\left\langle \frac{\mathrm{tr}(U_{\boldsymbol{x}} U_{\boldsymbol{y}}^\dagger)}{N_c} \right\rangle (Y) \xrightarrow{\boldsymbol{x}\to\boldsymbol{y}} 1 \tag{2.23}$$

The next most simple example of the importance of coincidence limits appeared when we investigated the limit $\boldsymbol{x}_3 \to \boldsymbol{x}_4$ in the amplitude matrix of $(q\bar{q})^2$ correlators (eq. (2.19)):

$$\mathcal{A}(Y) := \begin{pmatrix} \left\langle \frac{\operatorname{tr}(U_{\boldsymbol{x_1}} U^\dagger_{\boldsymbol{x_2}}) \operatorname{tr}(U_{\boldsymbol{x_3}} U^\dagger_{\boldsymbol{x_4}})}{N_c^2} \right\rangle_Y & \left\langle \frac{\operatorname{tr}(U_{\boldsymbol{x_1}} t^a U^\dagger_{\boldsymbol{x_2}}) \operatorname{tr}(U_{\boldsymbol{x_3}} t^a U^\dagger_{\boldsymbol{x_4}})}{N_c \sqrt{d_A/4}} \right\rangle_Y \\ \left\langle \frac{\operatorname{tr}(U_{\boldsymbol{x_1}} U^\dagger_{\boldsymbol{x_2}} t^b) \operatorname{tr}(U_{\boldsymbol{x_3}} U^\dagger_{\boldsymbol{x_4}} t^b)}{N_c \sqrt{d_A/4}} \right\rangle_Y & \left\langle \frac{\operatorname{tr}(U_{\boldsymbol{x_1}} t^a U^\dagger_{\boldsymbol{x_2}} t^b) \operatorname{tr}(U_{\boldsymbol{x_3}} t^a U^\dagger_{\boldsymbol{x_4}} t^b)}{d_A/4} \right\rangle_Y \end{pmatrix} \tag{2.24}$$

$$\xrightarrow{\boldsymbol{x_3} \to \boldsymbol{x_4}} \begin{pmatrix} \left\langle \frac{\operatorname{tr}(U_{\boldsymbol{x_1}} U^\dagger_{\boldsymbol{x_2}})}{N_c} \right\rangle_Y & 0 \\ 0 & \left\langle \frac{\widetilde{U}^{ab}_{\boldsymbol{z}} \operatorname{tr}(t^a U_{\boldsymbol{x}_1} t^b U^\dagger_{\boldsymbol{x}_2})}{C_F N_c} \right\rangle_Y \end{pmatrix} \tag{2.25}$$

The important observation here was that the limit $\boldsymbol{x}_3 \to \boldsymbol{x}_4$ shows that $\mathcal{A}(Y)$ encodes the evolution equation for the dipole operator. We expect that in general, the amplitude matrix of higher n-point correlators will always encode the evolution equations of lower n-point correlators in the appropriate coincidence limits [1]. Therefore, preserving coincidence limits is plausibly of critical importance, because these limits intimately entwine the true evolution equations of observables. Then by requiring that we preserve all of these limits for any Wilson line correlator, we impose a natural group-theoretic constraint on the possible parameterisations we might consider.

Now we outline the method of R. Moerman and H. Weigert that obeys all of these properties. First, we observe that we can write

$$\langle \mathcal{A} \rangle(Y) = \langle \mathcal{A}_1 \rangle(Y) + \langle \mathcal{A}_2 \rangle(Y) \tag{2.26}$$

where $\mathcal{A}_1, \mathcal{A}_2$ are the symmetric and antisymmetric parts of $\mathcal{A}$ respectively. Notice that this separation of symmetric and antisymmetric parts holds for all Y, because JIMWLK evolution evolves these matrices independently. Then, by defining[1]

$$\mathcal{M}_s(Y) = -\left(\frac{d}{dY} \langle \mathcal{A}_s \rangle(Y) \right) \langle \mathcal{A}_s \rangle^{-1}(Y) \tag{2.27}$$

we trivially have that

$$\frac{d}{dY} \langle \mathcal{A} \rangle(Y) = -\frac{1}{2} \sum_{s=1}^{2} \left(\mathcal{M}_s(Y) \langle \mathcal{A}_s \rangle(Y) + \langle \mathcal{A}_s \rangle(Y) \mathcal{M}_s^t(Y) \right) \tag{2.28}$$

[1] We have always assumed that these matrices are differentiable in writing the JIMWLK equation and as long as the initial condition is invertible, $\langle \mathcal{A} \rangle(Y)$ is invertible for any Y.

The general solution to the differential equation (2.28) is given by

$$\langle\mathcal{A}\rangle(Y) = \sum_{s=1}^{2} \mathcal{P}_s(Y, Y_0)\ \langle\mathcal{A}_s\rangle(Y_0)\ \mathcal{P}_s^t(Y, Y_0) \tag{2.29a}$$

where $\langle\mathcal{A}_s\rangle(Y_0)$ is some Y-independent initial condition and $\mathcal{P}_s(Y, Y_0)$ is the Y-ordered exponential

$$\mathcal{P}_s(Y, Y_0) := P\exp\bigg(-\frac{1}{2}\int_{Y_0}^{Y} dY'\mathcal{M}_s(Y')\bigg) \tag{2.29b}$$

Clearly the symmetric and antisymmetric parts of eq. (2.29) evolve independently as desired.

At this point, we have not introduced any new information, or any dependence on the JIMWLK equation, except that the symmetric and antisymmetric parts of $\langle\mathcal{A}\rangle(Y)$ evolve independently. Where we make progress is that R. Moerman and H. Weigert argue that they have found the most general parameterisation of $\mathcal{M}_s(Y)$ that respects all group-theoretic coincidence limits. The parameters are an infinite set of Y-dependent functions $G^k(Y)$ and can be truncated at any desired finite order. One can think of the $G^k(Y)$ as loosely analogous to *structure functions* and we will refer to them as *color structure functions*, which is consistent with the terminology introduced in [1].

The aforementioned parameterisation is implemented by considering the following operators

$$\hat{L}_s^k(Y) := (-1)^k \int_{\boldsymbol{x}_1\cdots\boldsymbol{x}_k} G^{km}_{s\,\boldsymbol{x}_1\cdots\boldsymbol{x}_k}(Y)\,\mathcal{C}_m^{a_1\cdots a_k}\, i\bar{\nabla}^{a_1}_{\boldsymbol{x}_1}\cdots i\bar{\nabla}^{a_k}_{\boldsymbol{x}_k} \tag{2.30a}$$

$$\hat{L}_s(Y) := \sum_{k=2}^{k'} \hat{L}_s^k(Y) \tag{2.30b}$$

$$\hat{R}_s^k(Y) := \int_{\boldsymbol{x}_1\cdots\boldsymbol{x}_k} G^{km}_{s\,\boldsymbol{x}_1\cdots\boldsymbol{x}_k}(Y)\,(\mathcal{C}_m^{a_1\cdots a_k})^*\, i\nabla^{a_1}_{\boldsymbol{x}_1}\cdots i\nabla^{a_k}_{\boldsymbol{x}_k} \tag{2.30c}$$

$$\hat{R}_s(Y) := \sum_{k=2}^{k'} \hat{R}_s^k(Y) \tag{2.30d}$$

where k' is some desired order of truncation, repeated indices are summed over, the functions $G^{km}_{s\,\boldsymbol{x}_1\cdots\boldsymbol{x}_k}(Y)$ are the aforementioned *color structure functions*[1], and the objects $\mathcal{C}_m^{a_1\cdots a_k}$ form a basis for the space of color singlets as a subspace of tensors with k adjoint indices. We shall refer to the $\mathcal{C}_m^{a_1\cdots a_k}$ as *adjoint color structures*; they are the primary object of study in this dissertation.[2]

[1] We introduce additional indices where necessary so that in full generality, there is a color structure function for each adjoint color structure, for each value of s.

[2] Particularly, the question that is addressed in the following chapter is how to choose this basis of adjoint color structures.

The motivation for the operators in eq. (2.30) comes as the natural generalisation of the $k' = 2$ case (the "Gaussian truncation"), which was investigated in [19,20] and the $k' = 3$ case, which was investigated in [20,21]. In the previous work on the $k' = 2$ case, only the operator $\hat{L}^2_s(Y)$ was considered[1] and the only possible adjoint color structure with two adjoint indices is the Kronecker delta. This gives

$$\hat{L}^2_s(Y) := \int_{\boldsymbol{x}_1\boldsymbol{x}_2} G^2_{\boldsymbol{x}_1\boldsymbol{x}_2}(Y)\, \delta^{a_1a_2}\, \nabla^{a_1}_{\boldsymbol{x}_1} i\nabla^{a_2}_{\boldsymbol{x}_2} \tag{2.31}$$

In the previous work on the $k' = 3$ case, again only the operators involving the right invariant vector fields were considered and the set of adjoint color structures with three adjoint indices was chosen[2] to be the $d^{a_1a_2a_3}, if^{a_1a_2a_3}$. This lead to[3]

$$\hat{L}^3_s(Y) := \int_{\boldsymbol{x}_1\boldsymbol{x}_2\boldsymbol{x}_3} \left(G^{3d}_{\boldsymbol{x}_1\boldsymbol{x}_2\boldsymbol{x}_3}(Y)\, d^{a_1a_2a_3} + G^{3f}_{\boldsymbol{x}_1\boldsymbol{x}_2\boldsymbol{x}_3}(Y)\, if^{a_1a_2a_3}\right) i\nabla^{a_1}_{\boldsymbol{x}_1} i\nabla^{a_2}_{\boldsymbol{x}_2} i\nabla^{a_3}_{\boldsymbol{x}_2} \tag{2.32}$$

Then by allowing these cases to generalise to arbitrary k', we obtain the operators introduced in eq. (2.30). The operators $\hat{L}_s(Y), \hat{R}_s(Y)$ in eq. (2.30) have the behaviour

$$\langle \hat{L}_s\,(Y)\mathcal{A}\rangle(Y) = \mathcal{M}_s(Y)\langle\mathcal{A}\rangle(Y) \tag{2.33a}$$

$$\langle \hat{R}_s\,(Y)\mathcal{A}\rangle(Y) = \langle\mathcal{A}\rangle(Y)\,\mathcal{M}^t_s(Y) \tag{2.33b}$$

and it is argued in [1] that this is the most general way that matrix multiplication on the left and right by any $\mathcal{M}_s(Y)$ can be parameterised in terms of color structure functions. Then, eq. (2.33) gives us

$$\sum_{s=1}^{2}\langle(\hat{L}_s + \hat{R}_s)\mathcal{A}_s\rangle(Y) = \sum_{s=1}^{2}\Big(\mathcal{M}_s(Y)\langle\mathcal{A}_s(Y)\rangle + \langle\mathcal{A}_s(Y)\rangle\mathcal{M}^t_s(Y)\Big) \tag{2.34}$$

which is the RHS of eq. (2.28). The last step of this method is to substitute $\langle\mathcal{A}\rangle(Y)$ (parameterised by these color structure functions) into the JIMWLK equation to obtain a closed set of equations for the color structure functions, which now encodes the separate evolution of symmetric and antisymmetric parts of $\langle\mathcal{A}\rangle(Y)$, respects all group-theoretic coincidence limits (because the left and right-invariant vector fields commute with taking coincidence limits), and approximates JIMWLK evolution at finite N_c, as desired.

[1] In the recent work of R. Moerman and H. Weigert, it was realised that both the left invariant and right invariant vector fields were needed to preserve independent evolution of symmetric and antisymmetric parts of the amplitude matrix [1], hence the introduction here of the operators $\hat{R}_s(Y)$ and degrees of freedom $G^k_s(Y)$ for each of the symmetric and antisymmetric parts. This was not included earlier in the literature.

[2] We will see in the next chapter that this choice is not arbitrary, rather it directly results from considerations involving irreducible representations of $SU(N_c)$.

[3] In our convention, $\hat{L}^3_s(Y)$ differs from previous work by a factor of -1.

There is one remaining property that we have not addressed: sensitivity to the symmetries of interchanging coordinates in the transverse plane within $\langle\mathcal{A}\rangle(Y)$. This is addressed in the following chapter, with the punchline being that this is directly determined by our choice of adjoint color structures $\mathcal{C}_m^{a_1\cdots a_k}$.

For completeness, we conclude this section by showing that we can directly calculate the expression for this parameterisation of $\mathcal{M}_s(Y)$ in full generality, as was done in [1]. This is most easily facilitated by introducing the following diagrammatic notation:

(Anti-)Wilson lines are represented by the following diagrams

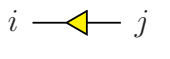

(2.35a)

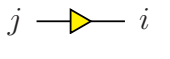

(2.35b)

If each Wilson line has a unique transverse coordinate, an arbitrary product of Wilson line pairs is given by

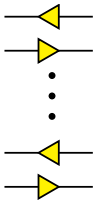

(2.35c)

If each Wilson line has the same transverse coordinate, then we use the diagram

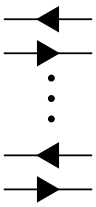

(2.36)

The action of the left and right-invariant vector fields on the Wilson lines

$$i\bar{\nabla}^a_{\boldsymbol{x}}U_{\boldsymbol{y}} = -\delta_{\boldsymbol{xy}}t^aU_{\boldsymbol{x}}, \quad i\bar{\nabla}^a_{\boldsymbol{x}}U^\dagger_{\boldsymbol{y}} = \delta_{\boldsymbol{xy}}U^\dagger_{\boldsymbol{x}}t^a, \tag{2.37a}$$

$$i\nabla^a_{\boldsymbol{x}}U_{\boldsymbol{y}} = \delta_{\boldsymbol{xy}}U_{\boldsymbol{x}}t^a, \quad i\nabla^a_{\boldsymbol{x}}U^\dagger_{\boldsymbol{y}} = -\delta_{\boldsymbol{xy}}t^aU^\dagger_{\boldsymbol{x}} \tag{2.37b}$$

is given diagrammatically by

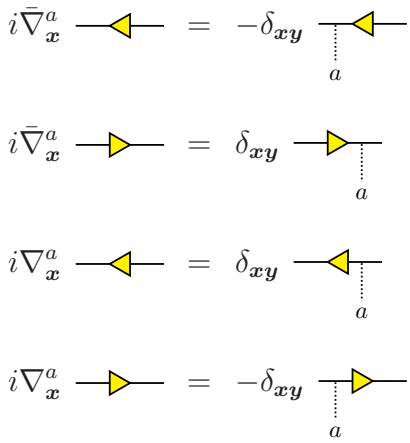

(2.38a)

(2.38b)

(2.38c)

(2.38d)

where the dotted lines labeled by an adjoint index indicate the insertion of a generator. Then the diagrams encoding the action of the vector fields on a product of pairs of fundamental and anti-fundamental Wilson lines are given by[1]

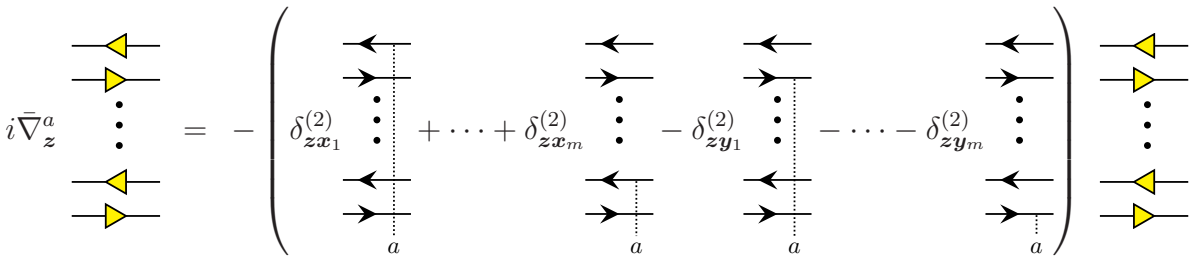

(2.39a)

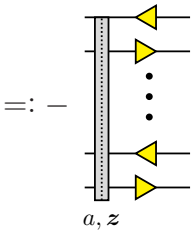

(2.39b)

where the diagram in the final line is just a notational device which represents the previous line. Similarly,

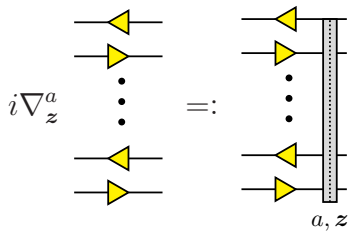

(2.40)

[1]Note that our convention for these diagrams differs from [1] by a factor of $\sqrt{2}$ for each Wilson line. We absorb these factors into the definition of our diagrams as it simplifies the presentation while changing nothing, whereas in [1] their choice of normalisation simplified later calculations that we won't need.

Let's calculate the action of the operators $\hat{L}_s(Y), \hat{R}_s(Y)$ on the amplitude matrix $\mathcal{A}$. The amplitude matrix in a given basis of singlet states is represented diagrammatically as

$$[\mathcal{A}]^i{}_j \quad =: \quad$$

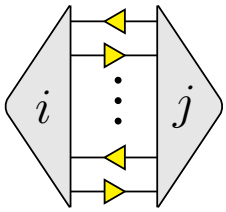

(2.41)

and so we have

$$\hat{L}_s(Y)[\mathcal{A}]^i{}_j = \sum_{k=1}^{k'}(-1)^k \int_{\boldsymbol{x}_1\cdots\boldsymbol{x}_k} G^{km}_{s\,\boldsymbol{x}_1\cdots\boldsymbol{x}_k}(Y)\,\mathcal{C}_m^{a_1\cdots a_k}\, i\bar{\nabla}^{a_1}_{\boldsymbol{x}_1}\cdots i\bar{\nabla}^{a_k}_{\boldsymbol{x}_k}$$

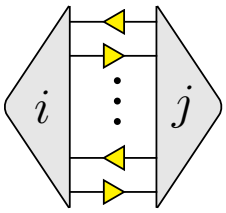

(2.42a)

$$= \sum_{k=1}^{k'} \int_{\boldsymbol{x}_1\cdots\boldsymbol{x}_k} G^{km}_{s\,\boldsymbol{x}_1\cdots\boldsymbol{x}_k}(Y)\,\mathcal{C}_m^{a_1\cdots a_k}$$

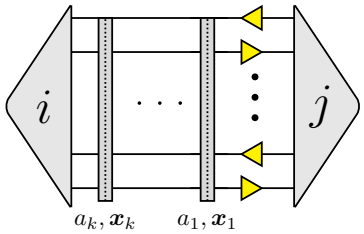

(2.42b)

$$= \sum_{k=1}^{k'}\sum_{l} \int_{\boldsymbol{x}_1\cdots\boldsymbol{x}_k} G^{km}_{s\,\boldsymbol{x}_1\cdots\boldsymbol{x}_k}(Y)\,\mathcal{C}_m^{a_1\cdots a_k}$$

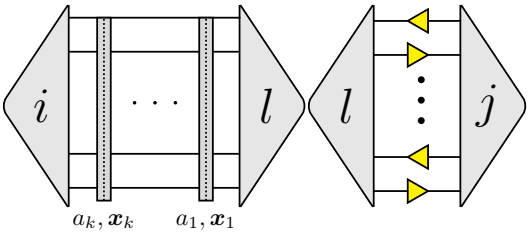

(2.42c)

$$= [\mathcal{M}(Y)]^i{}_l\,[\mathcal{A}]^l{}_j \tag{2.42d}$$

In the second to last line we inserted a complete set of singlet states, because as noted in [1],

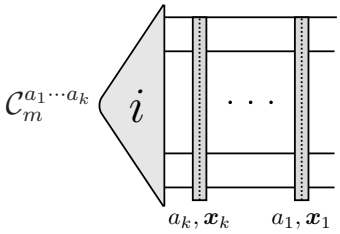

(2.43a)

is a singlet state in the sense that it is invariant under global $SU(N_c)$ transformations:

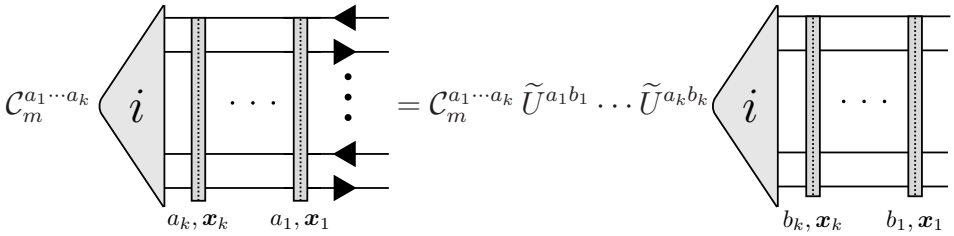

(2.43b)

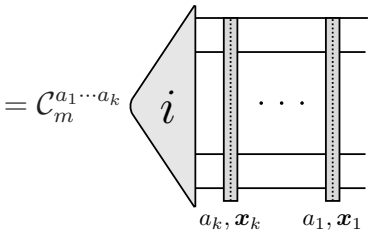

(2.43c)

where the $\widetilde{U}^{a_j b_j}$ are Wilson lines in the adjoint representation and we relabeled indices in the last line. Then altogether, we have explicitly shown that the parameterisation claimed in eq. (2.33) holds and that at k' order in the truncation

$$[\mathcal{M}(Y)]^i{}_j := \sum_{k=1}^{k'} \sum_l \int_{\boldsymbol{x}_1 \cdots \boldsymbol{x}_k} G^{km}_{s\, \boldsymbol{x}_1 \cdots \boldsymbol{x}_k}(Y)\, \mathcal{C}_m^{a_1\cdots a_k}$$

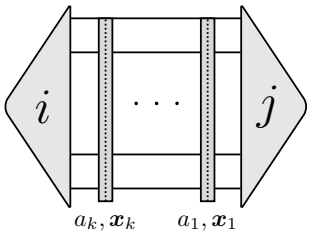

(2.44)

The argument for $\hat{R}_s(Y)$ follows in exactly the same fashion.

This concludes our brief summary of the parameterisation of R. Moerman and H. Weigert and so we move on to the promised discussion of the adjoint color structures.

Chapter 3

New color singlet space calculations

"If I had asked people what they wanted, they would have said 'faster horses.'"

Henry Ford

In the previous chapter, we identified the need to construct a basis for the space of singlets with purely adjoint indices in order to carry out the coincidence limit-preserving finite N_c truncation scheme of R. Moerman and H. Weigert. The purpose of this chapter is to give a detailed explanation of a new method for obtaining a basis for this space and motivate why the basis that we construct here improves upon existing approaches. We apply this method to write down the adjoint color structures for $k = 4$, because this is the highest order in k that is likely to be needed in practical applications in the near future. Throughout the chapter, N_c is kept as a free parameter, so that one can compare to the large N_c/BK limit whenever needed.

The chapter proceeds as follows: in Section 3.1, we define the *color singlet space*, which is significant in that the adjoint color structures form a basis for the subspace of tensors with purely adjoint indices within the color singlet space. In Section 3.2, we introduce the *trace basis*, which is a non-orthogonal basis for this space of tensors with purely adjoint indices and is standard in the literature. After discussing the strengths and weaknesses of the trace basis, Section 3.3 resolves some of these limitations by introducing a new basis for this space based on irreducible representations of the permutation group S_k. We show that this new construction reproduces the existing adjoint color structures used in the $k = 2$ and $k = 3$ cases (eq. (2.31) and eq. (2.32)) and in Section 3.3.3, we present a new basis for the $k = 4$ case using this method. This new approach has its own strengths and limitations which will we remark upon briefly, noting that the method used to perform this calculation falls within a deep mathematical theory of the representations of S_k on the space of tensors with purely adjoint indices. This mathematical theory will be presented in detail in the following chapter, which is a natural setting for a significantly more robust discussion of the properties of the calculations performed in this chapter.

3.1 Color singlet space

The adjoint color structures used in the truncaction presented in the previous chapter live in a vector space that is known as the *color singlet space*, which we now define following the conventions and exposition of [22,28]. Consider the vector space

$$(V \otimes \overline{V})^{\otimes n_q} \otimes A^{\otimes n_g} \tag{3.1a}$$

where

$$V \cong \mathbb{C}^{N_c}, \quad A \cong \mathbb{C}^{N_c^2-1} \tag{3.1b}$$

and $\overline{V}$ is the dual space of V. This space is acted on by (product) representations of $SU(N_c)$ in the following way: each V factor is acted upon by the fundamental representation, each $\overline{V}$ factor is acted upon by the anti-fundamental representation, and each A factor is acted upon by the adjoint representation[1].

Physically, the coordinates of quark (antiquark) fields are elements of V ($\overline{V}$) and the coordinates of gluon fields are elements of A (before complexification). n_q refers to the number of outgoing quarks plus the number of incoming anti-quarks in a scattering process (which is equal to the number of incoming quarks plus outgoing anti-quarks) and n_g refers to the number of incoming plus outgoing gluons [22]. Following convention in the literature, it is standard to refer to subspaces of $(V \otimes \overline{V})^{\otimes n_q} \otimes A^{\otimes n_g}$ that transform under the trivial representation of $SU(N_c)$ as *singlets* and to refer to subspaces that transform under other irreducible representations of $SU(N_c)$ as *multiplets*. QCD color confinement leads us to be specifically interested in subspaces that transform trivially under $SU(N_c)$ (we only observe color neutral objects in in/out states of any scattering experiment), that is the singlets. We call the space of all color singlets the *color singlet space*.

The *adjoint color structures* $\mathcal{C}_m^{a_1 \cdots a_k}$ that appear in the truncation presented in Section 2.3 are elements of the color singlet space. Specifically, they form a basis for the $A^{\otimes k}$ sector of the color singlet space, the space of color singlets within $A^{\otimes k}$, where we substitute the notation $k = n_g$ for the number of gluons to avoid clutter in calculations. We will refer to this sector as the *adjoint color singlet space* and denote the adjoint color singlet space $\mathcal{S}(A^{\otimes k})$.

We also note that $\mathcal{S}(A^{\otimes k})$ inherits an inner product from the canonical $SU(N_c)$ invariant scalar product on V [28]. If $A^{a_1 \cdots a_k}, B^{a_1 \cdots a_k} \in \mathcal{S}(A^{\otimes k})$, then this inherited inner product on $\mathcal{S}(A^{\otimes k})$ is given by

$$\langle A^{a_1 \cdots a_k}, B^{a_1 \cdots a_k} \rangle := \sum_{a_1, \ldots, a_k} \overline{A^{a_1 \cdots a_k}} B^{a_1 \cdots a_k} \tag{3.2}$$

where the overline denotes complex conjugation. One of our primary goals is to obtain a canonical orthogonal basis for the adjoint color singlet space, with orthogonality being with respect to this inner product.

[1] Note that the Lie algebra of $SU(N_c)$ is a real vector space and so the adjoint representation acts on a real vector space. In taking the adjoint representation to act on $\mathbb{C}^{N_c^2-1}$, it's implied that we've complexified the Lie algebra, $\mathfrak{su}(N_c) \otimes \mathbb{C} \cong \mathfrak{sl}(N_c, \mathbb{C})$, as is commonly done.

3.2 The trace basis

Given the adjoint color singlet space on k indices, one basis of interest is the so-called *trace basis*. The trace basis is formed from all possible k-index products of traces of products of $\mathfrak{su}(N_c)$ generators. For clarity, the trace basis for $k = 2, 3, 4$ is given below

$$k = 2 : \{\mathrm{tr}(t^{a_1}t^{a_2})\} \tag{3.3a}$$
$$k = 3 : \{\mathrm{tr}(t^{a_1}t^{a_2}t^{a_3}),\ \mathrm{tr}(t^{a_1}t^{a_3}t^{a_2})\} \tag{3.3b}$$
$$k = 4 : \{\mathrm{tr}(t^{a_1}t^{a_2}t^{a_3}t^{a_4}),\ \mathrm{tr}(t^{a_1}t^{a_3}t^{a_2}t^{a_4}),\ \mathrm{tr}(t^{a_1}t^{a_2}t^{a_4}t^{a_3}) \tag{3.3c}$$
$$\mathrm{tr}(t^{a_1}t^{a_3}t^{a_4}t^{a_2}),\ \mathrm{tr}(t^{a_1}t^{a_4}t^{a_2}t^{a_3}),\ \mathrm{tr}(t^{a_1}t^{a_4}t^{a_3}t^{a_2}), \tag{3.3d}$$
$$\mathrm{tr}(t^{a_1}t^{a_2})\,\mathrm{tr}(t^{a_3}t^{a_4}),\ \mathrm{tr}(t^{a_1}t^{a_3})\,\mathrm{tr}(t^{a_2}t^{a_4}),\ \mathrm{tr}(t^{a_1}t^{a_4})\,\mathrm{tr}(t^{a_2}t^{a_3})\} \tag{3.3e}$$

$k = 1$ does not appear in the above list, because the generators of $\mathfrak{su}(N_c)$ are traceless and so for $k = 1$, $\dim(\mathcal{S}(A)) = 0$ (obviously - the adjoint representation is a nontrivial irreducible representation and so has no singlet subspaces). Notice also that the trace basis for $k \geq 2$ has strictly fewer elements than the $k!$ possible way to permute k indices.

In fact, a major advantage of using the trace basis is that it gives us a practical formula for the dimension of the adjoint color singlet space. To see this, notice that if we choose to forget any additional structure other than the cyclicity of the trace, there is an isomorphism between trace basis elements for a given value of k and elements of S_k that have no *fixed points* and this isomorphism is defined according to cycle type. Some examples of this correspondence are given below

$$\mathrm{tr}(t^at^bt^c) \iff (123), \quad \mathrm{tr}(t^at^ct^b) \iff (132), \tag{3.4a}$$
$$\mathrm{tr}(t^at^bt^ct^d) \iff (1234), \quad \mathrm{tr}(t^at^b)\,\mathrm{tr}(t^ct^d) \iff (12)(34) \tag{3.4b}$$

In contrast, $(123)(4)$ cannot be represented in the trace basis, because the presence of a fixed point produces a zero when we consider the corresponding object $\mathrm{tr}(t^at^bt^c)\,\mathrm{tr}(t^d)$, because the generators of $\mathfrak{su}(N_c)$ are traceless.

The elements of S_k that have no fixed points are known as *derangements*. The number of derangements as a function of k is given by the *subfactorial* function and denoted $!k$. Then naively we have that the dimension of the adjoint color singlet space is given by the subfactorial [22, Sec. 1.2] and thus $\dim(\mathcal{S}(A^{\otimes k}))$ is given by the following combinatorial formula [29, pg. 67]:

$$\dim(\mathcal{S}(A^{\otimes k})) = !k := k! \sum_{j=0}^{n} \frac{(-1)^j}{j!} \tag{3.5a}$$
$$= \left[\frac{k!}{e}\right] \tag{3.5b}$$

where $[\,]$ denotes the "nearest integer" function and e is the base of the natural logarithm. Equation (3.5) gives $\dim(\mathcal{S}(A^{\otimes 3})) = 2$ and $\dim(\mathcal{S}(A^{\otimes 4})) = 9$ as expected from us explicitly writing out the trace basis earlier. However, the dimension of $\mathcal{S}(A^{\otimes k})$ is actually N_c-dependent in the sense that some of the trace basis elements become linearly dependent for various values of N_c.

In particular, eq. (3.5) only holds for $N_c \geq k$ [22], because there exist special $SU(N_c)$ identities that create linear dependencies whenever $k = N_c + 1$ [30].

Despite giving us a well-understood formula for the dimension of the adjoint color singlet space, **the trace basis is unsuitable for our purposes.** The major hindrances are:

Desirable properties that are not present in the trace basis

- The trace basis is not orthogonal with respect to the inner product in eq. (3.2) when $k > 2$. One option is of course to apply Gram-Schmidt orthogonalisation, although this can be undesirable as it and other similar orthogonalisation methods are somewhat arbitrary in terms of the vectors we select at each step in the procedure.
- The aforementioned N_c-dependence of the trace basis is not immediately obvious.

As we will see in the next section, the trace basis *will* be useful in helping us construct a canonical basis that takes major steps towards resolving both of the above issues.

3.3 Hermitian Young projection operator basis

In this section we construct a basis for the adjoint color singlet space that *nearly* captures the properties that we've said are desirable in the previous section. Despite falling short of our ultimate goal, we nonetheless feel that this method has made significant strides towards a resolution of this problem, with the final details being hopefully resolved by future research. We first outline this method, then give examples of this construction and further observations in later subsections.

Our starting point is to examine the adjoint color structures that were used in the Gaussian truncation [19, 20] and in the $k = 3$ generalisation of the Gaussian truncation [20, 21], so that we can develop the pattern that leads to a construction for all k. Here δ^{ab} formed a basis for $\mathcal{S}(A^{\otimes 2})$ (the space of singlets in $A^{\otimes 2}$), and the totally symmetric and totally antisymmetric symbols d^{abc} and if^{abc} formed a basis for $\mathcal{S}(A^{\otimes 3})$. The key insight is that each of these adjoint colour structures forms a basis for an irreducible representation of S_2 and S_3, respectively. This is somewhat unsurprising, because by permuting tensorial indices, we always have a representation of S_k on $\mathcal{S}(A^{\otimes k})$, which can be decomposed into irreducible representations.

Furthermore, methods are known [2] for constructing a set of orthogonal projections onto irreducible representations of $SU(N_c)$ in a decomposition of the k-fold tensor product of the fundamental representation of $SU(N_c)$ acting on $V^{\otimes k}$. These projection operators are elements of the group algebra of S_k (commonly denoted $\mathbb{C}[S_k]$) and by Schur-Weyl duality, the set of projection operators that project onto isomorphic copies of a given irreducible representation of $SU(N_c)$ form a basis for a single irreducible representation of S_k. Since these projection operators are orthogonal with respect to the inner product on the adjoint color singlet space (eq. (3.2)), one then has an orthogonal basis for $\mathbb{C}[S_k]$.

Then, towards our goal: one hopes that all that is necessary to obtain an orthogonal basis for the adjoint color singlet space is to act with these orthogonal projection operators on some other basis for $\mathcal{S}(A^{\otimes k})$ (for example the trace basis). We will see that δ^{ab} arises in this fashion when $k = 2$, as do the d^{abc} and if^{abc} symbols when $k = 3$. However, when $k = 4$, we will see that the basis that we construct in this manner fails to be fully orthogonal. We will briefly comment on why this occurs and on the strengths of using this basis nonetheless. This leads us to ultimately suggest that a simple repair using Gram-Schmidt orthogonalisation can be done with the few basis elements that fail to be orthogonal, until a full resolution is obtained. In fact, the full explanation of why orthogonality fails (and our suggestion for possible future research on a more satisfying resolution) is somewhat subtle and better explained with more advanced machinery in the next chapter.

3.3.1 Outline of the construction

Let's sketch how all of this works. The standard approach in the literature to organising information on irreducible representations of S_k and $SU(N_c)$ (and in particular on the projection operators that we're interested in) is to use the theory of *Young diagrams* and *Young tableaux*. A Young diagram associated with S_k is a collection of k boxes, left-aligned so that the number of boxes in a row is (not necessarily strictly) decreasing from top to bottom[1]. So for example the following are all Young diagrams:

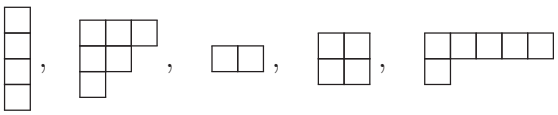

(3.6a)

whereas these are *not* Young diagrams:

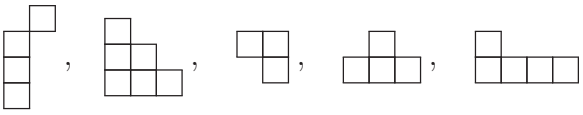

(3.6b)

A *standard Young tableau* is a Young diagram with k boxes and a number written in each box so that the numbers $1, 2, \ldots, k$ appear exactly once, with the numbers increasing both from left to right along rows and from top to bottom down columns. So these are standard Young tableaux:

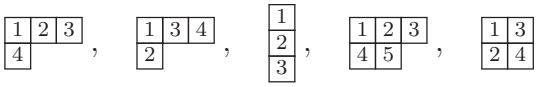

(3.7a)

while these are *not* standard tableaux:

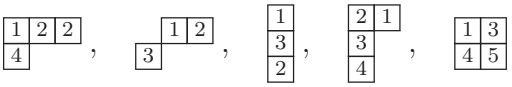

(3.7b)

By the above examples, we also note that there can be more than one standard tableau associated with a given Young diagram.

[1] In the French convention, the number of boxes in a row is (not necessarily strictly) decreasing from bottom to top. We instead use the English convention, which is common internationally.

In fact, it is a standard result in representation theory that the number of irreducible representations of S_k is equal to the number of Young diagrams with k boxes and that the dimension of each irreducible representation of S_k is equal to the number of standard tableaux associated with that irreducible representation's Young diagram (see [31]). So for example there are exactly two possible standard tableaux associated with the diagram $\square\!\square$:

$$\begin{array}{|c|c|}\hline 1&2\\\hline 3&4\\\hline\end{array}\,,\quad \begin{array}{|c|c|}\hline 1&3\\\hline 2&4\\\hline\end{array} \tag{3.8a}$$

while there are exactly three possible standard tableaux associated with the diagram $\begin{array}{|c|c|}\hline\multicolumn{1}{c}{}&\multicolumn{1}{c}{}\\\hline\multicolumn{1}{|c|}{}&\multicolumn{1}{c|}{}\\\hline\end{array}$:

$$\begin{array}{|c|c|c|}\hline 1&2&3\\\hline 4\\\cline{1-1}\end{array}\,,\quad \begin{array}{|c|c|c|}\hline 1&2&4\\\hline 3\\\cline{1-1}\end{array}\,,\quad \begin{array}{|c|c|c|}\hline 1&3&4\\\hline 2\\\cline{1-1}\end{array} \tag{3.8b}$$

and only one possible standard tableaux associated with the diagram $\square\square\square\square\square$:

$$\begin{array}{|c|c|c|c|c|}\hline 1&2&3&4&5\\\hline\end{array} \tag{3.8c}$$

and so we have (slightly abusing notation):

$$\dim\left(\begin{array}{|c|c|}\hline\multicolumn{1}{c}{}&\multicolumn{1}{c}{}\\\hline\multicolumn{1}{|c|}{}&\multicolumn{1}{c|}{}\\\hline\end{array}\right)=2,\quad \dim\left(\begin{array}{|c|c|c|}\hline\multicolumn{1}{c}{}&\multicolumn{1}{c}{}&\multicolumn{1}{c}{}\\\hline\multicolumn{1}{|c|}{}\\\cline{1-1}\end{array}\right)=3,\quad \dim\left(\begin{array}{|c|c|c|c|c|}\hline\multicolumn{1}{c}{}&\multicolumn{1}{c}{}&\multicolumn{1}{c}{}&\multicolumn{1}{c}{}&\multicolumn{1}{c}{}\\\hline\end{array}\right)=1 \tag{3.8d}$$

Furthermore, if λ is a Young diagram with k boxes, then corresponding to the irreducible representation of S_k associated with λ, there are $\dim(\lambda)$ isomorphic copies of a single distinct irreducible representation of $SU(N_c)$ in a decomposition of the k-fold tensor product of the fundamental representation of $SU(N_c)$ acting on $V^{\otimes k}$. In other words, the set of standard tableaux with k boxes is in one-to-one correspondence with the irreducible representations of $SU(N_c)$ that appear in this decomposition. This correspondence is known as *Schur-Weyl duality*.

In [2–4] a method was given for constructing what were referred to as Hermitian Young projection operators[1], which are elements of the group algebra $\mathbb{C}[S_k]$ and form a complete set of orthogonal projections onto the irreducible representations of $SU(N_c)$ on $V^{\otimes k}$. These operators obey the following properties:

[1]We could use any alternative orthogonal basis for irreducible $\mathbb{C}[S_k]$-modules, such as the basis constructed earlier in [32]. The choice to use the basis constructed by Alcock-Zeilinger and Weigert is motivated by the consideration that this seems to be the simplest basis with these properties that has been constructed thus far in the literature.

Properties of the Hermitian Young projection operators

- Decompostition of unity

$$\mathbb{1}^{\otimes k} = \sum_i P_i \tag{3.9}$$

- Transversality (Keppeler and Sjödahl's terminology [32])

$$P_i P_j = \delta_{ij} P_j, \quad \forall i, j \tag{3.10}$$

- Hermiticity

$$P_i^\dagger = P_i, \quad \forall i \tag{3.11}$$

where hermiticity in this context is defined with respect to the inner product on the adjoint color singlet space (eq. (3.2)) and refers to applying the transformation to $g \in \mathbb{C}[S_k]$

$$g = \sum_{i=1}^{k!} c_i g_i \overset{\dagger}{\mapsto} \sum_{i=1}^{k!} c_i^* g_i^{-1} \tag{3.12}$$

or equivalently, if we represent g in Birdtracks (Appendix A), then the diagram of $g^\dagger$ is given by reflecting the diagram of g across its vertical axis and reversing the direction of all arrows.

With respect to the inner product on the adjoint color singlet space (eq. (3.2)), transversality and hermiticity together mean that for any $v, w \in \mathcal{S}(A^{\otimes k})$

$$\langle P_i v, P_j w \rangle = v^\dagger P_i P_j w = \delta_{ij} v^\dagger P_i w \tag{3.13}$$

This means that we can uniquely (up to isomorphism) assign one of these Hermitian Young projection operators to each standard Young tableaux with k boxes. Then if we act with these operators on an arbitrary vector in $\mathcal{S}(A^{\otimes k})$, we're guaranteed to project onto a basis that is orthogonal with respect to this inner product, at least as long as each basis element is associated with a *different* irreducible representation of $SU(N_c)$ (or equivalently with a different standard Young tableau).

Before showing some examples, a final comment is in order. We know that the Hermitian Young projection operators are each associated to a standard Young tableaux, each of which is in turn associated with an irreducible representation of $SU(N_c)$ on $V^{\otimes k}$ (where each factor V is acted on by a copy of the fundamental representation). Then one might wonder what the relevance of the Hermitian Young projection operators is when we are actually interested in irreducible representations of S_k (or possibly $SU(N_c)$) on $\mathcal{S}(A^{\otimes k})$ and not $V^{\otimes k}$. The point is that, as mentioned earlier, the classical correspondence between irreducible representations of S_k and irreducible representations of $SU(N_c)$ known as Schur-Weyl duality tells us that the Hermitian Young projection operators project onto irreducible representations of $SU(N_c)$ on $V^{\otimes k}$.

Furthermore, these projection operators correspond to a full decomposition of the group algebra $\mathbb{C}[S_k]$ into irreducible representations of S_k. Since it is a standard result in representation theory that *every* irreducible representation of S_k appears in this decomposition [33, Sec. 3.7], then because we can always define a representation of S_k on $\mathcal{S}(A^{\otimes k})$ (by permuting indices in the tensor product), if we decompose $\mathcal{S}(A^{\otimes k})$ into irreducible representations of S_k, we can always associate each of the irreducible representations of S_k appearing in this decomposition with a Young diagram, which is in turn associated with the list of Hermitian Young projection operators that correspond to each standard tableaux associated with this Young diagram. The key difference between the case of irreducible representations of S_k on $\mathcal{S}(A^{\otimes k})$ and irreducible representations of S_k on $V^{\otimes k}$ is that in the case of $\mathcal{S}(A^{\otimes k})$, not every Young diagram appears in the decomposition - in other words, some of the Hermitian Young projection operators return a zero when acting on $\mathcal{S}(A^{\otimes k})$ (we'll see this explicitly in the next section). To make things more clear, we display this line of reasoning in Figure 3.1:

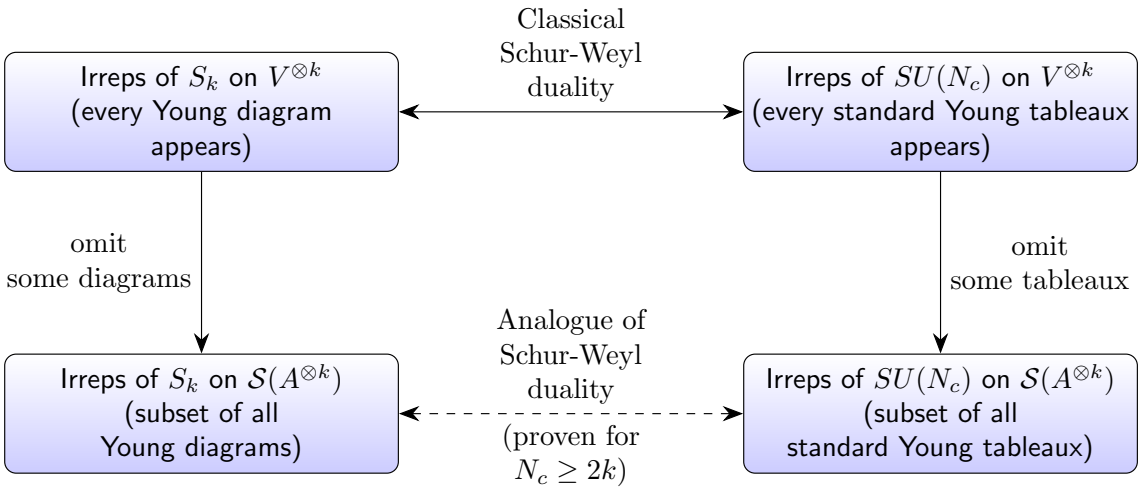

FIGURE 3.1: Flow chart explaining how Schur-Weyl duality connects the Hermitian Young projection operators and irreducible representations of $SU(N_c)$ on $V^{\otimes k}$ to irreducible representations of S_k on $\mathcal{S}(A^{\otimes k})$ (the adjoint color singlet space).

One might ask why we do not directly describe our construction in terms of irreducible representations of $SU(N_c)$ on $\mathcal{S}(A^{\otimes k})$, using the analogue of Schur-Weyl duality that is alluded to in Figure 3.1? The issue is that in seeking a proof of this analogue of Schur-Weyl duality, we have only found a proof in the literature that holds for $N_c \geq 2k$ [34, Sec. 4], whereas as explained earlier, we wish to work with $N_c \geq k$ or even arbitrary N_c. The authors of [34] do remark that this form of Schur-Weyl duality "will almost certainly hold for all N_c, k," but we have not yet shown this. So, for the time being, we take the point of view that we can completely circumvent proving that Schur-Weyl duality holds for $\mathcal{S}(A^{\otimes k})$ for all N_c by working solely with irreducible representations of S_k on $\mathcal{S}(A^{\otimes k})$, and we can still use the Hermitian Young projection operators via the motivation given in Figure 3.1. Henceforth, we shall continually refer to irreducible representations of S_k on the adjoint color singlet space and shall not return to this issue.

3.3.2 Hermitian Young projectors applied to the trace basis for $k = 2, 3$

Let's see how our construction works with some examples. Throughout this section we will make use of Birdtracks, which are defined in Appendix A (see also [35] for a standard reference). The diagrams for the Hermitian Young projection operators used in this section are taken (with permission) from [4] and can all be found in Figure 3 of that paper.

When $k = 2$, the Hermitian Young projectors associated with each irreducible representation of $SU(N_c)$ on $V \otimes V$ (equivalently: associated with each standard tableau with 2 boxes) are

$P_{\ytableaushort{12}} =$  , $P_{\ytableaushort{1,2}} =$  (3.14)

The trace basis for $k = 2$ has only one element $\mathrm{tr}(t^{a_1}t^{a_2})$ and so is of course already orthogonal. We calculate the action of the Hermitian Young projections on the indices of this single element:

$$P_{\ytableaushort{12}}\,\mathrm{tr}(t^{a_1}t^{a_2}) = \frac{1}{2}\big(\mathrm{tr}(t^{a_1}t^{a_2}) + \mathrm{tr}(t^{a_2}t^{a_1})\big) \tag{3.15a}$$

$$= \mathrm{tr}(t^{a_1}t^{a_2}) \tag{3.15b}$$

$$P_{\ytableaushort{1,2}}\,\mathrm{tr}(t^{a_1}t^{a_2}) = \frac{1}{2}\big(\mathrm{tr}(t^{a_1}t^{a_2}) - \mathrm{tr}(t^{a_2}t^{a_1})\big) \tag{3.15c}$$

$$= 0 \tag{3.15d}$$

So, using $\mathrm{tr}(t^{a_1}t^{a_2}) = \frac{1}{2}\delta^{a_1a_2}$, the only adjoint color structure that we have in this case is

$$\mathcal{C}_1^{a_1a_2} := \delta^{a_1a_2} \tag{3.16}$$

This is precisely the adjoint color structure used in the Gaussian truncation [19,20].

When $k = 3$ there are 3 different Young diagrams with 3 boxes and 4 standard tableaux in total. The associated Hermitian Young projection operators are:

$P_{\ytableaushort{123}} =$  (3.17a)

$P_{\ytableaushort{12,3}} = \frac{4}{3}$ 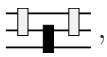 , $P_{\ytableaushort{13,2}} = \frac{4}{3}$  (3.17b)

$P_{\ytableaushort{1,2,3}} =$  (3.17c)

Let $v = c_1 \operatorname{tr}(t^{a_1} t^{a_2} t^{a_3}) + c_2 \operatorname{tr}(t^{a_2} t^{a_1} t^{a_3})$ be an arbitrary element of $\mathcal{S}(A^{\otimes 3})$ with respect to the trace basis. Then the result of projecting v with the Hermitian Young operators is

$$P_{\begin{array}{|c|c|c|}\hline 1&2&3\\\hline\end{array}}\, v = \left(\frac{c_1+c_2}{2}\right)\big(\operatorname{tr}(t^{a_1}t^{a_2}t^{a_3}) + \operatorname{tr}(t^{a_2}t^{a_1}t^{a_3})\big) \tag{3.18a}$$

$$= \left(\frac{c_1+c_2}{4}\right) d^{a_1a_2a_3} \tag{3.18b}$$

$$P_{\begin{array}{|c|c|}\hline 1&2\\\hline 3\\\cline{1-1}\end{array}}\, v = 0, \qquad P_{\begin{array}{|c|c|}\hline 1&3\\\hline 2\\\cline{1-1}\end{array}}\, v = 0 \tag{3.18c}$$

$$P_{\begin{array}{|c|}\hline 1\\\hline 2\\\hline 3\\\hline\end{array}}\, v = \left(\frac{c_1-c_2}{2}\right)\big(\operatorname{tr}(t^{a_1}t^{a_2}t^{a_3}) - \operatorname{tr}(t^{a_2}t^{a_1}t^{a_3})\big) \tag{3.18d}$$

$$= \left(\frac{c_1-c_2}{4}\right) i f^{a_1a_2a_3} \tag{3.18e}$$

where both projections of v associated with the diagram $\begin{array}{|c|c|}\hline\multicolumn{2}{|c|}{}\\\hline&\\\hline\end{array}$ vanish because of the cyclicity of the trace. Then we have found the adjoint color structures

$$\mathcal{C}_1^{a_1a_2a_3} := d^{a_1a_2a_3}, \quad \mathcal{C}_2^{a_1a_2a_3} := i f^{a_1a_2a_3} \tag{3.19}$$

Notice that the d^{abc} and if^{abc} symbols are guaranteed to be orthogonal with respect to the inner product on the adjoint color singlet space because they resulted from different Hermitian Young projection operators and so they provide an orthogonal basis for $\mathcal{S}(A^{\otimes 3})$, defined in a canonical way. Furthermore, this basis directly demonstrates the N_c-dependence of $\mathcal{S}(A^{\otimes 3})$, because the d^{abc} symbol vanishes for $N_c = 1, 2$. This would have been otherwise more difficult to anticipate using the trace basis.

In the context of JIMWLK truncations, the basis using the d^{abc} and if^{abc} symbols was suggested in [20, Sec. 6] and was employed in [21] and we see now that these choices were not a coincidence: these adjoint color structures are a direct result of the decomposition of $\mathcal{S}(A^{\otimes 3})$ into irreducible representations and can be obtained by projecting onto these representations using a complete set of orthogonal projection operators.

3.3.3 New calculation: Hermitian Young projection operator basis, $k = 4$

When $k = 4$, we have the following Hermitian Young projection operators[1]

$P_{\ydiagram{4}} =$  (3.20a)

$P_{\ydiagram{3,1}} = \frac{3}{2}$ 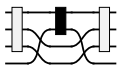 , $P_{\ydiagram{3,1}} = 2$ 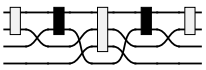 , $P_{\ydiagram{3,1}} = \frac{3}{2}$ 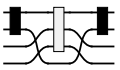 (3.20b)

$P_{\ydiagram{2,2}} = \frac{4}{3}$ 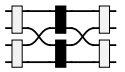 , $P_{\ydiagram{2,2}} = \frac{4}{3}$ 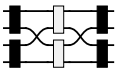 (3.20c)

$P_{\ydiagram{2,1,1}} = \frac{3}{2}$ 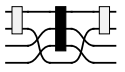 , $P_{\ydiagram{2,1,1}} = 2$ 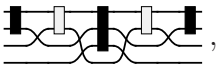 , $P_{\ydiagram{2,1,1}} = \frac{3}{2}$ 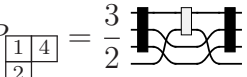 (3.20d)

$P_{\ydiagram{1,1,1,1}} =$  (3.20e)

Then if $v = \sum_i c_i v_i$ is an arbitrary element of $\mathcal{S}(A^{\otimes 4})$ with respect to the trace basis, we have the following projections, where we have rewritten traces in terms of the $\delta^{ab}, d^{abc}, if^{abc}$ symbols (repeated indices are summed over):

[1] Again, see Appendix A or [35] for an introduction to the diagrammatic notation used here.

$$P_{\begin{array}{|c|c|c|c|}\hline 1&2&3&4\\\hline\end{array}}\, v = \tilde{c}_1\Big(d^{a_1a_4m}d^{a_2a_3m} + d^{a_1a_3m}d^{a_2a_4m} + d^{a_1a_2m}d^{a_3a_4m}\Big) \tag{3.21a}$$

$$+ \tilde{c}_2\Big(\delta^{a_1a_4}\delta^{a_2a_3} + \delta^{a_1a_3}\delta^{a_2a_4} + \delta^{a_1a_2}\delta^{a_3a_4}\Big) \tag{3.21b}$$

$$P_{\begin{array}{|c|c|c|}\hline 1&2&3\\\hline 4\\\cline{1-1}\end{array}}\, v = 0, \quad P_{\begin{array}{|c|c|c|}\hline 1&2&4\\\hline 3\\\cline{1-1}\end{array}}\, v = 0, \quad P_{\begin{array}{|c|c|c|}\hline 1&3&4\\\hline 2\\\cline{1-1}\end{array}}\, v = 0 \tag{3.21c}$$

$$P_{\begin{array}{|c|c|}\hline 1&2\\\hline 3&4\\\hline\end{array}}\, v = \tilde{c}_3\Big(- d^{a_1a_4m}d^{a_2a_3m} - d^{a_1a_3m}d^{a_2a_4m} + 2d^{a_1a_2m}d^{a_3a_4m}\Big) \tag{3.21d}$$

$$- \tilde{c}_4\Big(\delta^{a_1a_4}\delta^{a_2a_3} + \delta^{a_1a_3}\delta^{a_2a_4} - 2\delta^{a_1a_2}\delta^{a_3a_4}\Big) \tag{3.21e}$$

$$P_{\begin{array}{|c|c|}\hline 1&3\\\hline 2&4\\\hline\end{array}}\, v = \tilde{c}_5\Big(d^{a_1a_4m}d^{a_2a_3m} - d^{a_1a_3m}d^{a_2a_4m}\Big) \tag{3.21f}$$

$$+ \tilde{c}_6\Big(\delta^{a_1a_4}\delta^{a_2a_3} - \delta^{a_1a_3}\delta^{a_2a_4}\Big) \tag{3.21g}$$

$$P_{\begin{array}{|c|c|}\hline 1&2\\\hline 3\\\cline{1-1}4\\\cline{1-1}\end{array}}\, v = \tilde{c}_7\Big(d^{a_2a_4m}if^{a_1a_3m} - d^{a_2a_3m}if^{a_1a_4m} + d^{a_1a_4m}if^{a_2a_3m} - d^{a_1a_3m}if^{a_2a_4m} \tag{3.21h}$$

$$+ 2d^{a_1a_2m}if^{a_3a_4m}\Big) \tag{3.21i}$$

$$P_{\begin{array}{|c|c|}\hline 1&3\\\hline 2\\\cline{1-1}4\\\cline{1-1}\end{array}}\, v = \tilde{c}_8\Big(2d^{a_3a_4m}if^{a_1a_2m} + d^{a_2a_4m}if^{a_1a_3m} - 3d^{a_2a_3m}if^{a_1a_4m} - d^{a_1a_4m}if^{a_2a_3m} \tag{3.21j}$$

$$+ 3d^{a_1a_3m}if^{a_2a_4m}\Big) \tag{3.21k}$$

$$P_{\begin{array}{|c|c|}\hline 1&4\\\hline 2\\\cline{1-1}3\\\cline{1-1}\end{array}}\, v = \tilde{c}_9\Big(d^{a_3a_4m}if^{a_1a_2m} - d^{a_2a_4m}if^{a_1a_3m} + d^{a_1a_4m}if^{a_2a_3m}\Big) \tag{3.21l}$$

$$P_{\begin{array}{|c|}\hline 1\\\hline 2\\\hline 3\\\hline 4\\\hline\end{array}}\, v = 0 \tag{3.21m}$$

The relationship between the coefficients $\tilde{c}_i$ and c_i is relatively unimportant, as in any practical application we would normalise each basis element, although for completeness this relationship is given in Appendix B.1. Notice that again some of the projections vanish, because of the cyclicity of the trace. In addition to this, a new feature emerges at $k = 4$: some of the Hermitian Young projection operators project v onto 2-dimensional subspaces. This information is summarised in the following table:

0-dimensional subspaces	$P_{\begin{array}{|c|c|c|}\hline 1&2&3\\\hline\end{array}\!\!\begin{array}{|c|}\hline 4\\\hline\end{array}} v, \quad P_{\begin{array}{|c|c|c|}\hline 1&2&4\\\hline\end{array}\!\!\begin{array}{|c|}\hline 3\\\hline\end{array}} v, \quad P_{\begin{array}{|c|c|c|}\hline 1&3&4\\\hline\end{array}\!\!\begin{array}{|c|}\hline 2\\\hline\end{array}} v$
1-dimensional subspaces	$P_{\begin{array}{|c|c|}\hline 1&2\\\hline\end{array}\!\!\begin{array}{|c|}\hline 3\\\hline\end{array}\!\!\begin{array}{|c|}\hline 4\\\hline\end{array}} v, \quad P_{\begin{array}{|c|c|}\hline 1&3\\\hline\end{array}\!\!\begin{array}{|c|}\hline 2\\\hline\end{array}\!\!\begin{array}{|c|}\hline 4\\\hline\end{array}} v, \quad P_{\begin{array}{|c|c|}\hline 1&4\\\hline\end{array}\!\!\begin{array}{|c|}\hline 2\\\hline\end{array}\!\!\begin{array}{|c|}\hline 3\\\hline\end{array}} v$
2-dimensional subspaces	$P_{\begin{array}{|c|c|c|c|}\hline 1&2&3&4\\\hline\end{array}} v, \quad P_{\begin{array}{|c|c|}\hline 1&3\\\hline\end{array}\!\!\begin{array}{|c|c|}\hline 2&4\\\hline\end{array}} v, \quad P_{\begin{array}{|c|c|}\hline 1&2\\\hline\end{array}\!\!\begin{array}{|c|c|}\hline 3&4\\\hline\end{array}} v$

TABLE 3.1: Dimensions of the subspaces of the adjoint color singlet space that the Hermitian Young projection operators project onto when $k = 4$

One confirms that the sum of the dimensions of the subspaces listed in Table 3.1 is 9, in agreement with the trace basis count at $k = 4$. Altogether, the projections in eq. (3.21) show that we have found the following adjoint color structures:

$$\mathcal{C}_1^{a_1a_2a_3a_4} := d^{a_1a_4m}d^{a_2a_3m} + d^{a_1a_3m}d^{a_2a_4m} + d^{a_1a_2m}d^{a_3a_4m} \tag{3.22a}$$
$$\mathcal{C}_2^{a_1a_2a_3a_4} := \delta^{a_1a_4}\delta^{a_2a_3} + \delta^{a_1a_3}\delta^{a_2a_4} + \delta^{a_1a_2}\delta^{a_3a_4} \tag{3.22b}$$
$$\mathcal{C}_3^{a_1a_2a_3a_4} := -d^{a_1a_4m}d^{a_2a_3m} - d^{a_1a_3m}d^{a_2a_4m} + 2d^{a_1a_2m}d^{a_3a_4m} \tag{3.22c}$$
$$\mathcal{C}_4^{a_1a_2a_3a_4} := \delta^{a_1a_4}\delta^{a_2a_3} + \delta^{a_1a_3}\delta^{a_2a_4} - 2\delta^{a_1a_2}\delta^{a_3a_4} \tag{3.22d}$$
$$\mathcal{C}_5^{a_1a_2a_3a_4} := d^{a_1a_4m}d^{a_2a_3m} - d^{a_1a_3m}d^{a_2a_4m} \tag{3.22e}$$
$$\mathcal{C}_6^{a_1a_2a_3a_4} := \delta^{a_1a_4}\delta^{a_2a_3} - \delta^{a_1a_3}\delta^{a_2a_4} \tag{3.22f}$$
$$\mathcal{C}_7^{a_1a_2a_3a_4} := d^{a_2a_4m}if^{a_1a_3m} - d^{a_2a_3m}if^{a_1a_4m} + d^{a_1a_4m}if^{a_2a_3m} - d^{a_1a_3m}if^{a_2a_4m} \tag{3.22g}$$
$$+ 2d^{a_1a_2m}if^{a_3a_4m} \tag{3.22h}$$
$$\mathcal{C}_8^{a_1a_2a_3a_4} := 2d^{a_3a_4m}if^{a_1a_2m} + d^{a_2a_4m}if^{a_1a_3m} - 3d^{a_2a_3m}if^{a_1a_4m} - d^{a_1a_4m}if^{a_2a_3m} \tag{3.22i}$$
$$+ 3d^{a_1a_3m}if^{a_2a_4m} \tag{3.22j}$$
$$\mathcal{C}_9^{a_1a_2a_3a_4} := d^{a_3a_4m}if^{a_1a_2m} - d^{a_2a_4m}if^{a_1a_3m} + d^{a_1a_4m}if^{a_2a_3m} \tag{3.22k}$$

where the normalisation for these adjoint color structures is displayed in Appendix B.1. We'll see later that the adjoint color structures in eq. (3.22) correspond to decomposing $\mathcal{S}(A^{\otimes 4})$ into irreducible representations of S_4. Since each irreducible representation of S_4 can be uniquely (up to isomorphism) associated with a Young diagram with 4 boxes, we denote the irreducible subspace of $\mathcal{S}(A^{\otimes k})$ associated with a Young diagram λ as $\mathcal{S}^\lambda$ and obtain the decomposition

$$\mathcal{S}(A^{\otimes 4}) \cong 2\,\mathcal{S}^{\begin{array}{|c|c|c|c|}\hline\end{array}} \oplus 2\,\mathcal{S}^{\begin{array}{|c|c|}\hline\end{array}\!\!\begin{array}{|c|c|}\hline\end{array}} \oplus \mathcal{S}^{\begin{array}{|c|}\hline\end{array}\!\!\begin{array}{|c|c|}\hline\end{array}\!\!\begin{array}{|c|}\hline\end{array}} \tag{3.23}$$

where the diagram associated with each irreducible representation is determined by looking at the standard tableau associated with each Hermitian Young projection operator and the prefactors in this decomposition are used to indicate a direct sum of multiple isomorphic copies of a particular irreducible subspace.

Let's review some of the properties of this new basis for $\mathcal{S}(A^{\otimes 4})$. Notice that as already stated, most of these objects are mutually orthogonal. The *exceptions* are

$$\langle \mathcal{C}_1^{a_1a_2a_3a_4}, \mathcal{C}_2^{a_1a_2a_3a_4} \rangle \neq 0, \quad \langle \mathcal{C}_3^{a_1a_2a_3a_4}, \mathcal{C}_4^{a_1a_2a_3a_4} \rangle \neq 0, \quad \langle \mathcal{C}_5^{a_1a_2a_3a_4}, \mathcal{C}_6^{a_1a_2a_3a_4} \rangle \neq 0 \tag{3.24}$$

The point is that each of these pairs of adjoint color structures arise from the *same* Hermitian Young projection operator and so had no chance at being orthogonal given this construction, although each pair is orthogonal to every other basis element (as predicted by eq. (3.13)). In fact, this will occur for all $k > 3$ (we have directly verified this for $k = 5$, although don't display the lengthy calculation here). There is an underlying structure to the representations of S_k that explains this occurrence and possible avenues for future research into resolving this problem, but we postpone this discussion to the next chapter, where we introduce the necessary mathematical machinery in detail. Until this question is resolved, we suggest the use of Gram-Schmidt orthogonalisation (or any other analogous procedure) on non-orthogonal elements within these subspaces.

Next, observe that as promised, the N_c-dependence is manifest in this basis: when $N_c = 2$ the d^{abc} symbols are all zero and so the space becomes 3-dimensional, with only $\mathcal{C}_2^{a_1a_2a_3a_4}, \mathcal{C}_4^{a_1a_2a_3a_4}, \mathcal{C}_6^{a_1a_2a_3a_4}$ surviving. Furthermore, there is a special $SU(N_c)$ identity arising from the characteristic equation of the group that holds only for $N_c = 3$ [30, 36, 37] that becomes relevant:

$$d^{a_1a_4m}d^{a_2a_3m} + d^{a_1a_3m}d^{a_2a_4m} + d^{a_1a_2m}d^{a_3a_4m} \overset{N_c=3}{=} \frac{1}{3}(\delta^{a_1a_4}\delta^{a_2a_3} + \delta^{a_1a_3}\delta^{a_2a_4} + \delta^{a_1a_2}\delta^{a_3a_4}) \tag{3.25}$$

So we see that when $N_c = 3$, the adjoint color singlet space is 8-dimensional (and not 9-dimensional as predicted by the trace basis), because $\mathcal{C}_1^{a_1a_2a_3a_4}$ and $\mathcal{C}_2^{a_1a_2a_3a_4}$ become collinear. In particular, this N_c-dependent collinearity could *only* have happened to elements that arise from the same Hermitian Young projection operator - only elements that are not automatically orthogonal have a chance at becoming collinear for certain values of N_c.

Finally, we can make one additional observation about this basis that wasn't necessarily part of our original goals. On close inspection, we see that when $k \leq 4$ every adjoint color structure is either real or purely imaginary and furthermore, all adjoint color structures that are associated with the same Young diagram share the same attribute: a diagram either has *only* real adjoint color structures associated with it or it has *only* imaginary adjoint color structures associated with it. Explicitly:

	Real	Imaginary	Mixed complex
☐☐☐☐ (d-type)	$\mathcal{C}_1$		
☐☐☐☐ (δ-type)	$\mathcal{C}_2$		
⊞ (d-type)	$\mathcal{C}_3, \mathcal{C}_5$		
⊞ (δ-type)	$\mathcal{C}_4, \mathcal{C}_6$		
⊟		$\mathcal{C}_7, \mathcal{C}_8, \mathcal{C}_9$	

TABLE 3.2: The adjoint color structures at $k = 4$ are all real or purely imaginary, according to their associated Young diagram.

In the next chapter we will prove that for all k, every adjoint color structure obtained in this manner is always real or purely imaginary. Furthermore, we show that we can always determine a priori exactly which color structures will be real and which will be imaginary, according to the irreducible representation of S_k that they are associated with through the Young diagrams, although the exact relationship between real and imaginary adjoint color structures and Young diagrams is more subtle than suggested just by the cases $k \leq 4$. From the cases $k \leq 4$, we might have been tempted to say that it is *only* the Young diagram that determines whether an adjoint color structure is real or purely imaginary, but as we will see in the next chapter, it's unclear that this is true (we have not proven this yet). Rather, it is both the Young diagram, and further underlying structure of S_k that seems to be relevant, which motivates the additional distinction we make in Table 3.2 between δ and d-type adjoint color structures.

3.4 Summary of Chapter 3

In this chapter we've seen that the adjoint color structures used in our new method for obtaining approximate solutions to the JIMWLK equation form a basis for the adjoint color singlet space, which is an inner product space composed of all singlets within the k-fold tensor product of the adjoint representation. We've seen that the trace basis spans the adjoint color singlet space, but is undesirable for use in our approximation primarily because it is not orthogonal, but also because it obscures the N_c-dependence of the adjoint color singlet space. This lead us to the primary topic of this dissertation: a new method for generating bases for the adjoint color singlet space at arbitrary k and N_c, based on irreducible representations of S_k and Hermitian Young projection operators that project onto irreducible representations of $SU(N_c)$. All of this is organised according to Young diagrams and Young tableaux: there is a one-to-one correspondence between irreducible representations of S_k and Young diagrams with k boxes, and standard Young tableaux with k boxes and Hermitian Young projection operators.

We have shown that our new method for generating bases for the adjoint color singlet space always produces a basis that is orthogonal across elements associated with different Hermitian Young projection operators, but orthogonality inevitably fails between elements that result from the same Hermitian Young projection operator. For example, we saw that at $k = 4$

$$\mathcal{C}_3^{a_1a_2a_3a_4} := -d^{a_1a_4m}d^{a_2a_3m} - d^{a_1a_3m}d^{a_2a_4m} + 2d^{a_1a_2m}d^{a_3a_4m} \tag{3.26a}$$

$$\mathcal{C}_4^{a_1a_2a_3a_4} := \delta^{a_1a_4}\delta^{a_2a_3} + \delta^{a_1a_3}\delta^{a_2a_4} - 2\delta^{a_1a_2}\delta^{a_3a_4} \tag{3.26b}$$

both resulted from the Hermitian Young projection operator associated with the standard tableau $\begin{array}{|c|c|}\hline 1 & 2 \\ \hline 3 & 4 \\ \hline \end{array}$ and so $\mathcal{C}_3^{a_1a_2a_3a_4}$ and $\mathcal{C}_4^{a_1a_2a_3a_4}$ are both independently orthogonal to all other basis elements, but are not orthogonal to each other. We've postponed a more detailed discussion of why this happens to the next chapter and have argued that any deviations from orthogonality can be repaired using Gram-Schmidt orthogonalisation until further research definitively resolves this issue in a more natural way.

We've argued for other benefits of using the Hermitian Young projection operator basis. First of all, this basis makes substantial strides towards automatically capturing all N_c-dependence of the adjoint color singlet space. In this basis, we can easily track the appearance of the d^{abc} symbols (which vanish for $N_c = 2$). Furthermore, we saw that at $k = 4$ a well-known identity [30, 36, 37] appears naturally by $\mathcal{C}_1^{a_1a_2a_3a_4}$ and $\mathcal{C}_2^{a_1a_2a_3a_4}$ becoming collinear at $N_c = 3$ and have noted that similar identities that hold for higher k [30, 37] are constrained by our construction to only relate basis elements resulting from the same Hermitian Young projection operator (because only elements that are not automatically orthogonal have a chance of becoming collinear for certain values of N_c). Lastly, while this wasn't a goal stated when we outlined our truncation scheme in the previous chapter, it turns out that the Hermitian Young projection operator basis always has basis elements that are real or purely imaginary and the type of the basis element can be determined before performing any projections using representation-theoretic methods that are discussed in the next chapter.

We've ultimately aimed to introduce this construction by example and direct calculation, with the specific intent of producing a useful basis for $\mathcal{S}(A^{\otimes 4})$, as this is the highest order in k that is of practical significance to our truncation scheme in the near future. However, everything discussed in this chapter can be understood within a more abstract mathematical framework that reveals special structures and properties of this construction for arbitrary k. This framework is the topic of the next chapter.

Chapter 4

Tricks from representation theory teach us more about the Hermitian Young projection operator basis

"Your math is great, but your physics is dismal."

Einstein (to Georges Lemaître)

In the previous chapter we learned several important properties of the adjoint color singlet space and our basis obtained using the Hermitian Young projection operators:

Important results from the previous chapter

- We can select a basis for the adjoint color singlet space by combining information about the irreducible representations of S_k with what is already known about color singlets from the trace basis. It is unsurprising that this seems to be a "natural" approach, because we tend to think of irreducible representations as the fundamental "building blocks" of any representation and in physics we often aim to decompose objects according to their underlying symmetries.
- For a given value of k, some irreducible representations *do not* appear in a decomposition of the adjoint color singlet space (for example, if we examine Equation (3.18), none of the elements of the Hermitian Young projection operator basis for $\mathcal{S}(A^{\otimes 3})$ correspond to the irreducible representation associated with the Young diagram $\begin{array}{|c|c|}\hline \multicolumn{1}{|c}{} \\ \hline \end{array}$).
- In the Hermitian Young projection operator basis, all subspaces corresponding to each Hermitian Young projection operator are mutually orthogonal. However, if a subspace has dimension greater than one, then the basis elements spanning this subspace need not be orthogonal to each other.

Then, one might ask: is there is a more systematic way to carry out this decomposition? We will show in this chapter that the answer to this question is yes.

Furthermore, the methods of this chapter will shed light on other properties of the Hermitian Young projection operator basis. We will see that the failures of orthogonality that were noticed in the previous chapter are intimately related to underlying

symmetries of the adjoint color singlet space under subgroups of S_k, and that we can systematically classify these symmetries. This is significant, because it hints at how one might produce a fully orthogonal basis for the adjoint color singlet space using the Hermitian Young projection operators, without the need for Gram-Schmidt orthogonalisation. However, we have been unable to fully resolve this puzzle at present, with this chapter detailing everything that we have uncovered thus far.

We'll also see that the theory developed here allows us to prove that for arbitrary k, all elements of the Hermitian Young projection operator basis are either real or purely imaginary. Further, we can determine which property each adjoint color structure will have without need to perform any lengthy calculations involving the Hermitian Young projection operators. The fact that the elements of the Hermitian Young projection operator basis are always real or purely imaginary is useful because this fulfills the assumptions required for lemmas classifying the real and imaginary parts of matrices of CGC correlators (proven by R. Moerman in related work [1]).

A final strength of the methods presented in this chapter is that all of the results pertaining to the adjoint color singlet space are presented at the level of representations and make no reference to the Hermitian Young projection operators, or any particular basis. This means that if one later learns that it is more desirable to use another set of projection operators to project onto irreducible representations of S_k or $SU(N_c)$, all of the results of this chapter will still hold.

In proceeding with the discussion of systematically decomposing the adjoint color singlet space into irreducible representations, recall that one approach to decomposing $\mathcal{S}(A^{\otimes k})$ into irreducible representations is to first decompose $A^{\otimes k}$, and then to find the subspace of singlets within this decomposition. In general, this is a lengthy process that can be circumvented by noting certain underlying symmetries and invariants of $\mathcal{S}(A^{\otimes k})$. The tool to do this is known as *character theory*[1], a subject describing invariants and orthogonality relations associated with irreducible representations that is intimately related to fourier analysis in special cases. For a measure of context, character theory appears in chemistry [38] and in molecular and condensed matter physics [39, 40], usually whenever symmetries under finite groups are present[2]. Given that symmetries associated with permutation groups appear in our work, it's unsurprising that character theory also proves useful in our context.

Finding these invariants can itself be a computationally intensive task. However, in the case of $\mathcal{S}(A^{\otimes k})$, symmetry allows us to circumvent this problem. It turns out that we can systematically classify subspaces of $\mathcal{S}(A^{\otimes k})$ that are invariant under certain subgroups of S_k and then determining the character invariants in $\mathcal{S}(A^{\otimes k})$ is rendered trivial by using the *induced representations* associated with these subgroups.

The most natural way to understand induced representations is as follows: suppose that we have a representation of a group G and instead we wish to work with a representation of a group H, which is a subgroup of G. This can be achieved by simply omitting the matrices that corresponds to elements of G that are not elements of H.

[1] Although I had read some of the classical mathematics texts on characters and it likely should have been obvious how to apply the theory in this context, I am deeply indebted to [23, App. A] (which we elaborate upon heavily) for making this method clear to me.

[2] Characters are defined for infinite groups as well as finite groups, however defining an inner product on characters of infinite groups isn't always a simple task (this is possible for example in the case of compact Lie groups [41, Ch. 12]) and so it is perhaps more common to see characters used in the finite group setting in physics.

What we obtain is a *restricted* representation. But at this point one might ask, can the "inverse" procedure be performed? That is, is there a canonical way to obtain a representation of G given a representation of H? The answer is yes - this is known as an induced representation.

Example: induced representations and the Poincaré group

Induced representations may be familiar from the classical example of the representation theory of the Poincaré group in relativistic field theory. Here one determines the *little group* that leaves a four-momentum p^μ invariant (the little group depends on whether p^μ is null, time-like, or space-like), then obtains unitary irreducible representations of the full Poincaré group as the representations *induced* from the little group [33, Sec. 10.4].

We will also make use of a powerful correspondence between restricted and induced representations known as *Frobenius reciprocity*. We'll see that Frobenius reciprocity is precisely what makes the process of calculating character invariants (and thus the decomposition of $\mathcal{S}(A^{\otimes k})$) in this setting trivial.

The chapter proceeds as follows: in Section 4.1 we introduce the concept of the character of a representation and show that characters obey orthogonality relations. This will allow us to decompose the adjoint color singlet space into irreducible representations. In Section 4.2, we motivate the need to work with modules and define these objects, then introduce induced representations, and derive Frobenius reciprocity, which relates the characters of induced representations to the more easily calculated characters of restricted representations. The key construction is then introduced in Section 4.3, where we show how to write the adjoint color singlet space as an induced representation and how the results of the previous sections then provides a simple formula for decomposing the adjoint color singlet space into irreducible representations. We also show in this section how this formula gives critical insight into why orthogonality failed in some instances for the Hermitian Young projector basis and what might be done in future to resolve this issue. We then proceed to work through this construction for the cases $k = 2, 3, 4$ in Section 4.4 and show that this produces the same results that we obtained by brute force in the previous chapter. Lastly, Section 4.5 shows how characters, induced representations, and Frobenius reciprocity allow us to prove that the adjoint color structures are either real or purely imaginary for all k. The method for calculating these properties directly from the representations themselves is given here.

4.1 Characters give us the multiplicity of irreducible representations

In this section we introduce the notion of the *character* of a representation. We will see that the characters of irreducible representations (known as *irreducible characters*) obey certain orthogonality relations which will allow us to determine the multiplicity of each irreducible representation in a decomposition of any representation. The primary motivation for making use of characters is that they can be used to determine

the decomposition of the adjoint color singlet space. This will be explored later in the chapter.

In this section G will always be a finite group, because ultimately our aim is to work with the permutation group S_k acting on $\mathcal{S}(A^{\otimes k})$ and so we have no need to develop the infinite case. Then given a representation $\rho : G \to GL(V)$ of G on a vector space V, the character of an element $g \in G$ is defined as

$$\chi_G^V := \operatorname{tr} \rho(g) \tag{4.1}$$

That is, the character of an element of G on V is just the trace of the matrix representation of G corresponding to V. This is well-defined without making reference to any basis for the matrix representation, because the trace is basis-independent. We will always work with finite-dimensional representations and so we won't need to do any additional work to make sure that the trace is well-defined. From this definition it follows that characters obey the following properties:

Properties of characters

- Characters are constant on conjugacy classes (the standard terminology is that they are *class functions*). This is because of the cyclicity of the trace:

$$\chi_G^V(xgx^{-1}) = \chi_G^V(g), \quad \forall\, x, g \in G \tag{4.2}$$

- Isomorphic representations have the same characters, again by the cyclicity of the trace.

- The complex conjugate of the character of $g \in G$ is the character of g^{-1}:

$$\overline{\chi_G^V(g)} = \chi_G^V(g^{-1}) \tag{4.3}$$

  This follows because every representation of a finite group (and of compact Lie groups) is isomorphic to a *unitary representation* (a representation where each matrix representing each group element is a unitary matrix). See [42, Sec. 4.3]. We define $\tilde{\rho} : G \to GL(V)$ to be a unitary representation that is isomorphic to ρ and then because isomorphic representations have isomorphic characters, we have that

$$\overline{\chi_G^V(g)} = \overline{\operatorname{tr}(\tilde{\rho}(g))} = \operatorname{tr}\left((\tilde{\rho}(g))^\dagger\right) \overset{\tilde{\rho}^\dagger \tilde{\rho}^{-1} = \mathbb{1}}{=} \operatorname{tr}\left((\tilde{\rho}(g))^{-1}\right) = \operatorname{tr}\left(\tilde{\rho}(g^{-1})\right) = \chi_G^V(g^{-1}) \tag{4.4}$$

What makes characters extremely useful is that we can define the following inner product on characters:

$$\langle \chi_G^X, \chi_G^Y \rangle_G := \frac{1}{|G|} \sum_{g \in G} \overline{\chi_G^X(g)} \chi_G^Y(g) \tag{4.5a}$$

$$= \frac{1}{|G|} \sum_{g \in G} \chi_G^X(g^{-1}) \chi_G^Y(g), \quad \text{(see eq. (4.3))} \tag{4.5b}$$

where $\overline{\chi_G^X(g)}$ is the complex conjugate of $\chi_G^X(g)$. If we think of a character as a vector $\chi = (\chi(g_1), \chi(g_2), \ldots, \chi(g_{|G|}))$ in $\mathbb{C}^{|G|}$, then the inner product eq. (4.5a) is just the canonical inner product on this complex vector space (up to a normalisation factor). What makes this inner product extremely useful is that if X, Y are two irreducible representations of G, their characters (henceforth known as *irreducible characters*) are orthogonal with respect to the inner product eq. (4.5):

$$\langle \chi_G^X, \chi_G^Y \rangle_G = \begin{cases} 0 & X \ncong Y \\ 1 & X \cong Y \end{cases} \quad X, Y \text{ irreducible} \tag{4.6a}$$

We won't prove the orthogonality relations given in Equation (4.6) (see any introductory book on the representation theory of finite groups such as [31, 43, 44])[1], but we have seen inner products and orthogonality relations analogous to eq. (4.6) in other contexts, such as in fourier analysis and quantum mechanics.

[1]While this isn't the standard text for a general introduction to representation theory, I found the first chapter of Sagan's book [31] to contain the most clear introduction and proofs of these notions for finite groups.

Example: connection between fourier analysis and the character inner product

The inner product in eq. (4.5a) (and analogous variants) appears in fourier analysis. For example, in signal processing, one samples a signal at n evenly-spaced points and obtains a list of data $\{x_m\}_{m=0}^{n-1}$. Then the data can be expanded as the fourier series

$$x_m = \frac{1}{n}\sum_{j=0}^{n-1} X_j \, e^{(\frac{2\pi m i}{n})j} \tag{4.7}$$

where the data X_j is the discrete fourier transform of the data x_j. Define

$$f : Z_n \to \mathbb{C} \tag{4.8a}$$
$$f(m) := x_m \tag{4.8b}$$

where Z_n is the cyclic group of order n and recall that since Z_n is abelian, all of its n irreducible representations are one dimensional, with irreducible characters

$$\chi^m(j) = e^{(\frac{2\pi m i}{n})j} \tag{4.9}$$

Then we have

$$f(m) = x_m = \left\langle \hat{f}, \chi^m \right\rangle_{Z_n} \tag{4.10}$$

where $\hat{f}$ is the discrete fourier transform of f and $\langle \cdot, \cdot \rangle_G$ is the inner product defined in eq. (4.5). In fact, one performs fourier analysis on any locally compact abelian group using characters and orthogonality relations analogous to Equation (4.6) (integrals replace sums where necessary). The classical fourier transform is one such example. However, character analysis and fourier analysis no longer coincide when we generalise to the nonabelian case.

For our purpose, what is important is that the orthogonality relations between irreducible characters in eq. (4.6) allow us to determine the multiplicity (number of times) that an irreducible representation of G appears in a decomposition of any representation of G (up to isomorphism). To see this, consider a reducible representation of G on a vector space V. Then V has the following unique decomposition (up to isormorphim)

$$V = \bigoplus_j X^j \tag{4.11}$$

where each X^j is an irreducible representation of G. We can group together isomorphic irreducible representations so that we have

$$V \cong \bigoplus_i (\underbrace{W^i \oplus \cdots \oplus W^i}_{m_i \text{ copies}}) =: \bigoplus_i (m_i W^i) \tag{4.12}$$

where the set of W^i is the full set of possible irreducible representations of G and m_i

is the number of times that W^i appears in the decomposition eq. (4.11) (up to isomorphism). Then for any $g \in G$

$$\chi_G^V(g) = \sum_i m_i \chi_G^{W^i}(g) \tag{4.13}$$

because isomorphic representations have the same characters and the trace of a direct sum is the sum of the traces. Then, because of the orthogonality relations in eq. (4.6), the number of times an irreducible representation W^i appears (up to isomorphism) in the decomposition eq. (4.11) is given by

$$m^i = \left\langle \chi_G^V, \chi_G^{W^i} \right\rangle_G \tag{4.14}$$

We'd like to use eq. (4.14) to find which irreducible representations appear when we project the adjoint color singlet space to a basis associated with irreducible representations of S_k. Luckily, the irreducible characters of S_k are well known, but it isn't immediately obvious how to calculate the character associated with the adjoint color singlet space for each k. It turns out that finding these characters is facilitated by the theory of *induced representations*, which is the topic of the next section.

4.2 Modules, induced representations, and Frobenius reciprocity

Our goal is to decompose the adjoint color singlet space into irreducible representations of S_k, which will explain why some of the Hermitian Young projection operators return 0 when acting on the adjoint color singlet space. We've seen in eq. (4.14) of the previous section that this can be done by using characters, as long as we can calculate the character of the full representation of S_k on the adjoint color singlet space at arbitrary k. In the next section we'll see that a trick involving induced representations and Frobenius reciprocity (a powerful correspondence between restricted and induced representations) allows us to calculate the character of the adjoint color singlet space without much difficulty and so our purpose in this section is to give some background on these concepts. In light of this, the style of this section will be considerably more similar to the mathematics literature than the rest of this dissertation. If the reader is familiar with modules, induced representations, and Frobenius reciprocity, then this section can be seamlessly skipped.

The appearance of induced representations encourages us to work with *modules* instead of the standard approach in physics of discussing representations "on" a vector space, particularly because modules are the natural setting to introduce Frobenius reciprocity. Modules are nothing more than a slight generalisation of vector spaces to the case where the scalars now come from a ring instead of from a field. In our case, the ring that we're particularly interested in is the *group algebra* (also known as the *group ring*), because we'll see that formulating our work in terms of the group algebra, modules, and irreducible submodules captures the same information as working with representations and irreducible representations. In some sense, modules allows us to simply organise the information encoded in the theory of representations and vector

spaces as a single mathematical object. Once this has been established, we'll see how this reformulation naturally gives us the correspondence between induced representations and restricted representations known as Frobenius reciprocity. Let's begin.

One way to think of modules is that they are simply comprised of an abelian group and a function that allows another algebraic object to "act" on this abelian group. We recall these definitions and give some examples. A reasonable starting point is to recall the definition of a group action on a set:

Definition 4.2.1 (Group action)**.** *A left group action on a set X is a function*

$$\cdot : G \times X \to X \tag{4.15a}$$

such that

$$e \cdot x = x, \quad e \in G,\ \forall x \in X \tag{4.15b}$$
$$(g_1 g_2) \cdot x = g_1 \cdot (g_2 \cdot x), \quad \forall g_1, g_2 \in G,\ \forall x \in X \tag{4.15c}$$

A right group action is defined in the obvious analogous way:

$$\circ : X \times G \to X \tag{4.15d}$$

such that

$$x \cdot e = x, \quad e \in G,\ \forall x \in X \tag{4.15e}$$
$$x \circ (g_1 g_2) = (x \circ g_1) \circ g_2, \quad \forall g_1, g_2 \in G,\ \forall x \in X \tag{4.15f}$$

So effectively the only difference between a left and right action is the order in which a product of group elements $g_1 g_2$ acts on elements of X.

Examples: group actions

Some examples of group actions are:

- The group composition law in any group induces a left action of the group on itself:

$$g \cdot x := gx, \quad g \in G, x \in G \tag{4.16}$$

- Left (or right) actions need not be notationally "on the left (right)". One easily checks that conjugation of group elements by other group elements

$$g \cdot x := gxg^{-1}, \quad g \in G, x \in G \tag{4.17}$$

  also satisfies the properties of a left action.

When we have a (left or right) group action on X, we will use the standard terminology of a "(left or right) G-action" on X. One defines actions for more complicated algebraic objects that "act" on other algebraic objects, where the important detail is that

all of the operations must be compatible with each other in the obvious ways. For example, if we have a representation ρ of G on a vector space V, then we always have a G-action on V defined as

$$g \cdot v = \rho(g)v \tag{4.18}$$

which is compatible with all of the vector space and group operations by definition of ρ.

If V is a vector space defined over the field $\mathbb{K}$, we can also think of V as being the result of defining scalar multiplication as a $\mathbb{K}$-action on the underlying abelian group structure of the vector space - that is a vector space is just an abelian group with a $\mathbb{K}$-action. This leads to the natural generalisation of a vector space that we've said we'll get some benefits from using: a *module* is just a vector space where the scalars come from a ring instead of a field. Since the field was commutative with respect to multiplication, the left and right-actions coincide (refer to Definition 4.2.1 if this isn't immediately clear), whereas rings are not necessarily commutative and so we take care to describe whether we are using a left or right action:

Definition 4.2.2 (***R***-Module)**.** *A left R-module is an abelian group with a left R-action defined on it, where R is a (not necessarily commutative) ring*[1] *and this R-action is compatible with the abelian group sum and the two ring operations in the obvious way. A right R-module differs only in that a right R-action is used.*

So we've learned that groups can act on themselves, that representations have something to do with G-actions on vector spaces, and there exists objects called modules which are slight generalisations of vector spaces and involve scalars from rings instead of fields. Then we can show that the familiar discussion of group representations "on" vector spaces can be reformulated in the language of modules if we can find an appropriate ring action. The correct ring to use is called the *group algebra* (sometimes called the *group ring*), which is standard in discussing representation theory in terms of modules:

Definition 4.2.3 (Group algebra over a field)**.** *The group algebra of G over a field $\mathbb{K}$, denoted $\mathbb{K}[G]$, is the set of all finite k-linear combinations of elements of G:*

$$x \in \mathbb{K}[G] \iff x = \sum_{g \in G} k_g g, \quad k_g \in \mathbb{K}, \text{ (and the sum is finite)} \tag{4.19}$$

We specialise to the field of complex numbers $\mathbb{C}$ for the remainder of this work. For an example of a group algebra, notice that the Hermitian Young projectors of Section 3.3.1 are each elements of the group algebra of S_k.

[1] There is no general agreement on whether a ring should be defined to have a multiplicative identity, with some authors preferring the term *unital* ring for the case when they do. We will define our rings to always be unital for simplicity.

Then, given a representation

$$\rho : G \to GL(V) \tag{4.20}$$

of G on a vector space V, we can unambiguously define a representation of the group algebra on V, by extending ρ by linearity:

$$\rho : \mathbb{C}[G] \longrightarrow \text{End}(V) \tag{4.21}$$

Then it becomes clear that working with ρ and V is exactly equivalent to defining V as a $\mathbb{C}[G]$-module[1], by defining the $\mathbb{C}[G]$-action as

$$g \cdot v = \rho(g)v, \quad \forall g \in \mathbb{C}[G] \tag{4.22}$$

and ensuring compatibility with all group and ring identities. Similarly, the character of a module is simply the character of its associated representation.

In summary, we've learned that the representation theory of finite groups on vector spaces can be reformulated as the study of the action of the group algebra on the underlying abelian group structure of the vector space. What about irreducible representations? We need the following definitions:

Definition 4.2.4 (Submodule of an $\boldsymbol{R}$-Module)**.** *Let M be a left R-module. If N is a subgroup of M (thinking of just the abelian group structure on M) and N is closed under the left R-action on M, then we say that N is a submodule of M.*

Definition 4.2.5 (Irreducible module)**.** *We call a module with no nontrivial submodules "irreducible."*

With some work, one can show that decomposing representations into irreducible representations is exactly the same as decomposing the analogous module into a direct sum of irreducible submodules[2]. Altogether we have done nothing special: we have simply traded the idea of studying group homomorphisms acting on vector spaces through the automorphism group with the study of $\mathbb{C}[G]$-modules. In the latter case, everything is packaged as a single mathematical object. We have promised that this reformulation will pay off when we introduce Frobenius reciprocity to study the characters of induced representations (induced modules), so we move on to define restricted and induced modules.

Given a left $\mathbb{C}[G]$-module M and H a subgroup of G, there is an obvious way to make M into a $\mathbb{C}[H]$-module: simply restrict the $\mathbb{C}[G]$-action to elements of $\mathbb{C}[H]$ and everything is well-defined. This is known as the *restricted* module and denoted $\text{Res}^G_H M$. Conversely, given a left $\mathbb{C}[H]$-module N, it turns out (possibly surprisingly) that there is a canonical way to construct a left $\mathbb{C}[G]$-module from $\mathbb{C}[H]$ and N, which is known as the *induced module* and denoted $\text{Ind}^G_H N$. To do this, we'll need to discuss bimodules, which involve two rings (for our purpose: group algebras), and tensor products.

[1] Note $(ke) \cdot v = \rho(ke)v = kv, \ \forall k \in \mathbb{C}$ and so defining V as a $\mathbb{C}[G]$-module immediately defines a multiplication of elements of V by scalars in the field $\mathbb{C}$, which is the same as V being a vector space over $\mathbb{C}$.

[2] It is perhaps more common to see the terminology *simple* modules rather than irreducible modules, but both are used often enough that we feel that using this terminology to ease our presentation is justified.

Definition 4.2.6 (Bimodule)**.** *M is a bimodule if it has compatible left R-action and right S-action. We say that M is a (R, S)-module.*

Notice that the group algebra itself can always be viewed as a $(\mathbb{C}[G], \mathbb{C}[G])$-module and so whenever we're studying the representation theory of finite groups like S_k, we have a bimodule structure available to us.

Now let's discuss tensor products. Recall that if V, W are vector spaces over $\mathbb{C}$, then the elements of the tensor product space $V \otimes_{\mathbb{C}} W$ are objects $v_i \otimes_{\mathbb{C}} w_j$ with the following identifications

$$(v_1 + v_2) \otimes_{\mathbb{C}} w \sim v_1 \otimes_{\mathbb{C}} w + v_2 \otimes_{\mathbb{C}} w \tag{4.23a}$$

$$v \otimes_{\mathbb{C}} (w_1 + w_2) \sim v \otimes_{\mathbb{C}} w_1 + v \otimes_{\mathbb{C}} w_2 \tag{4.23b}$$

$$k(v \otimes_{\mathbb{C}} w) \sim (kv) \otimes_{\mathbb{C}} w \sim v \otimes_{\mathbb{C}} (kw) \tag{4.23c}$$

The key difference in defining the tensor product of modules M and N over the same ring R, is that R is not necessarily commutative and so we need to modify the third rule for scalar multiplication by requiring M to be a right R-module, N a left R-module, and defining

$$r \cdot (m \otimes_R n) \sim (m \circ r) \otimes_R n \sim m \otimes_R (r \cdot n), \quad r \in R \tag{4.24}$$

One might ask why we should define the tensor product in terms of a left and right R-module instead of say, two left R-modules, or two right R-modules. Well, suppose we used two left (or right) actions in our definition. Then we would have the equivalence chain:

$$(r_1 r_2) \cdot (m \otimes_R n) \sim r_1 \cdot \big(m \otimes_R (r_2 \cdot n)\big) \sim (r_1 \cdot m) \otimes_R (r_2 \cdot n) \sim r_2 \cdot \big((r_1 \cdot m) \otimes_R n\big) \tag{4.25a}$$

$$\sim (r_2 r_1) \cdot (m \otimes_R n) \tag{4.25b}$$

which of course isn't what we're trying to capture in general with a noncommutative ring, because $r_1 r_2 \neq r_2 r_2$.

In contrast to choosing two left actions or two right actions, defining the tensor product over a ring by using a left and right action means that these two actions are compatible, because if we carefully apply Definition 4.2.1 (noting that the critical difference between left and right actions is the order in which a product of elements is applied), then

$$(r_1 r_2) \cdot (m \otimes_R n) \sim r_1 \cdot \big(m \otimes_R (r_2 \cdot n)\big) \sim (m \circ r_1) \otimes_R (r_2 \cdot n) \sim r_2 \cdot \big((m \circ r_1) \otimes_R n\big) \tag{4.26a}$$

$$\sim (r_1 r_2) \cdot (m \otimes_R n) \tag{4.26b}$$

as desired. So now we know that our definition of the tensor product of R-modules makes sense. This allows us to reach our goal, which is to give the following definition for an induced module:

Definition 4.2.7 (Induced module)**.** *Let $H \leq G$ and N a left $\mathbb{C}[H]$-module. We view $\mathbb{C}[G]$ as a $(\mathbb{C}[G], \mathbb{C}[H])$-module by restricting the right action and define*

$$Ind_H^G N := \mathbb{C}[G] \otimes_{\mathbb{C}[H]} N \tag{4.27}$$

which is a left $\mathbb{C}[\mathbb{G}]$-module due to the "unused" left action on $\mathbb{C}[G]$:

$$g' \cdot (g \otimes_{\mathbb{C}[H]} n) := (g' \cdot g) \otimes_{\mathbb{C}[H]} n \tag{4.28}$$

Recall that our goal was to construct the "inverse" of a restricted representation/ module. In other words given a subgroup $H \leq G$ and a left action of the subalgebra $\mathbb{C}[H]$ on a space, we seek a canonical left action of $\mathbb{C}[G]$ on some module built from this $\mathbb{C}[H]$-module. Then Definition 4.2.7 certainly satisfies our desire to construct a left $\mathbb{C}[G]$-module out of the left $\mathbb{C}[\mathbb{H}]$-module N, but why this definition over any other? The point is that this definition is the "natural" counterpart to the restricted module, as a result of Frobenius reciprocity. In some sense, we can take Frobenius reciprocity to be *the* motivation for this definition. While the relationship between restricted and induced modules described by Frobenius reciprocity is actually much deeper than what we'll need for our purposes (see Appendix B.2 for details), a critical result of this definition for induced modules is that the following correspondence between induced and restricted characters holds:

Theorem 4.2.1 (Frobenius reciprocity for characters)**.** *Let H be a subgroup of G. Let M be a left $\mathbb{C}[G]$-module and let N be a left $\mathbb{C}[H]$-module. Then*

$$\langle \chi^{Ind_H^G N}, \chi^M \rangle_G = \langle \chi^N, \chi^{Res_H^G M} \rangle_H \tag{4.29}$$

where $Res_H^G M$ is the restricted left $\mathbb{C}[H]$-module obtained by only allowing elements of $\mathbb{C}[H]$ to be used in the $\mathbb{C}[G]$-action on M.

Proof. See Appendix B.2 for proof. □

We already know from eq. (4.14) that the inner product of characters can be used to determine the multiplicity of irreducible modules in the decomposition of a given module and we will see in the next section that we can construct the adjoint color singlet space as a direct sum of induced modules. Then the power of Theorem 4.2.1 in our context is that the induced characters, which may not be straightforward to calculate in general, are related to the restricted characters, which in our case are well-known. Furthermore, the right-hand side of eq. (4.29) is a simpler inner product to evaluate, because we only need to sum over the elements of a subgroup H, rather than the entire group G. That is, the relationship between induced and restricted characters that arises from Frobenius reciprocity allows us to efficiently decompose the adjoint color singlet space into irreducible representations. We now proceed to this explicit construction.

4.3 The construction

We now show that one can systematically decompose the adjoint color singlet space at arbitrary k into irreducible $\mathbb{C}[S_k]$-modules using characters, induced representations, and Frobenius reciprocity. In doing so, we will stumble across a clear explanation for why the Hermitian Young projection operator basis fails to be fully orthogonal: it turns out that the underlying cycle structure of S_k is responsible.

We saw in Section 3.2 that if we forget the $\mathfrak{su}(N_c)$ structure, the adjoint color singlet space with k adjoint indices is spanned by the derangements of S_k. We make this space into a left $\mathbb{C}[S_k]$-module with the left $\mathbb{C}[S_k]$-action given by conjugation by elements of S_k, extended by linearity:

$$D^k := \text{span}_{\mathbb{C}}\{\sigma \mid \sigma \text{ is a derangement in } S_k\} \tag{4.30a}$$

$$g \cdot \sigma = g\sigma g^{-1}, \quad g \in S_k \tag{4.30b}$$

The point here is that conjugation preserves cycle type and so maps derangements into derangements, meaning that D^k is $\mathbb{C}[S_k]$-invariant. The trick to calculating the character of this module is that D^k is actually isomorphic to a direct sum of modules induced by a particular $\mathbb{C}[H]$-action on a subspace of D^k, with $H \leq S_k$. Further, we will see that Frobenius reciprocity gives us access to these characters in terms of restricted characters that are trivial to calculate (Theorem 4.2.1).

Let's establish the isomorphism between D^k and the direct sum of modules induced by a subgroups of S_k. First, observe that since conjugation preserves cycle type, D^k is the direct sum of $\mathbb{C}[S_k]$-invariant submodules where each submodule is spanned by derangements of the same cycle type:

$$D^k \cong \bigoplus_{\mu} D_\mu \tag{4.31}$$

where we denote cycle type as an integer partition $\mu = (\mu_1, \ldots, \mu_n)$.

Example: the space of derangements in S_4

In S_4, the permutation (1234) has cycle type (4), because it only consists of one disjoint cycle of length 4, while the permutation $(12)(34)$ has cycle type $(2,2)$, because it can be written as a product of two disjoint cycles each of length 2. Then

$$D^4 \cong D_{(4)} \oplus D_{(2,2)} \tag{4.32}$$

because the only derangements in S_4 have cycle type (4) or $(2,2)$.

In fact each D_μ is isomorphic to an induced module. To see this, choose some derangement $\sigma_\mu \in S_k$ where σ_μ has cycle type μ and choose H_μ to be the maximal subgroup that leaves σ_μ invariant under the action of conjugation. This is known as the *centralizer*[1] of σ_μ:

$$H_\mu := C_{S_k}(\sigma_\mu) = \{g \mid g \in S_k,\, g\sigma_\mu g^{-1} = \sigma_\mu\} \tag{4.33}$$

In fact, we can explicitly say what subgroup $C_{S_k}(\sigma_\mu)$ is of S_k in general:

The group $C_{S_k}(\sigma_\mu)$

There are two cases:

- **Case 1**: If σ_μ is written as a product of disjoint cycles, then none of these disjoint cycles have the same length as each other. In other words, if we denote the cycle type $\mu = (\mu_1, \ldots, \mu_m)$, then $\mu_i \neq \mu_j,\ \forall i \neq j$. For example, $\mu = (2, 3, 3)$ is made up of disjoint cycles where two of these cycles are both length 3 and so we do not consider this cycle type in Case 1, but $\mu = (2, 6, 7, 9)$ is made of up disjoint cycles that are each of differing lengths and so Case 1 applies. Then

  $$C_{S_k}(\sigma_\mu) \cong Z_{\mu_1} \times \cdots \times Z_{\mu_m} \tag{4.34}$$

  where Z_n is the cyclic group with n elements. So for example the derangement $(12)(345)$ would have centralizer

  $$C_{S_k}((12)(345)) = \{e, (12), (345), (543), (12)(345), (12)(543)\} \cong Z_2 \times Z_3 \tag{4.35}$$

- **Case 2**: The cycle type μ indicates that σ_μ is made up of disjoint cycles where some of these cycles have the same lengths, eg. $\mu_i = \mu_j$ for some $i \neq j$. In this case there are additional symmetries to the derangement (because disjoint cycles commute and so one can swap disjoint cycles of the same length with each other without changing σ_μ) and so the centralizer can be larger than predicted in the first case. For example, $(12)(34)$ is invariant under

  $$Z_2 \times Z_2 \cong \{e, (12), (34), (12)(34)\} \tag{4.36}$$

  which describes the symmetries of cyclicly permuting indices within disjoint cycles as we did in Case 1, but does not take into account symmetries under swapping disjoint cycles of equal length. Then we can include the additional symmetries of swapping cycles of equal length by noticing that because (12) commutes with (34), $(12)(34)$ is also invariant under $(13)(24)$ (which swaps the disjoint cycles), which is not an element of $Z_2 \times Z_2$:

  $$(13)(24) \cdot (12)(34) = (13)(24)(12)(34)((13)(24))^{-1} = (34)(12) = (12)(34) \tag{4.37}$$

[1] In general, we would work with the *stablizer* subgroup of a given group G, which is defined as the subgroup of G that leaves the element that is being acted upon invariant. Since we have chosen our left action to be conjugation, the stablizer and centralizer coincide. We will continue to refer to the centralizer to emphasise the left action that we're using.

Then we deduce that the centralizer is a larger subgroup than $Z_2 \times Z_2$.

In general, in a given permutation there can be several different sets of disjoint cycles of equal length. Then if we recall that σ_μ was just some derangement in S_k with cycle type μ, we can define $s_1, \ldots, s_i$ to be the permutations that leave σ_μ invariant by all possible permutations of disjoint cycles of equal length and we can define $z_1, \cdots, z_j$ to be the permutations that generate the cyclic groups corresponding to symmetries within the disjoint cycles of σ_μ. Then

$$C_{S_k}(\sigma_\mu) = \langle s_1, \ldots, s_i, z_1, \ldots, z_j \rangle \tag{4.38}$$

that is, $C_{S_k}(\sigma_\mu)$ is the subgroup of S_k generated by all possible products of the permutations that implement symmetries of σ_μ under conjugation. In the example $\sigma_\mu = (12)(34)$, we would have centralizer

$$C_{S_k}((12)(34)) = \langle (13)(24), (12), (34) \rangle \cong D_8 \tag{4.39}$$

where D_8 is the dihedral group with 8 elements.

Then, returning to our discussion of the module induced by $H_\mu := C_{S_k}(\sigma_\mu)$, we define

$$W_\mu := \text{span}_{\mathbb{C}}\{\sigma_\mu\} \tag{4.40}$$

which is tautologically a one-dimensional left $\mathbb{C}[H_\mu]$-module with the left action again given by conjugation. Then the claim is that

$$D_\mu \cong \text{Ind}_{H_\mu}^{S_k} W_\mu \tag{4.41}$$

Let's show this. From Definition 4.2.7, we recall that $\text{Ind}_{H_\mu}^{S_k} W_\mu$ is spanned by elements of the type $g \otimes_{\mathbb{C}[H_\mu]} \sigma_\mu$ where g varies over S_k. But if we choose a transversal $g_1, \ldots, g_m$ of H_μ (a representative from each coset of H_μ), then because the collection of cosets $g_i H_\mu$ partitions S_k into disjoint sets, each $g = g_i h_j$ uniquely, where $h_j \in H_\mu$. But by the definition of the tensor product over $\mathbb{C}[H_\mu]$ (see eq. (4.24)), we have for each g

$$g \otimes_{\mathbb{C}[H_\mu]} \sigma_\mu = g_i h_j \otimes_{\mathbb{C}[H_\mu]} \sigma_\mu \sim g_i \otimes_{\mathbb{C}[H_\mu]} h_j \sigma_\mu h_j^{-1} = g_i \otimes_{\mathbb{C}[H_\mu]} \sigma_\mu \tag{4.42}$$

and so the collection $g_i \otimes_{\mathbb{C}[H_\mu]} \sigma_\mu$ forms a basis for $\text{Ind}_{H_\mu}^{S_k} W_\mu$. Then we see that $\text{Ind}_{H_\mu}^{S_k} W_\mu$ has dimension $[G : H_\mu]$ and is isomorphic to

$$D_\mu = \text{span}_{\mathbb{C}}\{g_i \sigma_\mu g_i^{-1} \mid g_i \text{ ranges over a transversal of } S_k \text{ by } H_\mu\} \tag{4.43a}$$

where the module isomorphism is given by

$$\phi : \text{Ind}_{H_\mu}^{S_k} W_\mu \longrightarrow V_\mu \tag{4.43b}$$

$$\phi(g_i \otimes_{\mathbb{C}[H_\mu]} \sigma_\mu) = g_i \sigma_\mu g_i^{-1} \tag{4.43c}$$

extended by linearity. This isomorphism is just a consequence of the well-known result

that a transversal of the cosets of the centralizer of some $x \in G$ is bijective to the conjugacy class of x. But this just says that $\mathrm{Ind}_{H_\mu}^{S_k} W_\mu$ is isomorphic to the span of all possible ways to conjugate the derangement σ_μ, which is just the span of all derangements of cycle type μ. Then we have altogether that the space of derangements that correspond to the adjoint color singlet space $\mathcal{S}(A^{\otimes k})$ is given by

$$D^k \cong \bigoplus_\mu \mathrm{Ind}_{H_\mu}^{S_k} W_\mu \tag{4.44}$$

The point of all of this is that we can now determine the multiplicity of any irreducible moduel in the adjoint color singlet space using characters and Frobenius reciprocity. Recall that the irreducible modules associated with S_k are in one-to-one correspondence with Young diagrams with k boxes and so we will use the notation λ to label an arbitrary Young diagram with k boxes. Then if χ^λ is the irreducible character associated with the irreducible $\mathbb{C}[S_k]$-module indexed by λ, we have from Equation (4.14) that the multiplicity of this irreducible module in a decomposition of the adjoint color singlet space is given by

$$m^\lambda = \left\langle \chi^{D^k}, \chi^\lambda \right\rangle_{S_k} = \sum_\mu \left\langle \chi^{\mathrm{Ind}_{H_\mu}^{S_k} W_\mu}, \chi^\lambda \right\rangle_{S_k} \tag{4.45}$$

where in the last equality we have used the fact that the character of a direct sum is the sum of the characters, and that isomorphic modules have the same characters. Then using Theorem 4.2.1 (Frobenius reciprocity for characters), we have

$$m^\lambda = \sum_\mu \left\langle \chi^{\mathrm{Ind}_{H_\mu}^{S_k} W_\mu}, \chi^\lambda \right\rangle_{S_k} = \sum_\mu \left\langle \chi^{W_\mu}, \chi^{\mathrm{Res}_{H_\mu}^{S_k} \lambda} \right\rangle_{H_\mu} \tag{4.46}$$

$\chi^{\mathrm{Res}_{H_\mu}^{S_k} \lambda}$ is an abuse of notation to denote the irreducible character χ^λ restricted to elements of H_μ. Now notice that we have defined the $\mathbb{C}[H_\mu]$-action on W_μ to always acts trivially and so the character associated with this module is always 1. This implies that

$$m^\lambda = \sum_\mu \left\langle \underbrace{\chi^{W_\mu}}_{=1}, \chi^{\mathrm{Res}_{H_\mu}^{S_k} \lambda} \right\rangle_{H_\mu} = \sum_\mu \underbrace{\frac{1}{|H_\mu|} \sum_{h \in H_\mu} \chi^\lambda(h)}_{=: m_\mu^\lambda} \tag{4.47}$$

Then collecting everything together, the multiplicity m^λ of the irreducible module corresponding to λ in a decomposition of the adjoint color singlet space for arbitrary k is just

$$m^\lambda = \sum_\mu m_\mu^\lambda \tag{4.48a}$$

$$m_\mu^\lambda := \frac{1}{|H_\mu|} \sum_{h \in H_\mu} \chi^\lambda(h), \qquad H_\mu := C_{S_k}(\sigma_\mu) \tag{4.48b}$$

where σ_μ is a single derangment of cycle type μ (the choice of representative does not change the resulting multiplicites).

Equation (4.48) is the critical formula that we've worked towards. It may seem slightly convoluted, but what is likely more illuminating in our context is what this allows us to *do*: we now have all of the ingredients necessary to state which irreducible modules show up in any decomposition of the adjoint color singlet space into irreducible modules, for any k. All we have to do is determine the different cycle types that appear in derangements in S_k (ie. every partition of k that doesn't have 1 in it), then write down the maximal subgroups H_μ that leave these cycle types invariant under conjugation, and then sum the irreducible characters of S_k evaluated at elements of each H_μ, normalising each of these sums by $|H_\mu|$. Speaking roughly, one might think of this process as determining underlying symmetries of the adjoint color singlet space and then averaging irreducible characters over these underlying symmetry groups to determine the irreducible structure of the full space. Then if we introduce the notation $\mathcal{S}^\lambda$ for the irreducible subspace of $\mathcal{S}(A^{\otimes k})$ associated with the Young diagram λ, we can translate our results obtained using subspaces of derangements back into results in terms of traces of elements of $\mathfrak{su}(N_c)$, using the correspondence between D^k and $\mathcal{S}(A^{\otimes k})$. This then gives the decomposition of $\mathcal{S}(A^{\otimes k})$ as

$$\mathcal{S}(A^{\otimes k}) \cong \bigoplus_{\lambda \text{ has } k \text{ boxes}} (\underbrace{\mathcal{S}^\lambda \oplus \cdots \oplus \mathcal{S}^\lambda}_{m^\lambda \text{ copies}}) =: \bigoplus_{\lambda \text{ has } k \text{ boxes}} (m^\lambda \mathcal{S}^\lambda) \tag{4.49}$$

with m^λ determined using eq. (4.48). This process will become clear as we work through some examples in the next subsection.

While it may not be obvious, eq. (4.48) also produces a deep explanation for why the Hermitian Young projection operator basis wasn't automatically fully orthogonal, as we discussed in the previous chapter. Equation (4.48) tells us that submodules separated according to cycle type can each contribute to the multiplicity of the *same* irreducible module appearing in a decomposition of $\mathcal{S}(A^{\otimes k})$. Then when we project onto this irreducible module (say with the Hermitian Young projection operators), we obtain one adjoint color structure for each cycle type that has a nonzero multiplicity for this irreducible representation. If this occurs, these adjoint color structures will not be orthogonal in general, because they all result from a single projection operator. This is a central result of this chapter.

For example, we saw in eq. (3.24) of the previous chapter that at $k = 4$

$$0 \neq \langle \mathcal{C}_1^{a_1a_2a_3a_4}, \mathcal{C}_2^{a_1a_2a_3a_4} \rangle \tag{4.50a}$$

where

$$\mathcal{C}_1^{a_1a_2a_3a_4} := d^{a_1a_4m}d^{a_2a_3m} + d^{a_1a_3m}d^{a_2a_4m} + d^{a_1a_2m}d^{a_3a_4m} \tag{4.50b}$$

$$\mathcal{C}_2^{a_1a_2a_3a_4} := \delta^{a_1a_4}\delta^{a_2a_3} + \delta^{a_1a_3}\delta^{a_2a_4} + \delta^{a_1a_2}\delta^{a_3a_4} \tag{4.50c}$$

In Section 4.4.3, we'll see that the reason that these basis elements fail to be orthogonal is precisely because $\mathcal{C}_1^{a_1a_2a_3a_4}$, $\mathcal{C}_2^{a_1a_2a_3a_4}$ arise from a submodule with associated cycle type (4), $(2,2)$ respectively. Each of these cycle types has a nonzero multiplicity for the irreducible $\mathbb{C}[S_4]$-module associated with the diagram $\square\square\square\square$[1]. This leads us to speculate that it may be possible to obtain a fully orthogonal basis for the adjoint color singlet space at arbitrary k if we can systematically write down a set of orthogonal projection operators onto submodules of different cycle types and combine these with the orthogonal Hermitian Young projection operators.

One last comment is in order: we have not yet spoken about the irreducible characters of S_k. Since characters are constant on conjugacy classes, it is standard to organize the irreducible characters of a group in a *character table*, where the rows vary over the irreducible representations of the group and the columns vary over the conjugacy classes. Furthermore, the irreducible representations of S_k are indexed by the Young diagrams and the conjugacy classes of S_k are determined by the cycle type of a permutation. So for example we would write the character table of S_2 as

	$[1^2]$	$[2]$
$\square\square$	1	1
$\begin{smallmatrix}\square\\\square\end{smallmatrix}$	1	-1

TABLE 4.1: Character table of S_2

where the notation $[1^2]$ indicates the conjugacy class made up of 2 1-cycles and $[2]$ indicates the conjugacy class made up of 2-cycles. Character tables for S_k for low values of k are widely available, but characters can also be calculated directly using the Murnaghan-Nakayama rule (see Section 4.10 of [31]) or the Frobenius formula (see Section 4.1 of [44]), which we don't elaborate on here. We now proceed to the next section, which contains several worked examples of the construction introduced in this section.

[1] Recall that this is the irreducible module that the Hermitian Young projection operator associated with the diagram $\square\square\square\square$ projects onto.

4.4 Examples for $k = 2, 3, 4$

This section provides the decomposition of the adjoint color singlet space for $k = 2, 3, 4$ using the construction of the previous section.

4.4.1 $k = 2$

Here the process is somewhat trivial. We begin with a single 2-index trace $\mathrm{tr}(t^a t^b)$ which is identified with the only derangement in S_2, which in cycle notation is given by (12). So the span of the derangements in this case is just given by

$$D^2 = D_{(2)} = \{c\,(12) \mid c \in \mathbb{C}\} \tag{4.51}$$

We only have a single choice for the representative $\sigma_{(2)}$ of this space with cycle type (2) and so $W_{(2)} = D^2$. We ask what maximal subgroup of S_2 leaves $W_{(2)}$ invariant when acted on by conjugation, and of course we have $H_{(2)} = C_{S_2}((12)) = S_2$, the whole group (remember conjugation just relabels the numbers within the cycle $\sigma_{(2)} := (12)$ and so both possible relabellings (12) and (21) are equal) . Then there is only a single coset of $H_{(2)}$, and a transversal is given by choosing the identity permutation $e = (1)(2)$. Then $e \otimes_{\mathbb{C}[S_2]} (12)$ is a basis for $\mathrm{Ind}_{H_{(2)}}^{S_2} W_{(2)}$ and $\mathrm{Ind}_{H_{(2)}}^{S_2} W_{(2)} \cong D^2$. Then using the character table for S_2 (Table 4.1) and the formula for the multiplicities of the irreducible modules (eq. (4.48)), we find

$$m^{\square\square} = \frac{1}{2}\sum_{h\in S_2} \chi^{\square\square}(h) = \frac{1}{2}(\chi^{\square\square}(e) + \chi^{\square\square}\big((12)\big)) = \frac{1}{2}(1+1) \tag{4.52a}$$

$$= 1 \tag{4.52b}$$

$$m^{\square} = \frac{1}{2}\sum_{h\in S_2} \chi^{\square}(h) = \frac{1}{2}(\chi^{\square}(e) + \chi^{\square}\big((12)\big)) = \frac{1}{2}(1-1) \tag{4.52c}$$

$$= 0 \tag{4.52d}$$

Therefore, if we recall that we have introduced the notation $\mathcal{S}^\lambda$ for the subspace of the adjoint color singlet space associated with the irreducible representation of S_k that is indexed by the Young diagram λ, we can translate the irreducible multiplicities obtained using the derangements of S_2 back into information about $\mathcal{S}(A^{\otimes 2})$ to obtain the decomposition

$$\mathcal{S}(A^{\otimes 2}) \cong \mathcal{S}^{\square\square} \tag{4.53}$$

This is exactly what we showed by brute force when we worked through the full calculation of applying all of the $k = 2$ Hermitian Young projection operators to $\mathcal{S}(A^{\otimes 2})$ in eq. (3.15).

4.4.2 $k = 3$

The trace basis for $k = 3$ is given by

$$\{\mathrm{tr}(t^{a_1}t^{a_2}t^{a_3}), \mathrm{tr}(t^{a_1}t^{a_3}t^{a_2})\} \tag{4.54}$$

which we identify with the set of derangements in S_3:

$$D^3 = \mathrm{span}_{\mathbb{C}}\{(123), (132)\} \tag{4.55}$$

Since every element of D^3 is of the same cycle type, we pick a single representative of this cycle type, say $\sigma_{(3)} := (123)$. Then $W_{(3)}$, as defined before, is given by

$$W_{(3)} := \mathrm{span}_{\mathbb{C}}\{(123)\} \tag{4.56}$$

The maximal subgroup of S_3 that leaves $W_{(3)}$ invariant under the left action by conjugation is $C_{S_3}((123)) = Z_3$, the cyclic group with 3 elements. Then $W_{(3)}$ is a left $\mathbb{C}[Z_3]$-module with action given by conjugation. $|S_3| = 6$ and $|Z_3| = 3$ and so by Lagrange's theorem, the number of left cosets of Z_3 in S_3 is 2. Then a left transversal is given by $\{e, (12)\}$ and so

$$\begin{aligned} \mathrm{Ind}_{Z_3}^{S_3} W_{(3)} &= \mathrm{span}_{\mathbb{C}}\{e \otimes_{\mathbb{C}[Z_3]} (123),\ (12) \otimes_{\mathbb{C}[Z_3]} (123)\} && \text{(4.57a)} \\ &\cong \mathrm{span}_{\mathbb{C}}\{(123), (132)\} && \text{(4.57b)} \\ &= W_{(3)} = D^3 && \text{(4.57c)} \end{aligned}$$

The character table for S_3 is

	$[1^3]$	$[3]$	$[2\ 1]$
	1	1	1
	1	1	-1
	2	-1	0

TABLE 4.2: Character table of S_3

Then from eq. (4.48), the multiplicity of any irreducible module corresponding to a diagram λ in the decomposition of the adjoint color singlet space with $k = 3$ is given by

$$\begin{aligned} m^\lambda &= \frac{1}{3}\sum_{h\in Z_3} \chi^\lambda(h) && \text{(4.58a)} \\ &= \frac{1}{3}\big(\chi^\lambda([1^3]) + 2\chi^\lambda([3])\big) && \text{(4.58b)} \end{aligned}$$

where we have abused notation slightly to indicate that because characters are constant on conjugacy classes, we need really only indicate what conjugacy class the elements

of Z_3 lie in, which simplifies the sum. Then we have

$$m^{\ydiagram{3}} = \frac{1}{3}(1+2) = 1 \tag{4.59a}$$

$$m^{\ydiagram{2,1}} = \frac{1}{3}(1+2) = 1 \tag{4.59b}$$

$$m^{\ydiagram{2,1}} = \frac{1}{3}(2-2) = 0 \tag{4.59c}$$

Using the correspondence between the derangements D^3 and the adjoint color singlet space $\mathcal{S}(A^{\otimes 3})$, we use these multiplicities to obtain the decomposition

$$\mathcal{S}(A^{\otimes 3}) \cong \mathcal{S}^{\ydiagram{3}} \oplus \mathcal{S}^{\ydiagram{2,1}} \tag{4.60}$$

which was exactly what was calculated using the Hermitian Young projection operators in Equation (3.18).

4.4.3 $k = 4$

Let's repeat the construction for $k = 4$, which is the first nontrivial example in the sense that the set of derangements in S_4 begins to have more than one cycle type. We have that the space of derangements in S_4 decomposes into the spaces of derangements in S_4 with cycle type (4) and with cycle type $(2,2)$:

$$D^4 \cong D_{(4)} \oplus D_{(2,2)} \tag{4.61}$$

because at $k = 4$ the adjoint color singlet space is spanned by traces of the type $\mathrm{tr}(t^{a_1}t^{a_2}t^{a_3}t^{a_4})$ and of the type $\mathrm{tr}(t^{a_1}t^{a_2})\,\mathrm{tr}(t^{a_3}t^{a_4})$.

Let's first work with $D_{(4)}$, the 6-dimensional space of elements of S_4 with cycle type $\mu = (4)$ (made into a module with left $\mathbb{C}[S_4]$-action given by conjugation extended by linearity). If we choose a representative of this space $\sigma_{(4)} := (1234)$, then the maximal subgroup of S_4 that leaves $\sigma_{(4)}$ invariant when acted upon by conjugation is $C_{S_4}(\sigma_{(4)}) = Z_4$, the cyclic group with 4 elements. Since $|S_4| = 24$ and $|Z_4| = 4$, Lagrange's theorem tells us that $[S_4 : Z_4] = 6$ and so we'll need 6 elements of S_4 to form a transversal of S_4 by Z_4. One such choice is

$$\{e, (34), (23), (234), (243), (24)\} \tag{4.62}$$

and so we find that

$$D_{(4)} \cong \mathrm{Ind}_{Z_4}^{S_4} W_{(4)} \tag{4.63}$$

Similarly, if we consider $D_{(2,2)}$, which is the space of all permutations in S_4 with cycle type $(2,2)$, then if we choose the representative of this space $\sigma_{(2,2)} := (12)(34)$ as a candidate to generate $W_{(2,2)}$, the maximal subgroup of S_4 that leaves $\sigma_{(2,2)}$ invariant when acting by conjugation is D_8[1], the dihedral group with 8 elements. Then we have

[1]Take care not to mix up D_8 with $D_{(8)}$. The former is a group, the later is a space of derangements, as indicated by the presence of a cycle type (8) in the subscript.

that $[S_4 : D_8] = 3$ and so we expect a left transversal of S_4 by D_8 to have 3 elements. One such choice is

$$\{e, (23), (24)\} \tag{4.64}$$

and one checks that through all of the tricks defined before that

$$D_{(2,2)} \cong \mathrm{Ind}_{D_8}^{S_4} W_{(2,2)} \tag{4.65}$$

And finally

$$D^4 \cong \mathrm{Ind}_{Z_4}^{S_4} W_{(4)} \oplus \mathrm{Ind}_{D_8}^{S_4} W_{(2,2)} \tag{4.66}$$

Then to calculate the multiplicities of irreducible $\mathbb{C}[S_4]$-modules in decomposing D^4, we consider derangements of cycle type (4) and $(2,2)$ separately. The character table of S_4 is

	$[1^4]$	$[2^2]$	$[2\ 1^2]$	$[4]$	$[3\ 1]$
	1	1	1	1	1
	1	1	-1	-1	1
	2	2	0	0	-1
	3	-1	1	-1	0
	3	-1	-1	1	0

TABLE 4.3: Character table of S_4

The derangements of cycle type (4) have $H_{(4)} = Z_4$, the cyclic group with 4 elements. Then $m_{(4)}^{\lambda}$ in eq. (4.48) (simplified by taking into account that characters are constant on conjugacy classes) is

$$m_{(4)}^{\lambda} = \frac{1}{4}\big(\chi^{\lambda}([1^4]) + 2\chi^{\lambda}([4]) + \chi^{\lambda}([2^2])\big) \tag{4.67}$$

Substituting the values in from the character table of S_4 gives

$$m_{(4)}^{\ydiagram{4}} = \frac{1}{4}(1+2+1) = 1 \tag{4.68a}$$

$$m_{(4)}^{\ydiagram{1,1,1,1}} = \frac{1}{4}(1-2+1) = 0 \tag{4.68b}$$

$$m_{(4)}^{\ydiagram{2,2}} = \frac{1}{4}(2+0+2) = 1 \tag{4.68c}$$

$$m_{(4)}^{\ydiagram{3,1}} = \frac{1}{4}(3-2-1) = 0 \tag{4.68d}$$

$$m_{(4)}^{\ydiagram{2,1,1}} = \frac{1}{4}(3+2-1) = 1 \tag{4.68e}$$

Therefore at $k = 4$, the subspace of the adjoint color singlet space associated with $D_{(4)}$ decomposes as $\mathcal{S}^{\ydiagram{4}} \oplus \mathcal{S}^{\ydiagram{2,2}} \oplus \mathcal{S}^{\ydiagram{2,1,1}}$.

In the case of the derangements with cycle type $\mu = (2, 2)$, we found that $H_{(2,2)} = D_8$, the dihedral group with 8 elements. Explicitly:

$$D_8 \cong \{e, (12), (34), (12)(34), (13)(24), (14)(23), (1324), (1423)\} \tag{4.69}$$

Then $m^{\lambda}_{(2,2)}$ in eq. (4.48) is given by

$$m^{\lambda}_{(2,2)} = \frac{1}{8}\big(\chi^{\lambda}([1^4]) + 2\chi^{\lambda}([4]) + 3\chi^{\lambda}([2^2]) + 2\chi^{\lambda}([2\,1^2])\big) \tag{4.70}$$

Substituting the values from the character table of S_4 gives

$$m^{\ydiagram{4}}_{(2,2)} = \frac{1}{8}(1 + 2 + 3 + 2) = 1 \tag{4.71a}$$

$$m^{\ydiagram{1,1,1,1}}_{(2,2)} = \frac{1}{8}(1 - 2 + 3 - 2) = 0 \tag{4.71b}$$

$$m^{\ydiagram{2,2}}_{(2,2)} = \frac{1}{8}(2 + 0 + 6 + 0) = 1 \tag{4.71c}$$

$$m^{\ydiagram{3,1}}_{(2,2)} = \frac{1}{8}(3 - 2 - 3 + 2) = 0 \tag{4.71d}$$

$$m^{\ydiagram{2,1,1}}_{(2,2)} = \frac{1}{8}(3 + 2 - 3 - 2) = 0 \tag{4.71e}$$

and so at $k = 4$, the subspace of the adjoint color singlet space that is associated with $D_{(2,2)}$ decomposes as $\mathcal{S}^{\ydiagram{4}} \oplus \mathcal{S}^{\ydiagram{2,2}}$.

Then altogether, we have that the full adjoint color singlet space when $k = 4$ decomposes as[1]

$$\mathcal{S}(A^{\otimes 4}) \cong 2\,\mathcal{S}^{\ydiagram{4}} \oplus 2\,\mathcal{S}^{\ydiagram{2,2}} \oplus \mathcal{S}^{\ydiagram{2,1,1}} \tag{4.72}$$

This is precisely the result that we obtained earlier by directly applying the Hermitian Young projection operators to $\mathcal{S}(A^{\otimes 4})$ in eq. (3.23).

Now we can use the cycle structure of S_k to directly explain why the basis for $\mathcal{S}(A^{\otimes 4})$ generated in eq. (3.22) using the Hermitian Young projection operators failed to be fully orthogonal. Recall that in eq. (3.22), the Hermitian Young projection operators produced a basis $\{\mathcal{C}_1^{a_1a_2a_3a_4}, \ldots, \mathcal{C}_9^{a_1a_2a_3a_4}\}$ for the decomposition that we've just determined in eq. (4.72). We found that the following elements failed to be orthogonal:

$$\langle \mathcal{C}_1^{a_1a_2a_3a_4}, \mathcal{C}_2^{a_1a_2a_3a_4} \rangle \neq 0, \quad \langle \mathcal{C}_3^{a_1a_2a_3a_4}, \mathcal{C}_4^{a_1a_2a_3a_4} \rangle \neq 0, \quad \langle \mathcal{C}_5^{a_1a_2a_3a_4}, \mathcal{C}_6^{a_1a_2a_3a_4} \rangle \neq 0 \tag{4.73}$$

[1] Recall from eq. (4.12) and eq. (4.49) that we use prefactors as notation to indicate a direct sum of multiple isomorphic copies of a given irreducible subspace.

We focus on the non-orthogonal adjoint color structures

$$\mathcal{C}_3^{a_1a_2a_3a_4} := -d^{a_1a_4m}d^{a_2a_3m} - d^{a_1a_3m}d^{a_2a_4m} + 2d^{a_1a_2m}d^{a_3a_4m} \tag{4.74}$$

$$\mathcal{C}_4^{a_1a_2a_3a_4} := \delta^{a_1a_4}\delta^{a_2a_3} + \delta^{a_1a_3}\delta^{a_2a_4} - 2\delta^{a_1a_2}\delta^{a_3a_4} \tag{4.75}$$

as an example, but the explanation that we give is fully general. The point here is that from eq. (3.21) we read off

$$P_{\begin{array}{|c|c|}\hline 1&2\\\hline 3&4\\\hline\end{array}}\,\mathcal{S}(A^{\otimes 4}) = \text{span}\{\mathcal{C}_3^{a_1a_2a_3a_4}, \mathcal{C}_4^{a_1a_2a_3a_4}\} \tag{4.76}$$

The fact that this subspace is two-dimensional (the span of two adjoint color structures) corresponds to the subspace $\mathcal{S}^{\boxplus}$ appearing twice in the decomposition of $\mathcal{S}(A^{\otimes 4})$ in eq. (4.72). But notice that we found earlier in eq. (4.66) that

$$D^4 \cong \text{Ind}_{Z_4}^{S_4} W_{(4)} \oplus \text{Ind}_{D_8}^{S_4} W_{(2,2)} \tag{4.77}$$

and the calculations of this section showed that one copy of $\mathcal{S}^{\boxplus}$ appeared in $\mathcal{S}(A^{\otimes 4})$ because of the irreducible representation corresponding to $\boxplus$ appearing in $\text{Ind}_{Z_4}^{S_4} W_{(4)}$ and the other copy of $\mathcal{S}^{\boxplus}$ appeared because of the irreducible representation corresponding to $\boxplus$ appearing $\text{Ind}_{D_8}^{S_4} W_{(2,2)}$. But $\text{Ind}_{Z_4}^{S_4} W_{(4)}$ was just the space of derangements that corresponded to all traces over four generators of $\mathfrak{su}(N_c)$ and $\text{Ind}_{D_8}^{S_4} W_{(2,2)}$ was the space of derangements corresponding to all traces of the type $\text{tr}(t^{a_1}t^{a_2})\,\text{tr}(t^{a_3}t^{a_4})$. **So altogether we conclude** that non-orthogonal adjoint color structures appeared because of the cycle structure of derangements in S_n. That is, because subspaces of derangements with different cycle types can independently contribute to the multiplicity of the *same* irreducible representation, any projection operator associated with this irreducible representation can produce multiple adjoint color structures, which will fail to be mutually orthogonal. To avoid this problem we will need to somehow enforce orthogonality between subspaces that correspond to derangements with differing cycle types, while will then plausibly modify our construction to produce a fully orthogonal basis for arbitrary k, without the need to use Gram-Schmidt orthogonalisation. Exploring this idea further is a topic for future research.

4.5 Characters tell us which adjoint color structures are real or purely imaginary

A pattern that one might have noticed from the explicit calculations of the previous chapter is that each adjoint color structure obtained by our construction is real or purely imaginary for $k = 2, 3, 4$ (the δ^{ab}, d^{abc}, and f^{abc} symbols are always real numbers). In this section we'll see that this property of this basis extends to arbitrary k and furthermore, it turns out that the machinery of characters, induced modules, and Frobenius reciprocity that we've developed in this chapter[1] allows us to also determine whether an adjoint color structure is real or purely imaginary, without carrying out any projections.

[1] We are again indebted to [23], which was where we first saw this method used.

The value of knowing that all adjoint color structures are real or purely imaginary and exactly which adjoint color structures have each property at arbitrary k is that these properties are needed for certain results proven by R. Moerman in related work on the real and imaginary parts of matrices of CGC correlators [1]. Moreover, the machinery developed here allows us to determine these properties at the level of representations, rather than as a result of using the Hermitian Young projection operators, and so if we should ever choose to use another set of projection operators onto irreducible representations of $SU(N_c)$ or S_k, the properties established in this section still hold.

The first step is to notice that in our paradigm where we identify trace basis elements with derangements, complex conjugation can be identified with a particular type of permutation, acting on the space of derangements by conjugation. Recall that the generators of $\mathfrak{su}(N_c)$ are hermitian and so for an arbitrary trace basis element we have the identification

$$\overline{\operatorname{tr}(t^{a_1}\cdots t^{a_m})\operatorname{tr}(t^{a_{m+1}}\cdots t^{a_{m+n}})\cdots} = \operatorname{tr}(t^{a_m}\cdots t^{a_1})\operatorname{tr}(t^{a_{m+n}}\cdots t^{a_{m+1}})\cdots \tag{4.78a}$$

$$\sim r\cdot(1\cdots m)((m+1)\cdots(m+n))\cdots := (m\cdots 1)((m+n)\cdots(m+1))\cdots \tag{4.78b}$$

So in other words, we choose r to be the permutation that reverses the order of each disjoint cycle in this given derangement, when it acts on the derangement by conjugation (in this section we will always use "$\cdot$" as notation for the left action of conjugation). Since r depends on the cycle type of the derangement $\mu = (\mu_1, \ldots, \mu_m)$, we label it r_μ and are able to write down r_μ explicitly. Let

$$\sigma_\mu = (1\cdots\mu_1)((\mu_1+1)\cdots(\mu_1+\mu_2))\cdots \tag{4.79}$$

then

$$r_\mu := \Big(\big(1\ \mu_1\big)\big(2(\mu_1-1)\big)\cdots\Big)\Big(\big((\mu_1+1)(\mu_1+\mu_2)\big)\big((\mu_1+2)(\mu_1+\mu_2-1)\big)\cdots\Big)\cdots \tag{4.80}$$

is the element of S_k that "complex conjugates" σ_μ. In other words, r_μ can be written as the disjoint transpositions that interchange the first and last element of each disjoint cycle in σ_μ, then the second and second-to-last element, and so on, resulting in the ordering of numbers within each disjoint cycle of σ_μ being reversed. Then because r_μ implements the analogue of complex conjugation for this particular derangement, we can think of

$$\rho_\mu^+ := \sigma_\mu + r_\mu\cdot\sigma_\mu \tag{4.81a}$$

as proportional to the "real part" of σ_μ and

$$\rho_\mu^- := \sigma_\mu - r_\mu\cdot\sigma_\mu \tag{4.81b}$$

as being proportional to the "imaginary part" of σ_μ.

We form

$$W_\mu^\pm := \text{span}_{\mathbb{C}}(\rho_\mu^\pm) \tag{4.82}$$

and we want to find the maximal subgroup $H_\mu \leq S_k$ such that $W_\mu^\pm$ is $\mathbb{C}[H_\mu]$-invariant, so that we can use our earlier tricks of induced modules, characters, and Frobenius reciprocity to make firm statements about when the real and imaginary parts of the adjoint color structures are zero.

Example: σ_μ, r_μ, $\rho_\mu^\pm$, $\text{Ind}_{H_\mu}^{S_k}(\rho_\mu^\pm)$ for $\mathcal{S}(A^{\otimes 3})$

Noting the correspondence between the space of derangements D^k and the adjoint color singlet space $\mathcal{S}(A^{\otimes k})$, we show by means of an example how complex conjugation in the adjoint color singlet space can be analogously implemented in the space of derangements. If we consider $\mathcal{S}(A^{\otimes 3})$, then we have the correspondences:

	D^k (derangements)	$\mathcal{S}(A^{\otimes 3})$ (traces basis)
σ_μ	(123)	$\text{tr}(t^{a_1}t^{a_2}t^{a_3})$
r_μ	(13)	complex conjugation
ρ_μ^+	$(123)+(321)$	$2\,\text{Re}\big(\text{tr}(t^{a_1}t^{a_2}t^{a_3})\big)$ $= \text{tr}(t^{a_1}t^{a_2}t^{a_3}) + \text{tr}(t^{a_3}t^{a_2}t^{a_1})$
ρ_μ^-	$(123)-(321)$	$2i\,\text{Im}\big(\text{tr}(t^{a_1}t^{a_2}t^{a_3})\big)$ $= \text{tr}(t^{a_1}t^{a_2}t^{a_3}) - \text{tr}(t^{a_3}t^{a_2}t^{a_1})$
$\text{Ind}_{H_\mu}^{S_k}(\rho_\mu^+)$	$\text{span}_{\mathbb{C}}\{(123)+(321),(132)+(231)\}$	$\text{span}_{\mathbb{C}}\{\text{Re}\big(\text{tr}(t^{a_1}t^{a_2}t^{a_3})\big),$ $\text{Re}\big(\text{tr}(t^{a_1}t^{a_3}t^{a_2})\big)\}$
$\text{Ind}_{H_\mu}^{S_k}(\rho_\mu^-)$	$\text{span}_{\mathbb{C}}\{(123)-(321),(132)-(231)\}$	$\text{span}_{\mathbb{C}}\{\text{Im}\big(\text{tr}(t^{a_1}t^{a_2}t^{a_3})\big),$ $\text{Im}\big(\text{tr}(t^{a_1}t^{a_3}t^{a_2})\big)\}$

So we see that if σ_μ is chosen to correspond to $\text{tr}(t^{a_1}t^{a_2}t^{a_3})$, then $\rho_\mu^\pm$ corresponds (up to a constant) to the real (respectively imaginary) part of of $\text{tr}(t^{a_1}t^{a_2}t^{a_3})$ and $\text{Ind}_{H_\mu}^{S_k}(\rho_\mu^\pm)$ corresponds to the span of the real (respectively imaginary) parts of the trace basis for $\mathcal{S}(A^{\otimes 3})$. Since the adjoint color structures are just built out of linear combinations of trace basis elements, $\text{Ind}_{H_\mu}^{S_k}(\rho_\mu^\pm)$ gives us access to the real and imaginary parts of any adjoint color structures used as a basis for $\mathcal{S}(A^{\otimes 3})$.

To find the maximal subgroup $H_\mu \leq S_k$ such that $W_\mu^\pm$ is $\mathbb{C}[H_\mu]$-invariant, observe that if $K_\mu := C_{S_k}(\sigma_\mu)$, then

$$r_\mu\, k\, r_\mu \in K_\mu, \quad \forall k \in K_\mu \tag{4.83}$$

That is, r_μ is an element of the *normalizer* of the centralizer of σ_μ (for proof, see Appendix B.3). So if we form the group $H_\mu := C_{S_k}(\rho_\mu^\pm) = \langle r_\mu, K_\mu \rangle$, which is comprised of all possible products of r_μ and elements of K_μ, then we have the following relations for H_μ acting on $\rho_\mu^\pm$:

Properties of the left H_μ-action on $\rho_\mu^\pm$

Let $k \in K_\mu := C_{S_k}(\sigma_\mu)$. The following relations hold

- Action of r_μ on $\rho_\mu^\pm$:

$$r_\mu \cdot \rho_\mu^\pm = \pm\, \rho_\mu^\pm, \qquad \text{(by construction)} \tag{4.84}$$

- Elements of K_μ leave $\rho_\mu^\pm$ invariant:

$$\begin{aligned} k \cdot \rho_\mu^\pm &= \sigma_\mu \pm (k r_\mu) \cdot \sigma_\mu = \sigma_\mu \pm (r_\mu k') \cdot \sigma_\mu, \quad (k' \in K_\mu, \text{ because } r_\mu\, k\, r_\mu \in K_\mu) \\ &= \rho_\mu^\pm \qquad\qquad (k' \text{ is in the centralizer of } \sigma_\mu) \end{aligned} \tag{4.85}$$

- Action of elements of the form $k r_\mu$ on $\rho_\mu^\pm$:

$$\begin{aligned} (k r_\mu) \cdot \rho_\mu^\pm &= \pm\, k \cdot \rho_\mu^\pm \\ &= \pm\, \rho_\mu^\pm, \qquad (k \text{ leaves } \rho_\mu^\pm \text{ invariant}) \end{aligned} \tag{4.86}$$

Altogether, since one can easily show that every element of H_μ is either an element of K_μ or of the form $k r_\mu$, these relations mean that $W_\mu^\pm$ is invariant under the left $\mathbb{C}[H_\mu]$-action of conjugation and thus is a left $\mathbb{C}[H_\mu]$-module. Furthermore, since K_μ was the maximal subgroup of S_k that left σ_μ invariant and working with $\rho_\mu^\pm$ introduces a single additional symmetry under r_μ (up to sign), then H_μ is the maximal subgroup of S_k that leaves $W_\mu^\pm$ invariant.

All of this leads to be able to apply Frobenius reciprocity to determine the multiplicity with which these "real" and "purely imaginary" subspaces appear in the adjoint color singlet space, using the methods of the previous section. First, what is $\mathrm{Ind}_{H_\mu}^{S_k}(\rho_\mu^\pm)$ in this case? Well, it's spanned by elements of the form

$$g_i \otimes_{\mathbb{C}[H_\mu]} \rho_\mu^\pm \tag{4.87}$$

where the g_i are elements of a transversal of S_k by H_μ. We previously said that these elements are isomorphic to

$$g_i \cdot \rho_\mu^\pm = g_i \cdot \sigma_\mu \pm (g_i\, r_\mu) \cdot \sigma_\mu = (g_i \sigma_\mu\, g_i^{-1}) \pm (g_i\, r_\mu\, g_i^{-1}) \cdot (g_i \sigma_\mu\, g_i^{-1}) \tag{4.88}$$

The first term on the right-hand side of the previous line just says "relabel the numbers in σ_μ according to the permutation g_i" and the second term just says "apply the analogously relabeled (with respect to g_i) reversal element to the relabeled version of σ_μ." In other words, the span of the elements $g_i \otimes_{\mathbb{C}[H_\mu]} \rho_\mu^\pm$ is isomorphic to the span of the "real" (respectively: "purely imaginary") parts of all possible derangements in S_k with cycle type μ, because all possible "real" (respectively "imaginary") parts of derangements are generated.

We know that we can always convert derangements back into elements of the trace basis and so the preceding argument shows that $\mathrm{Ind}_{H_\mu}^{S_k}(\rho_\mu^\pm)$ can be used to generate the space of all possible real ("+") or imaginary ("−") parts of trace basis elements.

Then, since the adjoint color structures are always built out of linear combinations of trace basis elements, if we can use $\mathrm{Ind}_{H_\mu}^{S_k}(\rho_\mu^\pm)$ to show that the real (imaginary) parts of the traces used to span a particular irreducible representation vanish, then we know that the corresponding real (imaginary) parts of the adjoint color structures used as a basis for this irreducible representation in $\mathcal{S}(A^{\otimes 3})$ must vanish. So we conclude that if an irreducible $\mathbb{C}[S_k]$-module has multiplicity 0 in a decomposition of $\mathrm{Ind}_{H_\mu}^{S_k}(\rho_\mu^\pm)$, this corresponds to the irreducible module being spanned by purely imaginary adjoint color structures (the "+" case is 0), or real adjoint color structures (the "-" case is 0).

Notice also that the characters of $W_\mu^\pm$ are trivial in the "+" case, but eq. (4.86) tells us that in the "-" case, any element of H_μ that is of the form kr_μ with $k \in K_\mu$ has character -1 instead (because the action of these elements is the left action that multiplies ρ_μ^- by -1). So then we have that the multiplicity of the irreducible $\mathbb{C}[S_k]$-module labeled by the Young diagram λ is given by

$$m_{\mu\pm}^\lambda = \frac{1}{2|K_\mu|}\left(\sum_{k\in K_\mu} \chi^\lambda(k) \pm \chi^\lambda(k\, r_\mu)\right) \tag{4.89}$$

where we recall that $K_\mu := C_{S_k}(\sigma_\mu)$ and we have simplified using $|H_\mu| = 2|K_\mu|$. Notice also that we have

$$m_\mu^\lambda = m_{\mu+}^\lambda + m_{\mu-}^\lambda \tag{4.90}$$

which *proves* that the adjoint color structures can only be real or purely imaginary, because together the real and purely imaginary parts exhaust the total possible multiplicity of irreducible modules that can occur in the decomposition.

In the next subsection we use the machinery developed in this section to work through some specific examples. We will see that we reproduce the results that were found in the previous chapter when we noticed that all adjoint color structures for $k = 2, 3, 4$ were real or purely imaginary.

4.5.1 Examples: real and purely imaginary irreducible modules for $k = 2, 3, 4$

$\boldsymbol{k = 2}$ - Here the reversal permutation that implements the analogue of complex conjugation is $r_{(2)} = (12)$, which is already an element of $K := C_{S_2}(\sigma_{(2)})$. Then we have that $H_{(2)} := C_{S_2}(\rho_{(2)}^\pm) = K_{(2)}$ and everything follows as in the previous section's character analysis, with the result that

$$m_{(2)}^\lambda = m_{(2)+}^\lambda \tag{4.91a}$$

$$\implies m_{(2)-}^\lambda = 0 \tag{4.91b}$$

and so the only adjoint color structure is real. This was of course clear by anticipating $\mathcal{C}_1^{a_1a_2} = \delta^{a_1a_2}$ or noticing that

$$\mathrm{tr}(t^{a_1}t^{a_2}) + (12)\cdot \mathrm{tr}(t^{a_1}t^{a_2}) = 2\,\mathrm{tr}(t^{a_1}t^{a_2}) \tag{4.92a}$$

while on the other hand

$$\mathrm{tr}(t^{a_1}t^{a_2}) - (12)\cdot \mathrm{tr}(t^{a_1}t^{a_2}) = 0 \tag{4.92b}$$

$\boldsymbol{k=3}$ - The reversal permutation in this case is $r_{(3)} = (13)$. We saw before that $K_{(3)} = Z_3$ and so $H_{(3)} := C_{S_3}(\rho^{\pm}_{(3)}) = S_3$. Notice also that the elements of type $kr_{(3)} \in S_3$ are the 3 permutations with cycle type $(2,1)$. Then, simplifying by recalling that characters are constant on elements of equal cycle type (conjugacy classes), we have

$$m^{\lambda}_{(3)\pm} = \frac{1}{6}\Big(\chi^{\lambda}([1^3]) + 2\chi^{\lambda}([3]) \pm 3\chi^{\lambda}([21])\Big) \tag{4.93}$$

The character table for S_3 is

	$[1^3]$	$[3]$	$[2\ 1]$
	1	1	1
	1	1	-1
	2	-1	0

TABLE 4.4: Character table of S_3

and so we have

$$m^{\ydiagram{3}}_{(3)+} = 1, \quad m^{\ydiagram{3}}_{(3)-} = 0 \tag{4.94a}$$

$$m^{\ydiagram{2,1}}_{(3)+} = 0, \quad m^{\ydiagram{2,1}}_{(3)-} = 1 \tag{4.94b}$$

This means that the single occurrence of $\mathcal{S}^{\ydiagram{3}}$ in the decomposition of $\mathcal{S}(A^{\otimes 3})$ is spanned by a real adjoint color structure and the single occurrence of $\mathcal{S}^{\ydiagram{2,1}}$ is spanned by a purely imaginary adjoint color structure. These are of course the $d^{a_1a_2a_3}$ and $if^{a_1a_2a_3}$ objects, respectively.

$\boldsymbol{k=4}$ - Here we start to have derangements with multiple cycle types. Let's start with the $\mu = (4)$ derangements. The reversal permutation is

$$r_{(4)} = (14)(23) \tag{4.95}$$

Then we have that

$$K_{(4)} = Z_4 \implies H_{(4)} := C_{S_4}(\rho^{\pm}_{(4)}) = D_8 \tag{4.96}$$

The permutations in D_8 that are of the form $kr_{(4)}$ are $(14)(23), (24), (13), (12)(34)$, while the remaining permutations from $K_{(4)} \leq H_{(4)}$ are $e, (1234), (4321), (13)(24)$. Then we have

$$m^{\lambda}_{(4)\pm} = \frac{1}{8}\Big(\chi^{\lambda}([1^4]) + 2\chi^{\lambda}([4]) + \chi^{\lambda}([2^2]) \pm 2\chi^{\lambda}([2^2]) \pm 2\chi^{\lambda}([21^2])\Big) \tag{4.97}$$

The character table of S_4 is

	$[1^4]$	$[2^2]$	$[2\ 1^2]$	$[4]$	$[3\ 1]$
	1	1	1	1	1
	1	1	-1	-1	1
	2	2	0	0	-1
	3	-1	1	-1	0
	3	-1	-1	1	0

TABLE 4.5: Character table of S_4

And so we have

$$m^{\square\square\square\square}_{(4)+} = 1, \quad m^{\square\square\square\square}_{(4)-} = 0 \tag{4.98a}$$

$$m^{\begin{smallmatrix}\square\square\\\square\square\end{smallmatrix}}_{(4)+} = 1, \quad m^{\begin{smallmatrix}\square\square\\\square\square\end{smallmatrix}}_{(4)-} = 0 \tag{4.98b}$$

$$m^{\begin{smallmatrix}\square\square\\\square\\\square\end{smallmatrix}}_{(4)+} = 0, \quad m^{\begin{smallmatrix}\square\square\\\square\\\square\end{smallmatrix}}_{(4)-} = 1 \tag{4.98c}$$

Which means that $\mathcal{C}_1^{a_1a_2a_3a_4}$ as a basis for $\mathcal{S}^{\square\square\square\square}$ and $\mathcal{C}_3^{a_1a_2a_3a_4}, \mathcal{C}_5^{a_1a_2a_3a_4}$ as a basis for $\mathcal{S}^{\begin{smallmatrix}\square\square\\\square\square\end{smallmatrix}}$ are real, while $\mathcal{C}_7^{a_1a_2a_3a_4}, \mathcal{C}_8^{a_1a_2a_3a_4}, \mathcal{C}_9^{a_1a_2a_3a_4}$ as a basis for $\mathcal{S}^{\begin{smallmatrix}\square\square\\\square\\\square\end{smallmatrix}}$ are purely imaginary, which was exactly what we saw by direct calculation in eq. (3.22).

Let's now turn to the $(2,2)$ derangements. The reversal permutation is

$$r_{(2,2)} = (12)(34) \tag{4.99}$$

and we have that

$$r_{(2,2)} \in D_8 = K_{(2,2)} \implies H_{(2,2)} := C_{S_4}(\rho^{\pm}_{(2,2)}) = K_{(2,2)} \tag{4.100}$$

Since the reversal permutation is already an element of $K_{(2,2)}$, a little thought gives us that

$$m^{\lambda}_{(2,2)-} = -m^{\lambda}_{(2,2)-} \implies m^{\lambda}_{(2,2)-} = 0 \tag{4.101}$$

(this can be verified by directly calculating the characters as well) and so

$$m^{\lambda}_{(2,2)} = m^{\lambda}_{(2,2)+} \tag{4.102}$$

which means that $\mathcal{C}_2^{a_1a_2a_3a_4}$ as a basis for $\mathcal{S}^{\square\square\square\square}$ and $\mathcal{C}_4^{a_1a_2a_3a_4}, \mathcal{C}_6^{a_1a_2a_3a_4}$ as a basis for $\mathcal{S}^{\begin{smallmatrix}\square\square\\\square\square\end{smallmatrix}}$ are real, which was again the result that we obtained by brute force in eq. (3.22).

4.6 Summary of Chapter 4

In this chapter we've seen that characters, induced representations, and Frobenius reciprocity give us a systematic method for decomposing the adjoint color singlet space into irreducible representations of S_k, or equivalently, into irreducible $\mathbb{C}[S_k]$-modules. The critical observation was that the characters associated with irreducible representations are orthonormal, which gives us a simple formula for the multiplicity of any irreducible representation in a decomposition of $\mathcal{S}(A^{\otimes k})$.

The rest of our effort was expended on showing how to use this formula to calculate the multiplicity of irreducible representations in the decomposition in practice. We were able to show that the adjoint color singlet space can actually be thought of as corresponding to the direct sum of $\mathbb{C}[S_k]$-modules induced by the subgroups of S_k that encode the symmetries of each cycle type of derangements in S_k. Then Frobenius reciprocity allowed us to relate the induced characters assigned to the adjoint color singlet space with the irreducible characters of S_k, which are widely-known. We were then able to show using this approach that we could reproduce the decomposition of the adjoint color singlet space for $k = 2, 3, 4$ that was found in the previous chapter using the Hermitian Young projection operators. As a bonus result, the method developed here was easily extended to investigate the real and imaginary parts of the adjoint color structures for arbitrary k. We proved that every adjoint color structure is always real or purely imaginary and that we can always predict whether an adjoint color structure will be real or purely imaginary at the level of representations, without actually constructing the basis element.

The motivation for pursuing the construction of this chapter originally came from wanting to determine a priori whether a given Hermitian projection operator would produce a nonzero result when acting on the adjoint color singlet space, with the thought being that at higher orders it might be more computationally efficient to only construct the projection operators and carry out the projections that were known to produce nonzero results. However, solving this problem has gained us significant additional value. We have learned that failures of orthogonality in the Hermitian Young projection operator basis occur precisely because of the cycle structure of derangments in S_k. Therefore, if we were able to construct orthogonal projections onto subspaces of derangement according to cycle type at arbitrary k, we could couple these cycle type projections with the Hermitian Young projection operators, which would likely systematically produce a fully orthogonal basis for the adjoint color singlet space. Then, the study of the real and imaginary parts of the adjoint color structures that was carried out using the methods of this chapter are of value to parallel work by R. Moerman on the real and imaginary parts of matrices of CGC correlators [1]. Finally, as mentioned earlier, since all of the constructions in this chapter are at the level of representations, all results here do not depend on the specific projection operators that are used to project on the irreducible representations of S_k. This means that what we have learned in this chapter is additionally valuable in that it remains valid should we ever modify the projection operators that we use in future.

Chapter 5

A digression: bounding simple Wilson line operators

"Don't let me catch anyone talking about the Universe in my department."

Ernest Rutherford

In the previous chapters we've focused on developing approximate descriptions of the JIMWLK evolution of CGC correlators. In this chapter, we take the complementary view: while exact solutions of the JIMWLK equation cannot be obtained at present, it is still possible to prove certain exact statements about CGC correlators. A short list of new proofs in this direction form the content of this chapter. In particular, we focus on the images of Wilson line operators in the complex plane, which have practical significance as well as fascinating aesthetic appeal. For example, consider the $q\bar{q}$ dipole operator

$$\hat{S}_{\boldsymbol{xy}} := \frac{\mathrm{tr}(U_{\boldsymbol{x}} U^{\dagger}_{\boldsymbol{y}})}{N_c} \tag{5.1}$$

Then the image of this operator in the complex plane is the region bounded by the *hypocycloid* with N_c cusps (Figure 5.1). One of the results of this chapter is to provide a proof that has not already appeared in the literature of this fact (Section 5.1).

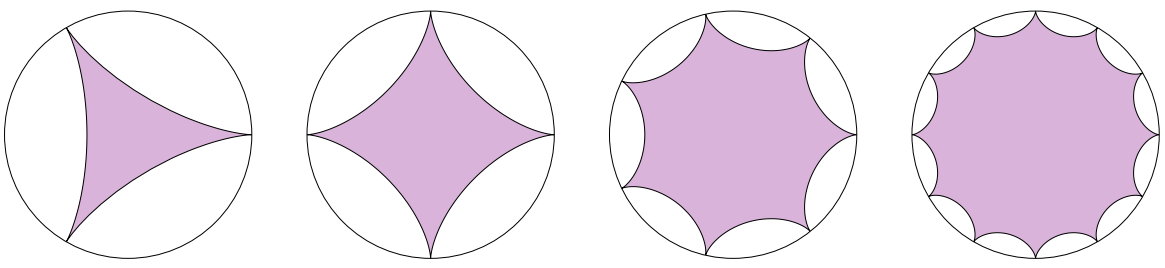

(A) $N_c = 3$ (B) $N_c = 4$ (C) $N_c = 7$ (D) $N_c = 12$

FIGURE 5.1: Hypocycloids with N_c cusps, circumscribed by the unit circle.

If we consider the next-most simple case, that is when we have 2 quark-antiquark pairs, we saw in Section 2.1.2 that the JIMWLK equation leads us to consider the evolution of a matrix of Wilson line correlators

$$\mathcal{A}(Y) := \begin{pmatrix} \left\langle \frac{\operatorname{tr}(U_{\boldsymbol{x_1}} U^\dagger_{\boldsymbol{x_2}}) \operatorname{tr}(U_{\boldsymbol{x_3}} U^\dagger_{\boldsymbol{x_4}})}{N_c^2} \right\rangle_Y & \left\langle \frac{\operatorname{tr}(U_{\boldsymbol{x_1}} t^a U^\dagger_{\boldsymbol{x_2}}) \operatorname{tr}(U_{\boldsymbol{x_3}} t^a U^\dagger_{\boldsymbol{x_4}})}{N_c \sqrt{d_A/4}} \right\rangle_Y \\ \left\langle \frac{\operatorname{tr}(U_{\boldsymbol{x_1}} U^\dagger_{\boldsymbol{x_2}} t^b) \operatorname{tr}(U_{\boldsymbol{x_3}} U^\dagger_{\boldsymbol{x_4}} t^b)}{N_c \sqrt{d_A/4}} \right\rangle_Y & \left\langle \frac{\operatorname{tr}(U_{\boldsymbol{x_1}} t^a U^\dagger_{\boldsymbol{x_2}} t^b) \operatorname{tr}(U_{\boldsymbol{x_3}} t^a U^\dagger_{\boldsymbol{x_4}} t^b)}{d_A/4} \right\rangle_Y \end{pmatrix} \tag{5.2}$$

where $d_A := N_c^2 - 1$ is the dimension of the adjoint representation. Numerical evidence suggests that the images of the operators appearing in the diagonal elements $\mathcal{A}_{11}(Y)$ and $\mathcal{A}_{22}(Y)$ are also the region in the complex plane bounded by the hypocycloid with N_c-cusps, while the images of the operators appearing in $\mathcal{A}_{12}(Y)$ and $\mathcal{A}_{21}(Y)$ seem to lie in some region bounded by a yet-to-be-determined geometric shape. While we have been unable to prove these observations thus far, we have been able to show that the image of each of these operators is contained in the unit circle, which is still a useful result, because it rules out blowup of these correlators under JIMWLK evolution. The results on bounding the entries of the two quark-antiquark pair amplitude matrix are the content of Section 5.2.

5.1 The image of the trace of $SU(n)$ matrices is the region bounded by the n-cusp hypocycloid

In this section, we provide a new proof that the image of the dipole operator is the region in the complex plane bounded by the hypocycloid with N_c cusps. The motivation for doing this is twofold: First, we find the commonly-cited proof in [45] to be overly terse. The only other proof that we are aware of in the literature [46, Sec. 3.2.2] follows a completely different approach from our proof and we were unable to verify its claims. Second, our hope is to prove analogous results for more complicated Wilson line operators and so one might hope that a clear proof of a simpler result will gives us clues as to how to proceed in more complicated scenarios.

Let's begin. We fix notation by recognising that the image of all possible $U_{\boldsymbol{x}} U^\dagger_{\boldsymbol{y}}$ products is simply the image of all special unitary matrices U and we will also use $n := N_c$ to reduce clutter. Then studying the image of the dipole operator is equivalent to determining the image of the function

$$f : SU(n) \to \mathbb{C} \tag{5.3a}$$

$$U \mapsto \frac{1}{n} \operatorname{tr} U = \frac{1}{n} \left(\sum_{i=1}^{n-1} z_i + \frac{1}{z_1 \cdots z_{n-1}} \right) \tag{5.3b}$$

where the z_i are the eigenvalues of U and we have used $\det U = 1$ to write z_n in terms of the other eigenvalues, without loss of generality (each eigenvalue lives on the unit circle and so there is no risk of dividing by 0).

In [45, sec. 3] the author states that the image of f is the n-cusp hypocycloid inscribed in the unit circle. A critical step in the argument relies on the statement that to obtain the boundary of the image, it is sufficient to set $n - 2$ of the partial derivatives

of f equal to zero, that is

$$\frac{\partial f}{\partial z_1} = \cdots = \frac{\partial f}{\partial z_{n-2}} = 0 \tag{5.4}$$

This result has been cited several times in the literature [21, 47–49], but as written, it is unclear why it should be true. Indeed, as noted in [50, 51] and as we shall see, even if we accept that the conditions eq. (5.4) return a family of critical points of f (which is true, but may or may not be immediately obvious), there is no reason why a one-dimensional family of critical points cannot lie in the interior of the image of the map. In fact, for $n \geq 4$, this occurs (see Figure 5.2). Thus, a full proof is needed and so we provide one.

Theorem 5.1.1. *Let $f : SU(n) \to \mathbb{C}$, $f(U) = \frac{1}{n}\operatorname{tr} U$. Then the image of f is the n-cusp hypocycloid, normalised so that it is inscribed in the unit circle.*

The proof proceeds by recalling some known results in differential geometry and establishing several lemmas. From now on we will think of f as the map

$$f : \mathbb{T}^{n-1} \to \mathbb{C} \tag{5.5a}$$

$$(\theta_1, \ldots, \theta_{n-1}) \mapsto \frac{1}{n}\left(\sum_{j=1}^{n-1} e^{i\theta_j} + e^{-i\sum_{k=1}^{n-1}\theta_k}\right) \tag{5.5b}$$

because after diagonalising the matrix U, we can always write the trace as a sum of exponentials. First, notice that f is continuous (it is just a sum of complex exponentials, which are continuous). Then because the torus $\mathbb{T}^{n-1}$ is compact and path-connected and f is continuous, $f(\mathbb{T}^{n-1})$ is compact and path-connected. Next, we establish that f is a *smooth* map between these manifolds.

Lemma 5.1.1. *f is smooth.*

Proof. See Appendix C.1. □

Notice that because the image of f is compact, its boundary is non-empty. We will recall the definition of a *critical value* of a smooth map and see that the boundary can only contain critical values, thus reducing the problem of finding the boundary of the image of f to a problem of determining the critical values of f and then checking if these critical values lie in the interior of the image. We will need the definition of the rank of a smooth map:

Definition 5.1.1. *(Rank of a smooth map) [52, pg. 96] Let $F : N \to M$ be smooth. The* rank *of F at $p \in N$ is defined as the rank of the differential at p: $dF_p : T_pN \to T_{F(p)}M$. If we choose charts $(U, x^1, \ldots, x^n)$ at p and $(V, y^1, \ldots, y^m)$ at $F(p)$, then*

$$rank F(p) = rank\left(\frac{\partial(y^i \circ F)}{\partial x^j}\right)(p) \tag{5.6}$$

where $\left(\frac{\partial(y^i \circ F)}{\partial x^j}\right)(p)$ is the Jacobian of F w.r.t. these charts.

It is also useful to recall at this point that the rank of a matrix is the number of linearly independent columns. Next, we turn to the definition of a critical value:

Definition 5.1.2. *(Critical value) [52, pg. 97] A point $p \in N$ is a* critical point *if the differential at p*

$$dF_p : T_pN \to T_{F(p)}M \tag{5.7}$$

fails to be surjective. The image of a critical point is said to be a critical value.

This leads us to state an important lemma that will establish a criterion to help us find points on the boundary of the image of f:

Lemma 5.1.2. *Let N be a compact smooth manifold without boundary and let M be a smooth manifold. Let N and M have dimensions n and m respectively, with $n > m$. If $F : N \to M$ is a smooth map, then the boundary of the image of F can only be populated by critical values.*

Proof. See Appendix C.2. □

Let's put this all together: f satisfies the criteria of Lemma 5.1.2 and so we know that the boundary of the image of f is populated solely by critical values of f, which is the same as saying that the differential is not surjective at each point that maps to the boundary of the image. Explicitly, in our case because dim $\mathbb{C} = 2$, failure for df to be surjective at a point means that with respect to some charts centered on that point, the rank of the Jacobian is < 2. So all we need to do is find out at which points $x \in \mathbb{T}^{n-1}$ the Jacobian of f has less than 2 linearly independent columns and we are guaranteed that some subset[1] of these points map to the boundary of the image of f.

Let's proceed. With respect to the obvious charts[2] on $\mathbb{T}^{n-1}$ and the charts we have used already on $\mathbb{C}$, the j-th column in the Jacobian is given by

$$\begin{pmatrix} J^1{}_j \\ J^2{}_j \end{pmatrix} = \begin{pmatrix} \partial_{\theta_j}(\pi^1 \circ f) \\ \partial_{\theta_j}(\pi^2 \circ f) \end{pmatrix} = \frac{1}{n} \begin{pmatrix} -\sin(\theta_j) - \sin(\sum_{k=1}^{n-1} \theta_k) \\ \cos(\theta_j) - \cos(\sum_{k=1}^{n-1} \theta_k) \end{pmatrix} \tag{5.8}$$

We are interested in values of θ_i such that the Jacobian does not have maximal rank, that is it has rank 0 or 1. We eliminate the less interesting case first (less interesting in the sense that it will not fully specify the boundary of the image of f), which is the rank zero case:

Lemma 5.1.3. *The critical values of f that arise due to f having rank zero occur at isolated points. In particular, these points are the n-th roots of unity.*

Proof. See Appendix C.3. □

If we now consider the case rank f = 1, we are able to classify all of the critical values of f, which will lead us closer to obtaining the boundary of the image of f.

[1] As we shall see and as was pointed out to me in public conversations here [51] and here [50], there do exist critical values that lie in the interior of the image of f, as well as on the boundary. However, this will not be as much of a hindrance to determining the boundary of the image as it may initially appear.

[2] We could for example choose the charts that cover $\theta_j \in (0, 2\pi)$ and then work through everything with the charts $\theta_j \in (-\pi, \pi)$ for completeness.

Theorem 5.1.2. *If we define*

$$g(\theta, p, c) := \frac{1}{n}\left(p\, e^{i\,\theta} + (n-p)\, e^{-i\left(\frac{p\,\theta + 2\pi c}{n-p}\right)}\right) \tag{5.9}$$

then the critical values of f are given by

$$\{g(\theta, p, c) \;\big|\; \quad -\frac{2\pi c}{n} \leq \theta \leq 2\pi - \frac{2\pi(p+c)}{n}, \quad p = 1, \ldots, n-1, \quad c = 0, \ldots, n-1\} \tag{5.10}$$

The parameter p arises because in the general rank 1 situation, the Jacobian of f has p columns that are equal (up to a factor of -1) and the remaining $n-p-1$ columns vanish. Geometrically, if a circle of radius $(n-p)/n$ rolls anti-clockwise inside of the unit circle, then $g(\theta, p, 0)$ describes the curve mapped out by a point P on this rolling circle. In particular, the point is taken to begin at $P_0 = (1, 0)$ and the next intersection of P with the unit circle occurs at the n-th root of unity if one counts p roots of unity clockwise from P_0, when $\theta = 2\pi(1 - (p+c)/n$. The parameter c rotates the family of curves $g(\theta, p, 0)$ clockwise by $2\pi c/n$ and so the critical values of f are the union of the family of curves where the initial points on the rolling circles begin at each of the roots of unity and connect to every other root of unity.

Proof. See Appendix C.4. □

Now that we understand that the entire discussion of which points are candidates for boundary points reduces to examining circles of specific radii rolling inside of the unit circle and determining for which values of p and c $g(\theta, p, c)$ lies in the interior of the image, we complete the proof of our main result Theorem 5.1.1 by proving that all points $g(\theta, p, c)$ lie on the n-cusp hypocycloid or in the interior of the region that it bounds. This last step follows immediately from Theorem 5.1.2 and so we inspect the content of this theorem more closely. Figure 5.2 shows the critical values of f for some values of n:

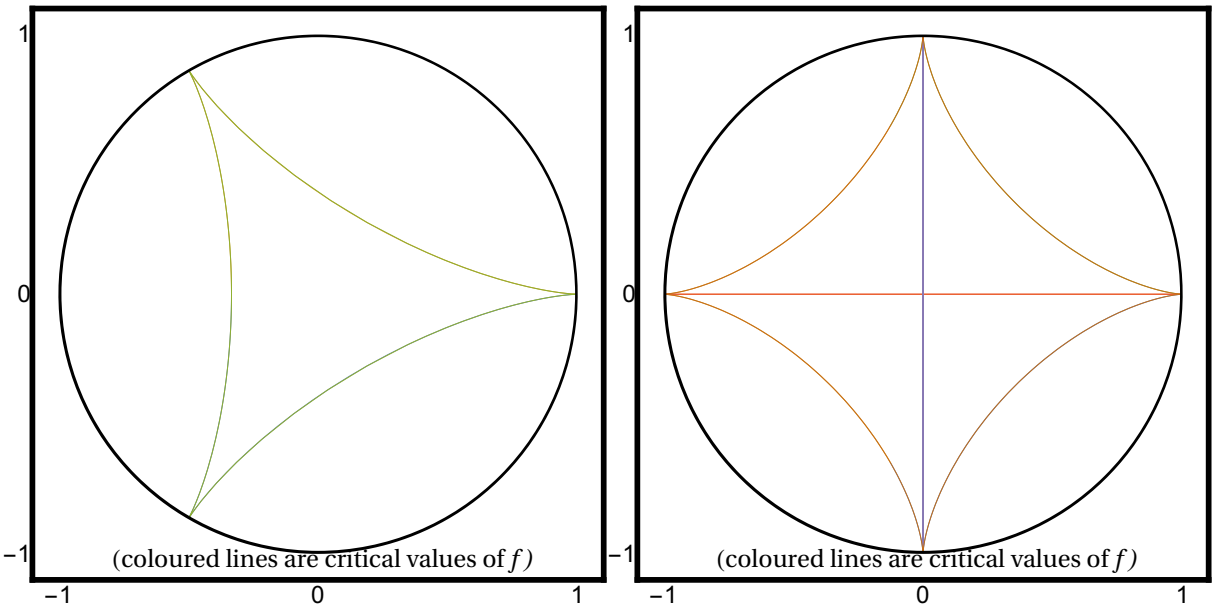

(A) $n = 3$ (B) $n = 4$

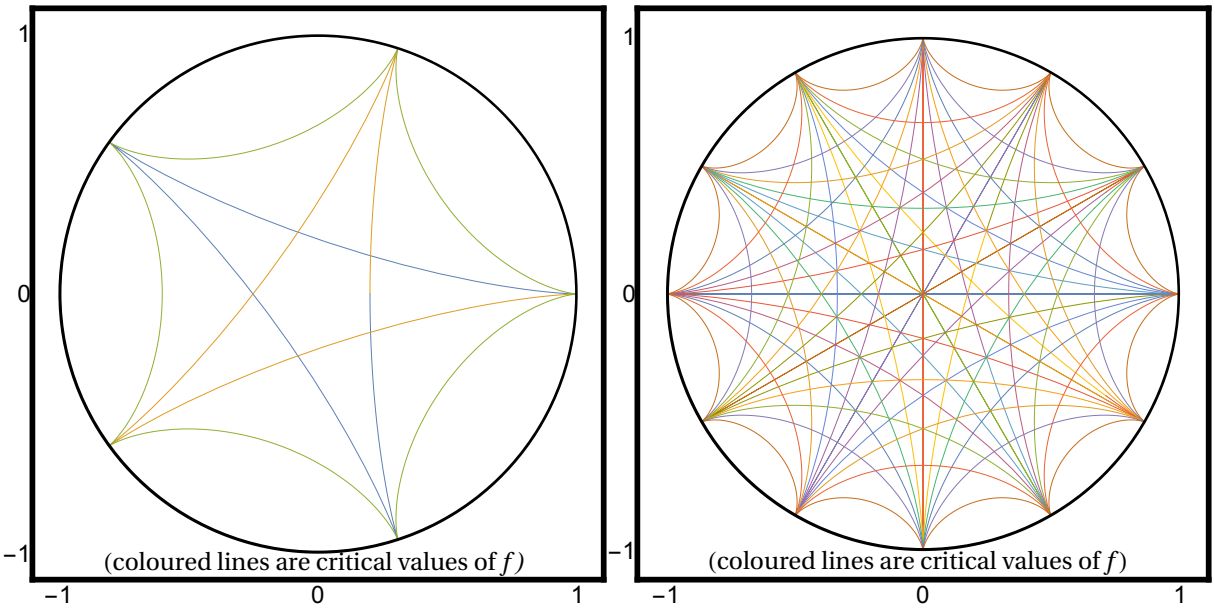

(C) $n = 5$ (D) $n = 12$

FIGURE 5.2: Visualisation of the critical values of f as derived in Theorem 5.1.2. For $n \geq 4$, there exist families of critical points that lie in the interior of the image of f.

As stated in Theorem 5.1.2, the critical values displayed in Figure 5.2 are a result of the curves $g(\theta, p, 0)$ being rotated through all[1] multiples of the n-th roots of unity. The curves $g(\theta, p, 0)$ are displayed in Figure 5.3:

[1]One might wonder if we could simply choose $c = 0$ and allow θ to vary over a larger domain to obtain all of the critical values of f. The answer is no for even values of $n \geq 6$: there are curves of critical values that cannot be obtained for any value of θ if $c = 0$.

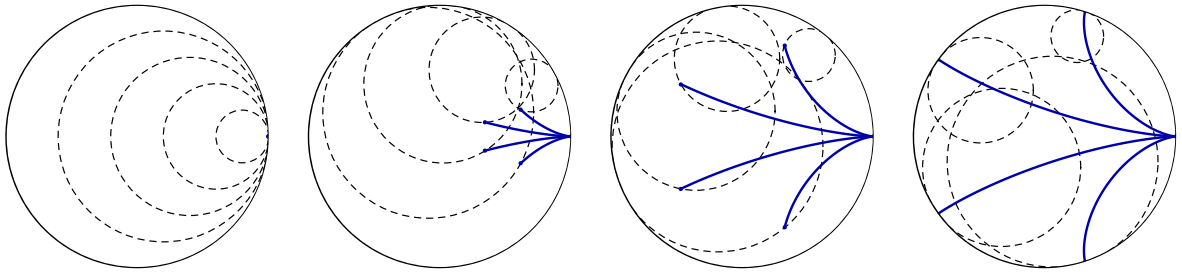

(A) $\theta = 0$ (B) $\theta = \frac{2}{5}\frac{2\pi(n-p)}{n}$ (C) $\theta = \frac{7}{10}\frac{2\pi(n-p)}{n}$ (D) $\theta = \frac{2\pi(n-p)}{n}$

FIGURE 5.3: The curves $g(\theta, p, 0)$, $n = 5$ (blue) as the circles with radii $(n-p)/n$, $p = 1, \ldots, n-1$ roll inside of the unit circle. These curves intersect the unit circle at the n-th roots of unity once each of the rolling circles has completed a full revolution.

The result of rotating the curves $g(\theta, p, 0)$ through the roots of unity is displayed in Figure 5.4:

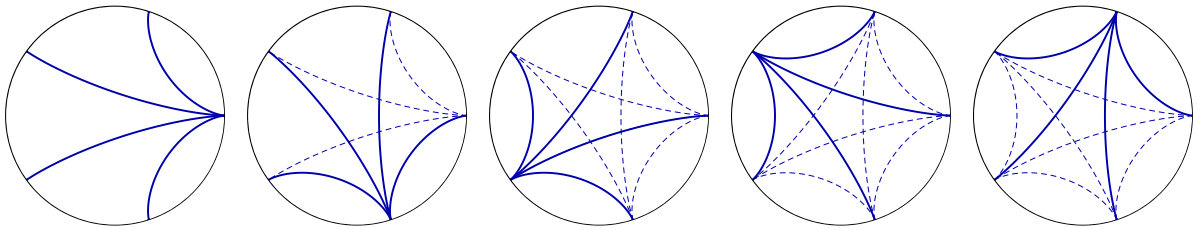

(A) $c = 0$ (B) $c = 1$ (C) $c = 2$ (D) $c = 3$ (E) $c = 4$

FIGURE 5.4: The curves $g(\theta, p, 0)$, $n = 5$ are rotated as $c = 0, \ldots, n-1$ varies, generating all of the critical values of f.

Then altogether, we have that for any n, the curve $g(\theta, n-1, 0),\ 0 \leq \theta \leq 2\pi/n$ forms a part of the boundary of the image of f, because it results from a rolling circle with radius $1/n$, which is the smallest possible radius among the rolling circles. Then because the critical values are symmetric under rotations by the n roots of unity, the boundary of the image of f is given by $g(\theta, n-1, c),\ 0 \leq \theta \leq 2\pi/n,\ c = 0, \ldots n-1$. But this is exactly the curve $g(\theta, n-1, 0),\ 0 \leq \theta \leq 2\pi$, which is the n-cusp hypocycloid. This completes the proof of Theorem 5.1.1. Notice that the proof given in [45] forms the boundary of the image by picking out the curves $g(\theta, n-1, 0),\ 0 \leq \theta \leq 2\pi$, but doesn't explain why we can ignore the other possible curves of critical values.

This proof of Theorem 5.1.1 has its benefits and its drawbacks. Recall that our hope is to be able to generalise this proof so that we can determine the images in the complex plane of slightly more complicated Wilson line operators. Certainly the precise discussion of critical values and method of considering all possible ways in which the Jacobian might fail to have maximal rank used in the proof of Theorem 5.1.1 is fully general. However, the resulting equations were significantly easier to massage into an interpretable form than the equations that arise when dealing with four point functions and so it may be the case that this method is not practically applicable to more

complicated Wilson line operators - we are not certain one way or the other as of yet. Nonetheless, the following section contains the heuristic results that we have so far for the four point functions.

5.2 Bounds on $(q\bar{q})^2$

In this section, we turn to the study of the images of the four-point operators describing two quark-antiquark pairs. We have seen in Section 2.1.2 that this means working with the amplitude matrix

$$\mathcal{A}(Y) := \begin{pmatrix} \left\langle \frac{\operatorname{tr}(U_{\boldsymbol{x_1}} U^\dagger_{\boldsymbol{x_2}}) \operatorname{tr}(U_{\boldsymbol{x_3}} U^\dagger_{\boldsymbol{x_4}})}{N_c^2} \right\rangle_Y & \left\langle \frac{\operatorname{tr}(U_{\boldsymbol{x_1}} t^a U^\dagger_{\boldsymbol{x_2}}) \operatorname{tr}(U_{\boldsymbol{x_3}} t^a U^\dagger_{\boldsymbol{x_4}})}{N_c \sqrt{d_A/4}} \right\rangle_Y \\ \left\langle \frac{\operatorname{tr}(U_{\boldsymbol{x_1}} U^\dagger_{\boldsymbol{x_2}} t^b) \operatorname{tr}(U_{\boldsymbol{x_3}} U^\dagger_{\boldsymbol{x_4}} t^b)}{N_c \sqrt{d_A/4}} \right\rangle_Y & \left\langle \frac{\operatorname{tr}(U_{\boldsymbol{x_1}} t^a U^\dagger_{\boldsymbol{x_2}} t^b) \operatorname{tr}(U_{\boldsymbol{x_3}} t^a U^\dagger_{\boldsymbol{x_4}} t^b)}{d_A/4} \right\rangle_Y \end{pmatrix} \tag{5.11}$$

We again switch notation to use $n := N_c$ to simplify our presentation. The Fierz identity allows us to cast the operators appearing in $[\mathcal{A}(Y)]_{12}$ and $[\mathcal{A}(Y)]_{22}$ in a form that is more amenable to analysis (the image of the operator in $[\mathcal{A}(Y)]_{21}$ is the same as that of $[\mathcal{A}(Y)]_{12}$). In the case of $[\mathcal{A}(Y)]_{12}$ we have

$$\frac{1}{n} \operatorname{tr}(U_{\boldsymbol{x_1}} t^a U^\dagger_{\boldsymbol{x_2}}) \operatorname{tr}(U_{\boldsymbol{x_3}} t^a U^\dagger_{\boldsymbol{x_4}}) = \frac{1}{n} \operatorname{tr}(U^\dagger_{\boldsymbol{x_4}} U_{\boldsymbol{x_3}} U^\dagger_{\boldsymbol{x_2}} U_{\boldsymbol{x_1}}) - \frac{1}{n^2} \operatorname{tr}(U_{\boldsymbol{x_1}} U^\dagger_{\boldsymbol{x_2}}) \operatorname{tr}(U_{\boldsymbol{x_3}} U^\dagger_{\boldsymbol{x_4}}) \tag{5.12}$$

and for $[\mathcal{A}(Y)]_{22}$ we have

$$\frac{1}{n^2-1} \operatorname{tr}(U_{\boldsymbol{x_1}} t^a U^\dagger_{\boldsymbol{x_2}} t^b) \operatorname{tr}(U_{\boldsymbol{x_3}} t^a U^\dagger_{\boldsymbol{x_4}} t^b) \tag{5.13a}$$

$$= \frac{1}{n^2-1} \Bigg(\operatorname{tr}(U_{\boldsymbol{x_1}} U^\dagger_{\boldsymbol{x_4}}) \operatorname{tr}(U^\dagger_{\boldsymbol{x_2}} U_{\boldsymbol{x_3}}) - \frac{1}{n} \operatorname{tr}(U_{\boldsymbol{x_1}} U^\dagger_{\boldsymbol{x_2}} U_{\boldsymbol{x_3}} U^\dagger_{\boldsymbol{x_4}}) \tag{5.13b}$$

$$- \frac{1}{n} \operatorname{tr}(U^\dagger_{\boldsymbol{x_4}} U_{\boldsymbol{x_3}} U^\dagger_{\boldsymbol{x_2}} U_{\boldsymbol{x_1}}) + \frac{1}{n^2} \operatorname{tr}(U_{\boldsymbol{x_1}} U^\dagger_{\boldsymbol{x_2}}) \operatorname{tr}(U_{\boldsymbol{x_3}} U^\dagger_{\boldsymbol{x_4}}) \Bigg) \tag{5.13c}$$

We gain some insight by numerically generating random $SU(n)$ matrices and checking their image under the operators in $\mathcal{A}(Y)$. Notice that it is sufficient to make the simplification that we generate

$$\mathcal{O}_{11} := \frac{1}{n^2} \operatorname{tr}(U_1) \operatorname{tr}(U_2) \tag{5.14a}$$

$$\mathcal{O}_{12} := \frac{1}{n} \operatorname{tr}(U_1 U_2) - \frac{1}{n^2} \operatorname{tr}(U_1) \operatorname{tr}(U_2) \tag{5.14b}$$

$$\mathcal{O}_{22} := \frac{1}{n^2-1} \Bigg(\operatorname{tr}(U_1 U_2) \operatorname{tr}(U_3) - \frac{1}{n} \operatorname{tr}(U_1 U_2 U_3) - \frac{1}{n} \operatorname{tr}(U_3 U_2 U_1) + \frac{1}{n^2} \operatorname{tr}(U_1) \operatorname{tr}(U_2 U_3) \Bigg) \tag{5.14c}$$

for random[1] $U_1, U_2, U_3 \in SU(n)$, where we group the unitary matrices according to

$$\mathcal{O}_{11} : U_{\boldsymbol{x_1}} U^\dagger_{\boldsymbol{x_2}} \to U_1, \quad U_{\boldsymbol{x_3}} U^\dagger_{\boldsymbol{x_4}} \to U_2 \tag{5.15a}$$

$$\mathcal{O}_{12} : U^\dagger_{\boldsymbol{x_2}} U_{\boldsymbol{x_1}} \to U_1, \quad U^\dagger_{\boldsymbol{x_4}} U_{\boldsymbol{x_3}} \to U_2 \tag{5.15b}$$

$$\mathcal{O}_{22} : U^\dagger_{\boldsymbol{x_4}} U_{\boldsymbol{x_3}} \to U_1, \quad U^\dagger_{\boldsymbol{x_3}} U_{\boldsymbol{x_1}} \to U_2, \quad U^\dagger_{\boldsymbol{x_2}} U_{\boldsymbol{x_3}} \to U_3 \tag{5.15c}$$

The result of simulating $\mathcal{O}_{11}, \mathcal{O}_{12}$, and $\mathcal{O}_{22}$ for random $U_1, U_2, U_3 \in SU(n)$ is displayed in Figures 5.5 to 5.7:

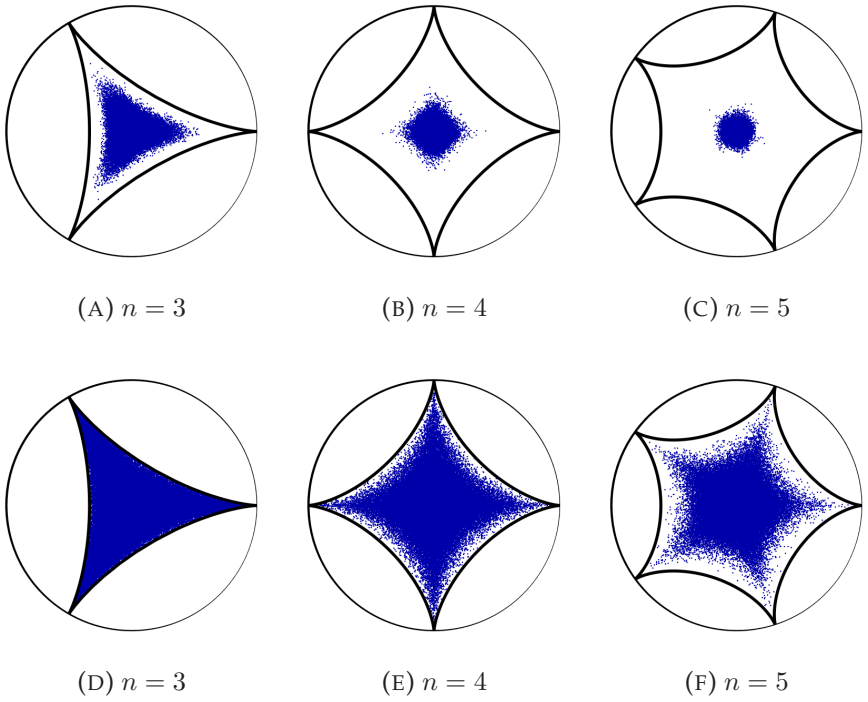

(A) $n = 3$ (B) $n = 4$ (C) $n = 5$

(D) $n = 3$ (E) $n = 4$ (F) $n = 5$

FIGURE 5.5: $\mathcal{O}_{11}$ generated for 100,000 random $SU(n)$ matrices (first row). Using only diagonal $SU(n)$ matrices fills out the image more clearly (second row). The unit circle and the n-cusp hypocycloid are overlaid.

[1]For a more detailed discussion of simulating random $SU(n)$ matrices, see [53].

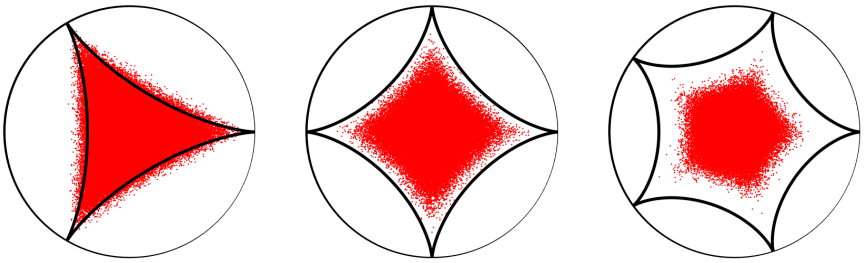

(A) $n = 3$ (B) $n = 4$ (C) $n = 5$

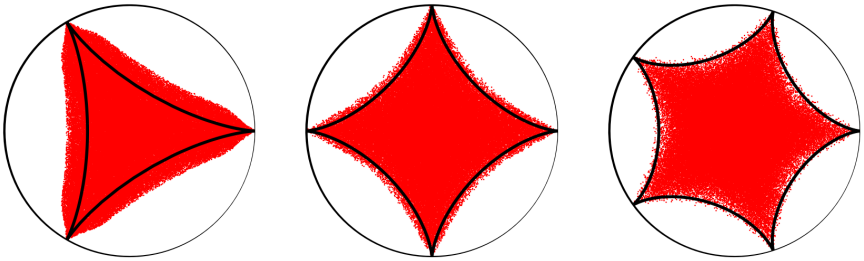

(D) $n = 3$ (E) $n = 4$ (F) $n = 5$

FIGURE 5.6: $\mathcal{O}_{12}$ generated for 100,000 random $SU(n)$ matrices (first row). Using only diagonal $SU(n)$ matrices fills out the image more clearly (second row). The unit circle and the n-cusp hypocycloid are overlaid.

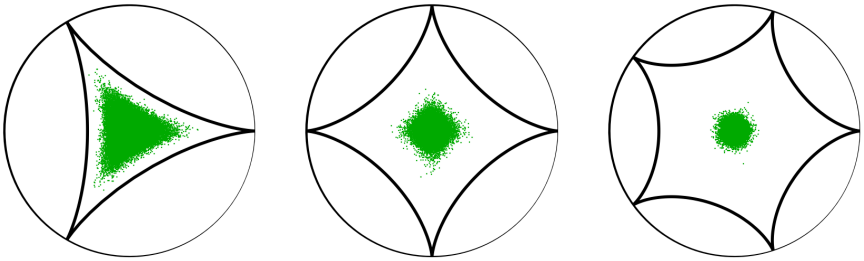

(A) $n = 3$ (B) $n = 4$ (C) $n = 5$

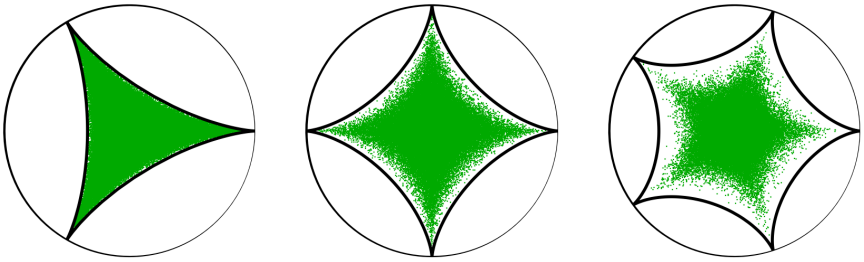

(D) $n = 3$ (E) $n = 4$ (F) $n = 5$

FIGURE 5.7: $\mathcal{O}_{22}$ generated for 100,000 random $SU(n)$ matrices (first row). Using only diagonal $SU(n)$ matrices fills out the image more clearly (second row). The unit circle and the n-cusp hypocycloid are overlaid.

Figures 5.5 to 5.7 carry several important features. First, it seems that the image of the operators $\mathcal{O}_{11}$ and $\mathcal{O}_{22}$ is again the n-cusp hypocycloid, whereas the image of $\mathcal{O}_{12}$ is very clearly *not* the n-cusp hypocycloid, although does appear to be bounded by the unit circle. We are currently unsure what geometric figure (if any name exists) the image of $\mathcal{O}_{12}$ fills out. Next, it seems clear that there is an effect that diagonal $SU(n)$ matrices are sufficient to fill out the boundary of the image of these operators. This is a useful simplifcation, although we do not currently have a proof of this observation. Lastly, it is an interesting feature that with increasing n there seems to be some suppression effect where the image of random matrices are more and more likely to cluster around the origin (although we don't expect this to mean that the conjectured images are not fully filled out by the entire group).

However, thus far we have been unable to prove any statements about the observed behaviour of the images of $\mathcal{O}_{11}, \mathcal{O}_{12}, \mathcal{O}_{22}$, except that all of these operators are bounded by the unit circle, which is a useful result for numerical simulations of JIMWLK evolution in that it rules out blowup. The image of $\mathcal{O}_{11}$ is trivially bounded by the unit circle: it is just the product of two dipole operators, each of which has norm ≤ 1 for all $U \in SU(n)$. The cases of $\mathcal{O}_{12}$ and $\mathcal{O}_{22}$ are addressed by Proposition 5.2.1 and Proposition 5.2.2 respectively.

Proposition 5.2.1. *For $SU(n)$ matrices U_1, U_2*

$$|\mathcal{O}_{12}| := \frac{1}{n}\left|\operatorname{tr}(U_1U_2) - \frac{1}{n}\operatorname{tr}(U_1)\operatorname{tr}(U_2)\right| \leq 1 \tag{5.16}$$

Proof. See Appendix C.5. □

Proposition 5.2.2. *For $SU(n)$ matrices U_1, U_2, U_3 with $n \geq 2$*

$$|\mathcal{O}_{22}| := \frac{1}{n^2-1}\left|\operatorname{tr}(U_2U_1)\operatorname{tr}(U_3) - \frac{1}{n}\operatorname{tr}(U_2U_3U_1) - \frac{1}{n}\operatorname{tr}(U_2U_1U_3) + \frac{1}{n^2}\operatorname{tr}(U_1)\operatorname{tr}(U_2U_3)\right| \tag{5.17a}$$

$$\leq 1 \tag{5.17b}$$

Proof. We provide two proofs of Proposition 5.2.2 in Appendix C.6. □

Altogether, we have that every entry of the amplitude matrix for two quark-antiquark pairs is bounded by the unit circle. This concludes the section.

5.3 Concluding remarks on bounding these operators

In this chapter, we have attempted to explore information about CGC correlators in a manner that is complementary to the approach of seeking approximate solutions to JIMWLK. Our first result was to show that the image of the dipole operator is bounded by the hypocycloid with N_c cusps, inscribed in the unit circle. While this observation is stated several times in the literature, this result has lacked clear proof. A proof has now been established in Section 5.1. Going beyond the dipole correlator to the case of two quark-antiquark pairs, we have seen numerical evidence that the diagonal elements of the amplitude matrix again have images that are bounded by the hypocycloid with N_c-cusps, although proof of this has eluded us thus far. We have also seen evidence that the off-diagonal elements of $\mathcal{A}(Y)$ in this case are explicitly *not* bounded by the N_c-cusp hypocycloid. Nonetheless, we were able to prove that both the diagonal and off-diagonal elements of the amplitude matrix for two quark-antiquark pairs are bounded by the unit circle.

In future we hope to be able to extend these preliminary results, possibly using the methods of Section 5.1 as a guide. We tentatively conjecture that the image of every diagonal element of $\mathcal{A}(Y)$ for an arbitrary number of Wilson lines always lies in the hypocycloid with N_c cusps. Furthermore, the unusual geometric structure of the images of the off-diagonal elements is intriguing and remains to be determined in general.

Chapter 6

Conclusions and outlook

"The early bird gets the worm, but the second mouse gets the cheese."

Unknown source

This dissertation has both resolved and paved the way for several new questions about CGC correlators under JIMWLK evolution.

We have seen that the full JIMWLK evolution of any CGC correlator results in an infinite hierarchy of coupled functional differential equations, with there being no known way to solve such a hierarchy currently. The standard approach in the literature to extracting analytic solutions from this hierarchy is to take the large N_c limit, which produces a single equation that depends on the dipole operators (the BK equation), but as we have noted, the BK equation makes certain correlators that only appear at finite N_c inaccessible. We briefly reviewed the finite N_c truncation scheme of R. Moerman and H. Weigert (see Section 2.3 and [1]), which is argued to be the most general finite N_c truncation scheme possible that still preserves independent evolution of symmetric and antisymmetric parts of any matrix of Wilson line correlators and preserves all group-theoretic coincidence limits imposed by JIMWLK, with both of these properties being known to hold for any exact solution of JIMWLK. This truncation scheme motivated the need to construct the adjoint color structures, which form a basis for the space of tensors with purely adjoint indices within the space of color singlets, which we call the adjoint color singlet space. We have been able to establish several exact properties of these adjoint color structures, some of which have lead to new questions that we hope will be resolved in future research.

Using approximate solutions (especially those of the new truncation scheme of R. Moerman and H. Weigert) to work through the problem of infinite hierarchies of coupled equations for the evolution of CGC correlators was a significant theme of this dissertation. But we have also devoted some energy to the secondary goal of investigating other properties of these CGC correlators that can be determined analytically without needing to solve these infinite hierarchies. In particular, we've shown that one can make powerful exact statements about the images of CGC operators in the complex plane and that several intriguing open questions arise from this research.

In conclusion, we summarise the new results presented in this dissertation and reiterate several open questions that have been encountered in this work. Where possible, we suggest plausible avenues of investigation that may help resolve these remaining questions, noting that these are interesting directions for future research.

6.1 New results established in this dissertation

One significant contribution of this dissertation is to give a new construction for the adjoint color structures that is entirely general in the sense that it can be systematically carried out for an arbitrary number of adjoint indices, at arbitrary N_c (Chapters 3 and 4). The construction is conceptually straightforward: we simply project the non-orthogonal trace basis for the adjoint color singlet space onto a set of orthogonal subspaces using the recently-discovered Hermitian Young projection operators [2–4]. If any of the subspaces that are projected onto have dimension greater than one, we use Gram-Schmidt orthogonalisation within these subspaces. Then, we obtain an orthogonal basis for the adjoint color singlet space, with the added strengths that we avoid having to construct every multiplet that appears in decomposition of $A^{\otimes k}$ (as is required by the construction of [22], for example), and each basis element encodes the symmetries of an irreducible representation of S_k associated with the Hermitian Young projection that created the basis element. This construction is further validated by showing that it reproduced the natural basis expected in the cases of two and three adjoint indices, and that with minimal effort we could explicitly write down a basis for the case of four adjoint indices (which is the maximum number of indices likely to be considered in practical application to R. Moerman and H. Weigert's truncation scheme in the near future).

The next series of results that we've presented in this dissertation were all established by introducing abstract mathematical concepts from representation theory in order to be able to predict which Hermitian Young projection operators would return non-zero projections when acting on the adjoint color singlet space, or equivalently, in order to predict the multiplicities of irreducible representations of S_k in decomposing the adjoint color singlet space (Chapter 4). The important realisation was that the adjoint color singlet space can always be viewed as the direct sum of representations of S_k induced by subgroups of S_k that describe the symmetries of derangements of different cycle types. This allowed us to calculate the irreducible multiplicities in a systematic and simple manner using the orthogonality of irreducible characters, because Frobenius reciprocity always allows us to relate the induced characters to restricted characters, which are trivial in this construction. Viewing the adjoint color singlet space in terms of induced representations and using Frobenius reciprocity also allowed us to show that every adjoint color structure is always real or purely imaginary, and for arbitrary k, we can always predict which adjoint color structures will be real or purely imaginary.

Lastly, this dissertation has contributed a short series of results on the images of Wilson line operators that are commonly used in the CGC context (Chapter 5). We have presented a new proof that the image of the dipole operator is the hypocycloid with N_c cusps, inscribed in the unit circle (equivalently: the image of the normalised trace of $SU(N_c)$ matrices is the N_c-cusp hypocycloid). We have also shown that all of the four-point Wilson line operators that appear in the $(q\bar{q})^2$ JIMWLK evolution amplitude matrix are bounded by the unit circle.

6.2 Open questions for future research

Our work here has both provided possible frameworks for answering several open questions about the JIMWLK evolution of CGC correlators and generate new research questions in this area.

While it has not been a focus of this dissertation, an important question is raised in using the truncation of R. Moerman and H. Weigert [1]: it is not currently known how to derive an error term for this truncation, or a systematic way of knowing how many terms in the expansion need to be included for desired accuracy in a given correlator's evolution. It has been suggested [54] that perhaps some progress might be made through trying to relate this expansion to the expansions in terms of Feynman diagrams that appear in the study of Multiple Gluon Exchange Webs [55–58], using the Magnus expansion [59].

Another topic that we have encountered but not fully resolved is the question of how to ensure that the Hermitian Young projection operator basis for the adjoint color singlet space is fully orthogonal, without needing to apply Gram-Schmidt orthogonalisation within orthogonal subspaces that are associated with each projection operator. One way of resolving this is to simply avoid our construction and instead recursively construct a full set of orthogonal projection operators onto every irreducible representation of $SU(N_c)$ in $A^{\otimes k}$ (see [22]), then disregard the operators that do not project onto singlets. But if one prefers the efficiency of directly constructing the basis for the singlets, then a possible resolution that we have noted is that one could systematically construct orthogonal projection operators that project onto derangements of differing cycle types and then combine these with the Hermitian Young projection operators, because orthogonality seems to fail exclusively when derangements of differing cycle types induce the same irreducible representation of S_k (Section 4.3).

Lastly, in the study of the images in the complex plane of Wilson line operators (Chapter 5), we have seen numerical evidence (Figures 5.5 to 5.7) that the operators appearing in the diagonal elements of the amplitude matrix for two quark-antiquark pairs are bounded by the hypocycloid with N_c cusps, and the operators appearing in the off-diagonal elements of this matrix are bounded by some unknown geometric shape that is larger than the N_c-cusp hypocycloid. However, a proof of these observations has eluded us thus far. We hope that one might use the method of Section 5.1 (where we proved that the image of the dipole operator is the N_c-cusp hypocycloid) to prove these statements, but the equations that appeared there can become unwieldy as the eigenvalues of multiple matrices become involved. Figures 5.5 to 5.7 seem to suggest that one can simplify things by using only diagonal $SU(N_c)$ matrices and then prove that the full image of these operators lies within the image obtained by only working with diagonal matrices. Perhaps this is enough for one to solve these equations directly via some clever arguments, or maybe what is needed is further constraints on the matrix arguments of these operators, supplemented by a proof that this is sufficient to bound the images. Even more ambitiously, one might conjecture that the operator in each diagonal element of the full untruncated (infinite) amplitude matrix is bounded by the N_c-cusp hypocycloid, which again may be difficult to prove for the reasons already mentioned.

Appendix A

Birdtracks for our purposes

We give a brief introduction to Birdtracks for reference so that this dissertation is relatively self-contained (for full development of the theory, see [35]). For our purposes, we will use Birdtracks to represent the action of elements of the symmetric group S_n on n-index objects by simply drawing lines with arrows to show where indices are mapped to. For example, we can compare the usual cycle notation for the symmetric group and Birdtracks in the case of the action of the two elements of S_2 on an object with 2 indices:

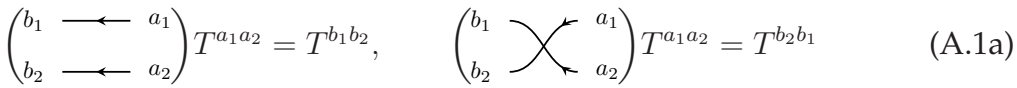

(A.1a)

$$\iff (1)(2)T^{a_1 a_2} = T^{a_1 a_2}, \qquad (12)T^{a_1 a_2} = T^{a_2 a_1} \tag{A.1b}$$

We will always act "from the left" as depicted above and otherwise we drop the labelling of indices and arrows on Birdtracks where the action is obvious from context.

Recall that for each n, we can form the totally symmetric and totally antisymmetric group algebra elements

$$\boldsymbol{S}_n := \frac{1}{n!} \sum_{\sigma \in S_n} \sigma, \qquad \boldsymbol{A}_n := \frac{1}{n!} \sum_{\sigma \in S_n} \text{sign}(\sigma)\, \sigma \tag{A.2}$$

These objects are of critical importance to constructing the Hermitian Young projection operators used in our method for constructing a basis for the adjoint color singlet space. In Birdtracks, $\boldsymbol{S}_n$ and $\boldsymbol{A}_n$ are represented by white rectangles and black rectangles respectively, with n ingoing and outgoing legs. For example, at $n = 4$ we write

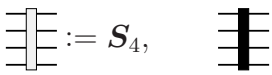

(A.3)

This notation is useful, because it compactly represents the $n!$ objects contained in symmetrizing or anti-symmetrizing on n indices. In addition, known results involving contraction between totally symmetric and totally antisymmetric objects are starkly visually represented. Some typical examples are:

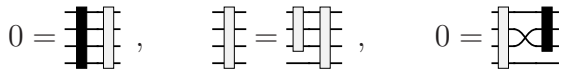

(A.4)

Appendix B

Proofs and calculations encountered in constructing the adjoint color structures

B.1 Intermediate steps in calculating the adjoint color structures, $k = 4$

When $k = 4$, we have the following Hermitian Young projection operators:

$P_{\begin{array}{|c|c|c|c|}\hline 1&2&3&4\\\hline\end{array}} =$  (B.1a)

$P_{\begin{array}{|c|c|c|}\hline 1&2&3\\\hline 4\\\cline{1-1}\end{array}} = \frac{3}{2}$ 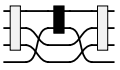 , $P_{\begin{array}{|c|c|c|}\hline 1&2&4\\\hline 3\\\cline{1-1}\end{array}} = 2$ 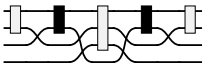 , $P_{\begin{array}{|c|c|c|}\hline 1&3&4\\\hline 2\\\cline{1-1}\end{array}} = \frac{3}{2}$ 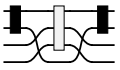 (B.1b)

$P_{\begin{array}{|c|c|}\hline 1&2\\\hline 3&4\\\hline\end{array}} = \frac{4}{3}$ 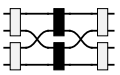 , $P_{\begin{array}{|c|c|}\hline 1&3\\\hline 2&4\\\hline\end{array}} = \frac{4}{3}$ 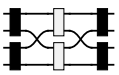 (B.1c)

$P_{\begin{array}{|c|c|}\hline 1&2\\\hline 3\\\cline{1-1}4\\\cline{1-1}\end{array}} = \frac{3}{2}$ 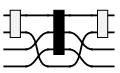 , $P_{\begin{array}{|c|c|}\hline 1&3\\\hline 2\\\cline{1-1}4\\\cline{1-1}\end{array}} = 2$ 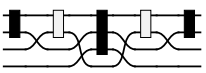 , $P_{\begin{array}{|c|c|}\hline 1&4\\\hline 2\\\cline{1-1}3\\\cline{1-1}\end{array}} = \frac{3}{2}$ 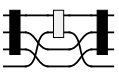 (B.1d)

$P_{\begin{array}{|c|}\hline 1\\\hline 2\\\hline 3\\\hline 4\\\hline\end{array}} =$  (B.1e)

The trace basis for $\mathcal{S}(A^{\otimes 4})$ has 9 elements, 6 of which have associated cycle type as derangements $\mu = (4)$ and 3 of which have associated cycle type $\mu = (2, 2)$. Then if $v = \sum_i c_i v_i$ is an arbitrary element of $\mathcal{S}(A^{\otimes 4})$ with respect to the trace basis, we have the

following projections:

$$P_{\ydiagram{4}}\, v = \frac{c_1'}{6}\Big(\operatorname{tr}(t^{a_1}t^{a_2}t^{a_3}t^{a_4}) + \operatorname{tr}(t^{a_1}t^{a_2}t^{a_4}t^{a_3}) + \operatorname{tr}(t^{a_1}t^{a_3}t^{a_2}t^{a_4}) \tag{B.2a}$$

$$+ \operatorname{tr}(t^{a_1}t^{a_3}t^{a_4}t^{a_2}) + \operatorname{tr}(t^{a_1}t^{a_4}t^{a_2}t^{a_3}) + \operatorname{tr}(t^{a_1}t^{a_4}t^{a_3}t^{a_2})\Big) \tag{B.2b}$$

$$+ \frac{c_2'}{3}\Big(\operatorname{tr}(t^{a_1}t^{a_4})\operatorname{tr}(t^{a_2}t^{a_3}) + \operatorname{tr}(t^{a_1}t^{a_3})\operatorname{tr}(t^{a_2}t^{a_4}) + \operatorname{tr}(t^{a_1}t^{a_2})\operatorname{tr}(t^{a_3}t^{a_4})\Big) \tag{B.2c}$$

$$P_{\begin{smallmatrix}\ydiagram{3}\\ \ydiagram{1}\end{smallmatrix}}\, v = 0, \quad P_{\begin{smallmatrix}\ydiagram{3}\\ \ydiagram{1}\end{smallmatrix}}\, v = 0, \quad P_{\begin{smallmatrix}\ydiagram{3}\\ \ydiagram{1}\end{smallmatrix}}\, v = 0 \tag{B.2d}$$

$$P_{\begin{smallmatrix}\ydiagram{2}\\ \ydiagram{2}\end{smallmatrix}}\, v = \frac{c_3'}{12}\Big(\operatorname{tr}(t^{a_1}t^{a_2}t^{a_3}t^{a_4}) + \operatorname{tr}(t^{a_1}t^{a_2}t^{a_4}t^{a_3}) - 2\operatorname{tr}(t^{a_1}t^{a_3}t^{a_2}t^{a_4}) \tag{B.2e}$$

$$+ \operatorname{tr}(t^{a_1}t^{a_3}t^{a_4}t^{a_2}) - 2\operatorname{tr}(t^{a_1}t^{a_4}t^{a_2}t^{a_3}) + \operatorname{tr}(t^{a_1}t^{a_4}t^{a_3}t^{a_2})\Big) \tag{B.2f}$$

$$- \frac{c_4'}{6}\Big(\operatorname{tr}(t^{a_1}t^{a_4})\operatorname{tr}(t^{a_2}t^{a_3}) + \operatorname{tr}(t^{a_1}t^{a_3})\operatorname{tr}(t^{a_2}t^{a_4}) - 2\operatorname{tr}(t^{a_1}t^{a_2})\operatorname{tr}(t^{a_3}t^{a_4})\Big) \tag{B.2g}$$

$$P_{\begin{smallmatrix}\ydiagram{2}\\ \ydiagram{2}\end{smallmatrix}}\, v = \frac{c_5'}{4}\Big(\operatorname{tr}(t^{a_1}t^{a_2}t^{a_3}t^{a_4}) - \operatorname{tr}(t^{a_1}t^{a_2}t^{a_4}t^{a_3}) - \operatorname{tr}(t^{a_1}t^{a_3}t^{a_4}t^{a_2}) \tag{B.2h}$$

$$+ \operatorname{tr}(t^{a_1}t^{a_4}t^{a_3}t^{a_2})\Big) \tag{B.2i}$$

$$+ \frac{c_6'}{2}\Big(\operatorname{tr}(t^{a_1}t^{a_4})\operatorname{tr}(t^{a_2}t^{a_3}) - \operatorname{tr}(t^{a_1}t^{a_3})\operatorname{tr}(t^{a_2}t^{a_4})\Big) \tag{B.2j}$$

$$P_{\begin{smallmatrix}\ydiagram{2}\\ \ydiagram{1}\\ \ydiagram{1}\end{smallmatrix}}\, v = \frac{c_7'}{4}\Big(\operatorname{tr}(t_{a_1}t_{a_2}t_{a_3}t_{a_4}) - \operatorname{tr}(t_{a_1}t_{a_2}t_{a_4}t_{a_3}) + \operatorname{tr}(t_{a_1}t_{a_3}t_{a_4}t_{a_2}) \tag{B.2k}$$

$$- \operatorname{tr}(t_{a_1}t_{a_4}t_{a_3}t_{a_2})\Big) \tag{B.2l}$$

$$P_{\begin{smallmatrix}\ydiagram{2}\\ \ydiagram{1}\\ \ydiagram{1}\end{smallmatrix}}\, v = \frac{c_8'}{12}\Big(\operatorname{tr}(t^{a_1}t^{a_2}t^{a_3}t^{a_4}) + \operatorname{tr}(t^{a_1}t^{a_2}t^{a_4}t^{a_3}) + 2\operatorname{tr}(t^{a_1}t^{a_3}t^{a_2}t^{a_4}) \tag{B.2m}$$

$$- \operatorname{tr}(t^{a_1}t^{a_3}t^{a_4}t^{a_2}) - 2\operatorname{tr}(t^{a_1}t^{a_4}t^{a_2}t^{a_3}) - \operatorname{tr}(t^{a_1}t^{a_4}t^{a_3}t^{a_2})\Big) \tag{B.2n}$$

$$P_{\begin{smallmatrix}\ydiagram{2}\\ \ydiagram{1}\\ \ydiagram{1}\end{smallmatrix}}\, v = \frac{c_9'}{6}\Big(\operatorname{tr}(t^{a_1}t^{a_2}t^{a_3}t^{a_4}) + \operatorname{tr}(t^{a_1}t^{a_2}t^{a_4}t^{a_3}) - \operatorname{tr}(t^{a_1}t^{a_3}t^{a_2}t^{a_4}) \tag{B.2o}$$

$$- \operatorname{tr}(t^{a_1}t^{a_3}t^{a_4}t^{a_2}) + \operatorname{tr}(t^{a_1}t^{a_4}t^{a_2}t^{a_3}) - \operatorname{tr}(t^{a_1}t^{a_4}t^{a_3}t^{a_2})\Big) \tag{B.2p}$$

$$P_{\begin{smallmatrix}\ydiagram{1}\\ \ydiagram{1}\\ \ydiagram{1}\\ \ydiagram{1}\end{smallmatrix}}\, v = 0 \tag{B.2q}$$

where

$$c_1' := c_1 + c_2 + c_3 + c_4 + c_5 + c_6 \tag{B.2r}$$
$$c_2' := c_7 + c_8 + c_9 \tag{B.2s}$$
$$c_3' := c_1 - 2c_2 + c_3 + c_4 - 2c_5 + c_6 \tag{B.2t}$$
$$c_4' := 2c_7 - c_8 - c_9 \tag{B.2u}$$
$$c_5' := c_1 - c_3 - c_4 + c_6 \tag{B.2v}$$
$$c_6' := c_8 - c_9 \tag{B.2w}$$
$$c_7' := c_1 - c_3 + c_4 - c_6 \tag{B.2x}$$
$$c_8' := c_1 + 2c_2 + c_3 - c_4 - 2c_5 - c_6 \tag{B.2y}$$
$$c_9' := c_1 - c_2 + c_3 - c_4 + c_5 - c_6 \tag{B.2z}$$

In the fundamental representation, we have the identity

$$t^a t^b = \frac{1}{2N_c}\delta^{ab}\mathbb{1} + \frac{1}{2}(d^{ab}{}_c + if^{ab}{}_c)t^c \tag{B.3}$$

and so we can rewrite all of the traces in terms of the $\delta^{ab}, d^{abc}, f^{abc}$ symbols. The result is:

$$P_{\begin{array}{|c|c|c|c|}\hline 1&2&3&4\\\hline\end{array}}\, v = \tilde{c}_1\Big(d^{a_1a_4m}d^{a_2a_3m} + d^{a_1a_3m}d^{a_2a_4m} + d^{a_1a_2m}d^{a_3a_4m}\Big) \tag{B.4a}$$

$$+ \tilde{c}_2\Big(\delta^{a_1a_4}\delta^{a_2a_3} + \delta^{a_1a_3}\delta^{a_2a_4} + \delta^{a_1a_2}\delta^{a_3a_4}\Big) \tag{B.4b}$$

$$P_{\begin{array}{|c|c|}\hline 1&2\\\hline 3&4\\\hline\end{array}}\, v = \tilde{c}_3\Big(-d^{a_1a_4m}d^{a_2a_3m} - d^{a_1a_3m}d^{a_2a_4m} + 2d^{a_1a_2m}d^{a_3a_4m}\Big) \tag{B.4c}$$

$$- \tilde{c}_4\Big(\delta^{a_1a_4}\delta^{a_2a_3} + \delta^{a_1a_3}\delta^{a_2a_4} - 2\delta^{a_1a_2}\delta^{a_3a_4}\Big) \tag{B.4d}$$

$$P_{\begin{array}{|c|c|}\hline 1&3\\\hline 2&4\\\hline\end{array}}\, v = \tilde{c}_5\Big(d^{a_1a_4m}d^{a_2a_3m} - d^{a_1a_3m}d^{a_2a_4m}\Big) \tag{B.4e}$$

$$+ \tilde{c}_6\Big(\delta^{a_1a_4}\delta^{a_2a_3} - \delta^{a_1a_3}\delta^{a_2a_4}\Big) \tag{B.4f}$$

$$P_{\begin{array}{|c|c|}\hline 1&2\\\hline 3\\\cline{1-1}4\\\cline{1-1}\end{array}}\, v = \tilde{c}_7\Big(d^{a_2a_4m}if^{a_1a_3m} - d^{a_2a_3m}if^{a_1a_4m} + d^{a_1a_4m}if^{a_2a_3m} - d^{a_1a_3m}if^{a_2a_4m} \tag{B.4g}$$

$$+ 2d^{a_1a_2m}if^{a_3a_4m}\Big) \tag{B.4h}$$

$$P_{\begin{array}{|c|c|}\hline 1&3\\\hline 2\\\cline{1-1}4\\\cline{1-1}\end{array}}\, v = \tilde{c}_8\Big(2d^{a_3a_4m}if^{a_1a_2m} + d^{a_2a_4m}if^{a_1a_3m} - 3d^{a_2a_3m}if^{a_1a_4m} - d^{a_1a_4m}if^{a_2a_3m} \tag{B.4i}$$

$$+ 3d^{a_1a_3m}if^{a_2a_4m}\Big) \tag{B.4j}$$

$$P_{\begin{array}{|c|c|}\hline 1&4\\\hline 2\\\cline{1-1}3\\\cline{1-1}\end{array}}\, v = \tilde{c}_9\Big(d^{a_3a_4m}if^{a_1a_2m} - d^{a_2a_4m}if^{a_1a_3m} + d^{a_1a_4m}if^{a_2a_3m}\Big) \tag{B.4k}$$

where

$$\tilde{c}_1 := \frac{c'_1}{24}, \quad \tilde{c}_2 := \frac{c'_1 + N_c c'_2}{12N_c}, \quad \tilde{c}_3 := \frac{c'_3}{24}, \quad \tilde{c}_4 := \frac{2c'_3 + N_c c'_4}{24N_c}, \quad \tilde{c}_5 := \frac{c'_5}{8}, \tag{B.4l}$$

$$\tilde{c}_6 := \frac{2c'_5 - N_c c'_6}{8N_c}, \quad \tilde{c}_7 := \frac{c'_7}{32}, \quad \tilde{c}_8 := \frac{c'_8}{96}, \quad \tilde{c}_9 := \frac{c'_9}{24} \tag{B.4m}$$

Then the associated adjoint color structures are

$$\mathcal{C}_1^{a_1a_2a_3a_4} := d^{a_1a_4m}d^{a_2a_3m} + d^{a_1a_3m}d^{a_2a_4m} + d^{a_1a_2m}d^{a_3a_4m} \tag{B.5a}$$
$$\mathcal{C}_2^{a_1a_2a_3a_4} := \delta^{a_1a_4}\delta^{a_2a_3} + \delta^{a_1a_3}\delta^{a_2a_4} + \delta^{a_1a_2}\delta^{a_3a_4} \tag{B.5b}$$
$$\mathcal{C}_3^{a_1a_2a_3a_4} := -d^{a_1a_4m}d^{a_2a_3m} - d^{a_1a_3m}d^{a_2a_4m} + 2d^{a_1a_2m}d^{a_3a_4m} \tag{B.5c}$$
$$\mathcal{C}_4^{a_1a_2a_3a_4} := \delta^{a_1a_4}\delta^{a_2a_3} + \delta^{a_1a_3}\delta^{a_2a_4} - 2\delta^{a_1a_2}\delta^{a_3a_4} \tag{B.5d}$$
$$\mathcal{C}_5^{a_1a_2a_3a_4} := d^{a_1a_4m}d^{a_2a_3m} - d^{a_1a_3m}d^{a_2a_4m} \tag{B.5e}$$
$$\mathcal{C}_6^{a_1a_2a_3a_4} := \delta^{a_1a_4}\delta^{a_2a_3} - \delta^{a_1a_3}\delta^{a_2a_4} \tag{B.5f}$$
$$\mathcal{C}_7^{a_1a_2a_3a_4} := d^{a_2a_4m}if^{a_1a_3m} - d^{a_2a_3m}if^{a_1a_4m} + d^{a_1a_4m}if^{a_2a_3m} - d^{a_1a_3m}if^{a_2a_4m} \tag{B.5g}$$
$$+ 2d^{a_1a_2m}if^{a_3a_4m} \tag{B.5h}$$
$$\mathcal{C}_8^{a_1a_2a_3a_4} := 2d^{a_3a_4m}if^{a_1a_2m} + d^{a_2a_4m}if^{a_1a_3m} - 3d^{a_2a_3m}if^{a_1a_4m} - d^{a_1a_4m}if^{a_2a_3m} \tag{B.5i}$$
$$+ 3d^{a_1a_3m}if^{a_2a_4m} \tag{B.5j}$$
$$\mathcal{C}_9^{a_1a_2a_3a_4} := d^{a_3a_4m}if^{a_1a_2m} - d^{a_2a_4m}if^{a_1a_3m} + d^{a_1a_4m}if^{a_2a_3m} \tag{B.5k}$$

where, in case we wish to normalise, the norms of these objects are given by

$$\|\mathcal{C}_1^{a_1a_2a_3a_4}\|^2 = 3\left(N_c^2-1\right)^2\left(N_c^2-4\right) \tag{B.5l}$$
$$\|\mathcal{C}_2^{a_1a_2a_3a_4}\|^2 = 3\left(N_c^4-1\right) \tag{B.5m}$$
$$\|\mathcal{C}_3^{a_1a_2a_3a_4}\|^2 = \frac{6\left(N_c^2-1\right)^2\left(N_c^2-4\right)\left(N_c^2-6\right)}{N_c^2} \tag{B.5n}$$
$$\|\mathcal{C}_4^{a_1a_2a_3a_4}\|^2 = 6\left(N_c^2-1\right)\left(N_c^2-2\right) \tag{B.5o}$$
$$\|\mathcal{C}_5^{a_1a_2a_3a_4}\|^2 = \frac{2\left(N_c^2-1\right)^2\left(N_c^2-4\right)\left(N_c^2-6\right)}{N_c^2} \tag{B.5p}$$
$$\|\mathcal{C}_6^{a_1a_2a_3a_4}\|^2 = 2\left(N_c^2-1\right)\left(N_c^2-2\right) \tag{B.5q}$$
$$\|\mathcal{C}_7^{a_1a_2a_3a_4}\|^2 = 8\left(N_c^2-1\right)^2\left(N_c^2-4\right) \tag{B.5r}$$
$$\|\mathcal{C}_8^{a_1a_2a_3a_4}\|^2 = 24\left(N_c^2-1\right)^2\left(N_c^2-4\right) \tag{B.5s}$$
$$\|\mathcal{C}_9^{a_1a_2a_3a_4}\|^2 = 3\left(N_c^2-1\right)^2\left(N_c^2-4\right) \tag{B.5t}$$

B.2 Deriving Frobenius reciprocity for characters

Here we establish Frobenius reciprocity between induced and restricted left R-modules and show that this results in the reciprocity of induced and restricted characters given in Theorem 4.2.1.

Given left R-modules M and N, Frobenius reciprocity is a direct consequence of the study of the abelian group $\mathrm{Hom}_R(M,N)$, which is the set of all R-module homomorphisms between M and N, with the group structure being addition of homomorphisms. The study of $\mathrm{Hom}_R(M,N)$ is ubiquitous in abstract algebra, but for our purposes, we show that Frobenius reciprocity is a special case of a canonical relationship between R-module homomorphisms and tensor products over rings. To see this, we make $\mathrm{Hom}_R(M,N)$ into a module in the following way: if M is a (R,S)-bimodule, then the right S-action on M becomes a canonical left S-action on $\mathrm{Hom}_R(M,N)$, making $\mathrm{Hom}_R(M,N)$ a left S-module. That is, we can read off the appropriate left action on $\mathrm{Hom}_R(M,N)$ from the following diagram

$$\begin{array}{ccc} M & \xrightarrow{\varphi} & N \\ {\scriptstyle\circ}\uparrow & \nearrow{\scriptstyle\cdot} & \\ M\times S & & \end{array} \tag{B.6}$$

and so we see that the left action on $\mathrm{Hom}_R(M,N)$ should be

$$\cdot : S\times \mathrm{Hom}_R(M,N)\to \mathrm{Hom}_R(M,N) \tag{B.7}$$

$$s\cdot\varphi(m) := \varphi(m\circ s),\quad \varphi\in\mathrm{Hom}_R(M,N),\ s\in S \tag{B.8}$$

The mnemonic is that forming $\mathrm{Hom}_R(M,N)$ "uses up" the left R-action on M and N, leaving only the S-action behind. The right S-action on M is chosen to remain so that the left S-action on $\mathrm{Hom}_R(M,N)$ is compatible with the left R-module structure on M and N. That is if $s\in S$, $m\in M$, $r\in R$, then

$$s\cdot\varphi(r\cdot m) := \varphi(r\cdot m\circ s), \quad \text{(definition of the left } S\text{-action on } \mathrm{Hom}_R(M,N)) \tag{B.9a}$$

$$= r\varphi(m\circ s), \quad (\varphi \text{ is a left } R\text{-module homomorphism}) \tag{B.9b}$$

$$= r(s\cdot\varphi)(m), \quad \text{(again using the } S\text{-action on } \mathrm{Hom}_R(M,N)) \tag{B.9c}$$

so the left S-action on $\mathrm{Hom}_R(M,N)$ is R-linear (and it is straightforward to check the other properties necessary to prove that this is a left action). So in a similar way to the argument for why one needs a right action on one of the underlying modules to define a left action on the tensor product of two modules, if we did not have a right action of one of the underlying modules in $\mathrm{Hom}_R(M,N)$, we could not define a desirable left-action on the Hom structure, because one checks that R-linearity would fail. These may perhaps seem like overly-technical points, but genuinely are necessary for the coming argument.

Altogether, the importance of introducing $\mathrm{Hom}_R(M,N)$ is so that we can state the following canonical property of tensor products of modules:

Proposition B.2.1 (Tensor-Hom adjunction)**.** *Let M be a (R,S)-bimodule, W a left S-module, and N a left R-module. Then*

$$Hom_R(M \otimes_S W, N) \cong Hom_S(W, Hom_R(M,N)) \tag{B.10}$$

Proof. The proof is very straightforward - see [60, Ch. 2.4.1] for details. Briefly: the crux of the proof is to define

$$f : \mathrm{Hom}_R(M \otimes_S W, N) \to \mathrm{Hom}_S(W, \mathrm{Hom}_R(M,N)) \tag{B.11}$$
$$f(\varphi)(m)(w) := \varphi(m \otimes_S w), \quad \varphi \in \mathrm{Hom}_R(M \otimes_S W, N),\ m \in M,\ w \in W \tag{B.12}$$

and then methodically verify all of the properties needed to prove that f is an isomorphism, which is a tedious but straightforward task. □

Frobenius reciprocity is a special case of the Tensor-Hom adjunction. To see this we'll also need the following observation: if we view a ring R as an (R,R)-module, then given a left R-module M, we have that

$$\mathrm{Hom}_R(R, M) \cong M \tag{B.13}$$

where the isomorphism is given by $\varphi \mapsto \varphi(e)$, extended by the R-module structure. Now we can state the critical result:

Theorem B.2.1 (Frobenius reciprocity)**.** *Let H be a subgroup of G. Let W be a left $\mathbb{C}[H]$-module and N a left $\mathbb{C}[G]$-module. Then the following isomorphism holds*

$$Hom_{\mathbb{C}[G]}(Ind_H^G W, N) \cong Hom_{\mathbb{C}[H]}(W, Res_H^G N) \tag{B.14}$$

Proof. Consider proposition B.2.1. Take $R = \mathbb{C}[G]$ and $S = \mathbb{C}[H]$. Then we can set $M = \mathbb{C}[G]$, restricting the canonical right action on $\mathbb{C}[G]$ to make it into a $(\mathbb{C}[G], \mathbb{C}[H])$-module. This gives

$$\mathrm{Hom}_{\mathbb{C}[G]}(\mathrm{Ind}_H^G W, N) \cong \mathrm{Hom}_{\mathbb{C}[H]}(W, \mathrm{Hom}_{\mathbb{C}[G]}(\mathbb{C}[G], N)) \tag{B.15}$$

By eq. (B.13), $\mathrm{Hom}_{\mathbb{C}[G]}(\mathbb{C}[G], N) \cong N$ if $\mathbb{C}[G]$ is viewed as a $(\mathbb{C}[G], \mathbb{C}[G])$-module and so when we view $\mathbb{C}[G]$ as a $(\mathbb{C}[G], \mathbb{C}[H])$-module, $\mathrm{Hom}_{\mathbb{C}[G]}(\mathbb{C}[G], N) \cong \mathrm{Res}_H^G N$, because N inherits the restricted left $\mathbb{C}[H]$-action from the $(\mathbb{C}[G], \mathbb{C}[H])$-module structure on $\mathbb{C}[G]$. □

Frobenius reciprocity then gives us a special relationship between the characters of the restricted and induced modules. First, we need one more critical theorem to tie everything together:

Theorem B.2.2. *Let M and N be left $\mathbb{C}[G]$-modules. Then*

$$dim(Hom_{\mathbb{C}[G]}(M,N)) = \frac{1}{|G|} \sum_{g \in G} \chi^M(g^{-1}) \chi^N(g) \tag{B.16a}$$
$$=: \langle \chi^M, \chi^N \rangle_G \tag{B.16b}$$

where χ^M, χ^N are the characters of the representations associated with the modules M, N.

Proof. See Theorem 12 of [61, Ch. 6.14] and preceding lemmas. □

Altogether, the isomorphism of Theorem B.2.1 tells us that

$$\dim(\mathrm{Hom}_{\mathbb{C}[G]}(\mathrm{Ind}_H^G W, N)) = \dim(\mathrm{Hom}_{\mathbb{C}[H]}(W, \mathrm{Res}_H^G N)) \tag{B.17}$$

and so Theorem B.2.2 gives us

$$\langle \chi^{\mathrm{Ind}_H^G W}, \chi^N \rangle_G = \langle \chi^W, \chi^{\mathrm{Res}_H^G N} \rangle_H \tag{B.18}$$

which is the relationship between induced and restricted characters cited in the main text.

B.3 A Proof that $r_\mu \in N_{S_k}(C_{S_k}(\sigma_\mu))$

We prove that r_μ is an element of the *normalizer* of the centralizer of σ_μ. That is, we claim that (note also that r_μ is of course its own inverse):

$$r_\mu \, h \, r_\mu \in C_{S_k}(\sigma_\mu), \quad \forall h \in C_{S_k}(\sigma_\mu) \tag{B.19}$$

To see this, first recall that in eq. (4.38) we established that every element of $C_{S_k}(\sigma_\mu)$ is generated by elements $s_1, \ldots, s_n, z_1, \ldots, z_m$ where the s_j elements leave σ_μ invariant by interchanging disjoint cycles of equal length (if any) and the z_i generate $Z_{\mu_1} \times \cdots \times Z_{\mu_m}$. So first notice that

$$r_\mu \, z_i r_\mu = (z_i)^{-1} \in Z_{\mu_i}, \quad \forall z_i \tag{B.20}$$

This is because z_i is an element of a cyclic group and so can always be written as

$$z_i = x^c, \quad x := \big((a+1)(a+2)\cdots(a+\mu_i)\big) \tag{B.21a}$$

for some integer c, and r_μ just reverses the ordering of the numbers in x and so $r_\mu \, x \, r_\mu = x^{-1}$, which gives

$$\begin{aligned} r_\mu \, z_i \, r_\mu &= r_\mu \, x \, r_\mu \cdots r_\mu \, x \, r_\mu && \text{(B.21b)} \\ &= x^{-1} \cdots x^{-1} && \text{(B.21c)} \\ &= z_i^{-1} && \text{(B.21d)} \end{aligned}$$

Next, notice that since each of the s_j just interchange disjoint cycles of the same length (if σ_μ has any disjoint cycles of the same length - the s_j are all zero if not) and r_μ just reverses the order of numbers within these cycles, then we have that reversing the order, then interchanging cycles, then reversing the order again leaves σ_μ unchanged, that is

$$r_\mu s_j r_\mu = s_j, \quad \forall s_j \tag{B.22}$$

One can prove this directly using r_μ written as a product of disjoint transpositions as we did in eq. (4.80). Then altogether, since any element of $C_{S_k}(\sigma_\mu)$ is generated by $s_1, \ldots, s_n, z_1, \ldots, z_m$, we have that

$$r_\mu \, h \, r_\mu \in C_{S_k}(\sigma_\mu), \quad \forall h \in C_{S_k}(\sigma_\mu) \tag{B.23}$$

Appendix C

Proofs necessary for bounding the images of simple Wilson line correlators

C.1 Lemma 5.1.1

Lemma. *Let f be defined as*

$$f : \mathbb{T}^{n-1} \to \mathbb{C} \tag{C.1a}$$

$$(\theta_1, \ldots, \theta_{n-1}) \mapsto \frac{1}{n}\left(\sum_{j=1}^{n-1} e^{i\theta_j} + e^{-i\sum_{k=1}^{n-1}\theta_k}\right) \tag{C.1b}$$

Then f is smooth.

Proof. Recall the following definition [52, pg. 64]

Definition C.1.1. *(Smoothness of a map in terms of components). Let $F : N \to M$ be a continuous map between two manifolds of dimensions n and m respectively. The following are equivalent:*

1. *The map $F : N \to M$ is C^∞ (it is smooth).*
2. *The manifold M has an atlas such that for every chart $(V, \psi) = (V, y^1, \ldots, y^m)$ in the atlas, the components $y^i \circ F : F^{-1}(V) \to \mathbb{R}$ of F relative to the chart are all C^∞.*

Such an atlas for $\mathbb{C}$ is provided by the single chart $(\mathbb{C}, \pi_1, \pi_2)$ where π_1, π_2 are the projections onto real and imaginary parts of $z \in \mathbb{C}$. Then we have

$$\pi_1 \circ f : \mathbb{T}^{n-1} \to \mathbb{R}, \qquad \pi_2 \circ f : \mathbb{T}^{n-1} \to \mathbb{R} \tag{C.2a}$$

$$\pi_1 \circ f((\theta_1, \ldots, \theta_{n-1})) = \frac{1}{n}\left(\sum_{j=1}^{n-1} \cos(\theta_j) + \cos(\sum_{k=1}^{n-1}\theta_k)\right) \tag{C.2b}$$

$$\pi_2 \circ f((\theta_1, \ldots, \theta_{n-1})) = \frac{1}{n}\left(\sum_{j=1}^{n-1} \sin(\theta_j) - \sin(\sum_{k=1}^{n-1}\theta_k)\right) \tag{C.2c}$$

Clearly $\pi_1 \circ f$ and $\pi_2 \circ f$ are smooth and so by Definition C.1.1, f is smooth. □

C.2 Lemma 5.1.2

Lemma. *Let N be a compact smooth manifold without boundary and let M be a smooth manifold. Let N and M have dimensions n and m respectively, with $n > m$. If $F : N \to M$ is a smooth map, then the boundary of the image of F can only be populated by critical values.*

Proof. Assume the contrary. Then because the image of F is compact, its boundary is non-empty and there exists a point $y \in M$ on the boundary of the image of F so that for some $x \in N$

$$dF_x : T_xN \to T_yM \tag{C.3}$$

is surjective. Then locally, F is an open map [62, pg. 169]. Then there exists a neighborhood U centered on x such that $F(U)$ is open. But $y \in F(U)$ and y lies on the boundary of a compact image by construction. Contradiction. Thus, no such y exists and so the differential cannot be surjective at every point $x \in N$ that maps to the boundary of the image of F. □

C.3 Lemma 5.1.3

Lemma. *The critical values of f that arise due to f having rank zero occur at isolated points. In particular, these points are the n-th roots of unity.*

Proof. If f has rank zero at a point, then every entry of the Jacobian is zero. This means that

$$0 \overset{!}{=} \frac{\partial}{\partial\theta_j}\mathrm{Re}f \quad \text{and} \quad 0 \overset{!}{=} \frac{\partial}{\partial\theta_j}\mathrm{Im}f, \quad \forall j = 1, \dots, n-1 \tag{C.4a}$$

$$\iff 0 \overset{!}{=} \frac{\partial f}{\partial\theta_j}, \quad \forall j = 1, \dots, n-1 \tag{C.4b}$$

$$\implies 1 = e^{i(\theta_j + \sum_{k=1}^{n-1}\theta_k)}, \quad \forall j = 1, \dots, n-1 \tag{C.4c}$$

$$\implies 2\pi m_j = \theta_j + \sum_{k=1}^{n-1}\theta_k, \qquad m_j \in \mathbb{Z}, \quad \forall j \in 1, \dots, n-1 \tag{C.4d}$$

Then we can sum over j to obtain

$$\sum_{k=1}^{n-1}\theta_k = \frac{2\pi c}{n}, \qquad c := \sum_{j=1}^{n-1} m_j \tag{C.5a}$$

$$\implies \theta_j = -\frac{2\pi c}{n} + 2\pi m_j, \quad \forall j \in 1, \dots, n-1 \tag{C.5b}$$

$$\implies f = \exp\left(-i\frac{2\pi c}{n}\right), \quad c \in \mathbb{Z} \tag{C.5c}$$

which describes the n-th roots of unity. □

C.4 Theorem 5.1.2

Theorem. *If we define*

$$g(\theta, p, c) := \frac{1}{n}\left(p\, e^{i\,\theta} + (n-p)\, e^{-i(\frac{p\,\theta + 2\pi c}{n-p})}\right) \tag{C.6}$$

then the critical values of f are given by

$$\{g(\theta, p, c) \;\big|\; -\frac{2\pi c}{n} \leq \theta \leq 2\pi - \frac{2\pi(p+c)}{n}, \quad p = 1, \ldots, n-1, \quad c = 0, \ldots, n-1\} \tag{C.7}$$

The parameter p arises because in the general rank 1 situation, the Jacobian of f has p columns that are equal (up to a factor of -1) and the remaining $n-p-1$ columns vanish. Geometrically, if a circle of radius $(n-p)/n$ rolls anti-clockwise inside of the unit circle, then $g(\theta, p, 0)$ describes the curve mapped out by a point P on this rolling circle. In particular, the point is taken to begin at $P_0 = (1, 0)$ and the next intersection of P with the unit circle occurs at the n-th root of unity if one counts p roots of unity clockwise from P_0, when $\theta = 2\pi(1 - (p+c)/n$. The parameter c rotates the family of curves $g(\theta, p, 0)$ clockwise by $2\pi c/n$ and so the critical values of f are the union of the family of curves where the initial points on the rolling circles begin at each of the roots of unity and connect to every other root of unity.

Proof. Let rank f = 1 (we will re-examine the case where rank f = 0 at the end of the proof). Then the Jacobian of f contains at least one non-zero column and exactly one linearly independent column. Without loss of generality (we can shuffle coordinates $\{\theta_j\}$ in the domain without changing the results of the theorem), we choose this to be the first column of the Jacobian. Then rank(f) = 1 at a point is equivalent to the simultaneous vanishing of the determinant of every 2×2 matrix formed by the first column and each other column of the Jacobian, because all non-vanishing column vectors must be collinear to each other. This means that

$$0 \stackrel{!}{=} \det \frac{1}{n} \begin{pmatrix} -\sin(\theta_1) - \sin(\sum_{k=1}^{n-1} \theta_k) & -\sin(\theta_i) - \sin(\sum_{k=1}^{n-1} \theta_k) \\ \cos(\theta_1) - \cos(\sum_{k=1}^{n-1} \theta_k) & \cos(\theta_i) - \cos(\sum_{k=1}^{n-1} \theta_k) \end{pmatrix}, \quad \forall i = 2, \ldots, n-1 \tag{C.8a}$$

$$\implies 0 = \sin(\theta_i - \theta_1) + \sin(\theta_1 + \sum_{k=1}^{n-1} \theta_k) - \sin(\theta_i + \sum_{k=1}^{n-1} \theta_k), \qquad \forall i = 2, \ldots, n-1 \tag{C.8b}$$

Let $x := \sum_{k=1}^{n-1} \theta_k$ for ease of notation. We can simplify the above condition further if we use the double angle identity on the first term and apply the following identities for

sums of sinusoids to the second and third term:

$$\sin(a)+\sin(b)=2\sin\left(\frac{a+b}{2}\right)\cos\left(\frac{a-b}{2}\right) \tag{C.9a}$$

$$\cos(a)-\cos(b)=-2\sin\left(\frac{a+b}{2}\right)\sin\left(\frac{a-b}{2}\right) \tag{C.9b}$$

Then for the determinant condition, we have that

$$0\overset{!}{=}\sin(\theta_i-\theta_1)+\sin(\theta_1+x)-\sin(\theta_i+x),\qquad \forall i=2,\dots,n-1 \tag{C.10a}$$

$$=2\sin\left(\frac{\theta_i-\theta_1}{2}\right)\cos\left(\frac{\theta_i-\theta_1}{2}\right)+2\sin\left(\frac{\theta_1-\theta_i}{2}\right)\cos(\frac{\theta_1+\theta_i+2x}{2}\right) \tag{C.10b}$$

$$=-4\sin\left(\frac{\theta_1-\theta_i}{2}\right)\sin\left(\frac{\theta_1+x}{2}\right)\sin\left(\frac{\theta_i+x}{2}\right),\quad x=\sum_{k=1}^{n-1}\theta_k,\quad \forall i=2,\dots,n-1 \tag{C.10c}$$

Notice that if the factor $\sin((\theta_1+x)/2)$ vanishes, then the first column in the Jacobian vanishes, which is not the case by assumption. We can see this by using the identities eq. (C.9) to rewrite an arbitrary column in the Jacobian:

$$\begin{pmatrix}\frac{\partial}{\partial\theta_j}\mathrm{Re}f\\ \frac{\partial}{\partial\theta_j}\mathrm{Im}f\end{pmatrix}=\frac{1}{n}\begin{pmatrix}-2\sin\left((\theta_j+\sum_{k=1}^{n-1}\theta_k)/2\right)\cos\left((\theta_j-\sum_{k=1}^{n-1}\theta_k)/2\right)\\ -2\sin\left((\theta_j+\sum_{k=1}^{n-1}\theta_k)/2\right)\sin\left((\theta_j-\sum_{k=1}^{n-1}\theta_k)/2\right)\end{pmatrix} \tag{C.11}$$

Then from the determinant condition eq. (C.10c), we must have that

$$0=\sin\left(\frac{\theta_1-\theta_i}{2}\right),\qquad \text{or}\qquad 0=\sin\left(\frac{\theta_i+x}{2}\right) \tag{C.12}$$

One of each condition must hold independently for each value of i if rank f=1. However, **both cannot hold simultaneously** for a given value of i, because this would mean that

$$\theta_i=\theta_1+2\pi q_i,\qquad \text{and}\qquad \theta_i=-x+2\pi s_i,\quad q_i,s_i\in\mathbb{Z} \tag{C.13}$$

which would again imply that $\sin((\theta_1+x)/2)$ vanishes, that is that the first column in the Jacobian vanishes, which is not the case by assumption. Note that separately, the first condition in eq. (C.13) says that the i-th column of the Jacobian equals the first column of the Jacobian up to a possible factor of -1 and the second condition in eq. (C.13) says that the i-th column of the Jacobian vanishes.

Altogether, the general situation is as follows: at a critical value where f is rank 1, p columns of the Jacobian are equal to the first column of the Jacobian (up to a possible factor of -1) and the remaning $n-p-1$ columns vanish. We can interchange coordinates $\{\theta_i\}$ in the chart in the domain of f so that, without loss of generality, for $i=2,\dots,p$, θ_i obeys the first condition in eq. (C.13) and for $i=p+1,\dots n-1$, θ_i obeys the second condition in eq. (C.13).

Then we can simplify the second condition in eq. (C.13) so that it is defined in terms of θ_1:

$$\theta_i = -\sum_{k=1}^{n-1} \theta_k + 2\pi s_i, \qquad i = p+1, \dots, n-1, \quad s_i \in \mathbb{Z} \tag{C.14a}$$

$$= -p\,\theta_1 - \sum_{j=p+1}^{n-1} \theta_j - 2\pi \sum_{k=1}^{p} q_k + 2\pi s_i, \quad i = p+1, \dots, n-1, \quad s_i, q_k \in \mathbb{Z} \tag{C.14b}$$

We can sum over i to obtain

$$\sum_{i=p+1}^{n-1} \theta_i = -p\,(n-p-1)\,\theta_1 - (n-p-1) \sum_{j=p+1}^{n-1} \theta_j - 2\pi(n-p-1) \sum_{k=1}^{p} q_k + 2\pi \sum_{i=p+1}^{n-1} s_i \tag{C.14c}$$

Relabelling indices and rearranging, we find

$$\sum_{i=p+1}^{n-1} \theta_i = -\frac{p\,(n-p-1)}{n-p}\theta_1 - \frac{2\pi(n-p-1)}{n-p} \sum_{k=1}^{p} q_k + \frac{2\pi}{n-p} \sum_{i=p+1}^{n-1} s_i \tag{C.14d}$$

Substituting this back into eq. (C.14b) gives

$$\theta_i = -\frac{p\,\theta_1}{n-p} - \frac{2\pi c}{n-p} + 2\pi s_i, \quad c := \sum_{k=1}^{p} q_k + \sum_{i=p+1}^{n-1} s_i, \quad i = p+1, \dots, n-1 \tag{C.14e}$$

Using the first condition in eq. (C.13) and the just-derived condition eq. (C.14e) for $i = 2, \dots p$ and $i = p+1, \dots, n-1$ respectively, we can rewrite every θ_i in f in terms of θ_1:

$$g(\theta, p, c) := \frac{1}{n}\left(p\,e^{i\,\theta} + (n-p)\,e^{-i\left(\frac{p\,\theta + 2\pi c}{n-p}\right)}\right), \quad p = 1, \dots, n-1, \quad c \in \mathbb{Z} \tag{C.15}$$

where we have dropped the subscript on θ_1 and for convenience we have dropped unnecessary additional factors of 2π in the complex exponents.

The set of all points $\{g(\theta, p, c)\}$ is the set of all critical values that occur when f has rank 1, as we have shown. However, we also recognise that $g(\theta, n-1, 0)$ defines the n-cusp hypocycloid inscribed in the unit circle. The points at which $g(\theta, n-1, 0)$ touches the unit circle are the n-th roots of unity, which are the critical values of f when f has rank 0, according to Lemma 5.1.3. Thus $\{g(\theta, p, c)\}$ contains all of the critical values of f, as claimed in the statement of the theorem.

Now let's prove the geometric interpretation of $g(\theta, p, c)$. First, we will derive the equation for the n-cusp hypocycloid and then modify this derivation to describe $g(\theta, p, c)$. The setup is displayed in Figure C.1[1]:

[1] I have essentially redrawn the animation of [63], modified to account for a slight modification in the derivation that I've chosen to use.

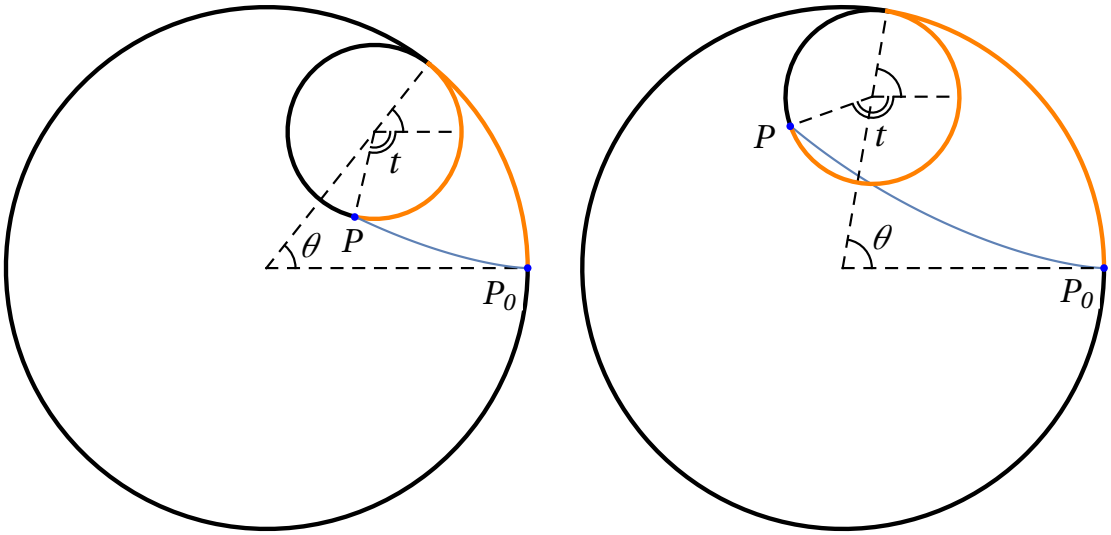

FIGURE C.1: A circle of radius r rolls inside of the unit circle. A point P on the inner circle begins at P_0 and traces out a hypocycloid (blue) as θ varies. The arc length $1 \cdot \theta$ on the unit circle is equal to $r(\theta + t)$ (orange).

A point P on a circle of radius r traces out a curve as this circle rolls inside of the unit circle. The point P has initial condition P_0 where we (temporarily) choose $P_0 = (1, 0)$. Then relative to the center of the small circle, the position of P is described by

$$\begin{pmatrix} x_1(t) \\ x_2(t) \end{pmatrix} := \begin{pmatrix} r\cos t \\ -r\sin t \end{pmatrix} \tag{C.16}$$

where t measures the angle (clockwise) from a line through the center of the smaller circle that is parallel to the x axis. The position of the center of the small circle relative to the center of the unit circle as θ varies is described by

$$\begin{pmatrix} y_1(\theta) \\ y_2(\theta) \end{pmatrix} := \begin{pmatrix} (1-r)\cos\theta \\ (1-r)\sin\theta \end{pmatrix} \tag{C.17}$$

We can relate θ and t by observing that the arc lengths in Figure C.1 are related by

$$\theta = r(\theta + t) \tag{C.18a}$$

$$\implies t = \left(\frac{1-r}{r}\right)\theta \tag{C.18b}$$

Then to describe the position of P relative to the center of the large circle as θ varies, we simply perform vector addition

$$\begin{pmatrix} P_1(\theta) \\ P_2(\theta) \end{pmatrix} := \begin{pmatrix} (1-r)\cos\theta + r\cos\left(\left(\frac{1-r}{r}\right)\theta\right) \\ (1-r)\sin\theta - r\sin\left(\left(\frac{1-r}{r}\right)\theta\right) \end{pmatrix} \tag{C.19}$$

Let's compare this to our case $g(\theta, p, c)$. If we identify $r = (n-p)/n$ (which is always positive, so this identification is valid) we have

$$\begin{pmatrix} \text{Re } g(\theta,p,k) \\ \text{Im } g(\theta,p,k) \end{pmatrix} = \begin{pmatrix} (1-r)\cos\theta + r\cos\left(\left(\frac{1-r}{r}\right)\theta + \frac{2\pi c}{nr}\right) \\ (1-r)\sin\theta - r\sin\left(\left(\frac{1-r}{r}\right)\theta + \frac{2\pi c}{nr}\right) \end{pmatrix}, \quad c = 0, \ldots, n-p-1 \tag{C.20}$$

If we choose

$$t = \left(\frac{1-r}{r}\right)\theta + \frac{2\pi c}{nr} \tag{C.21a}$$

$$\implies \theta + \frac{2\pi c}{n} = r(\theta + t), \quad c = 0, \ldots, n-p-1 \tag{C.21b}$$

then we observe that eq. (C.21b) is the equation for a point on a circle of radius $r = (n-p)/n$ rolling inside of the unit circle, where the point P began its motion at one of the n roots of unity, resulting in an additional term $2\pi c/n$ being added to θ, to give the correct arc lengths depicted in orange in Figure C.1. Furthermore, the point on the inner circle only touches the unit circle once it has completed a full revolution. The circumference of the inner circle is

$$\frac{2\pi(n-p)}{n} \tag{C.22}$$

which is equal to the arc length mapped out on the unit circle. If P_0 was at $\theta_0 = -2\pi c/n$, then this arc length corresponds to the angle

$$\theta = \frac{2\pi(n-p)}{n} - \frac{2\pi c}{n} = -\frac{2\pi(p+c)}{n} \tag{C.23}$$

after a rull revolution of the inner circle. This means that P_0 is located by counting c roots of unity clockwise from $(1, 0)$ and the curve traced out by P touches the unit circle for the first time after P_0 at a position located by counting p roots of unity clockwise from P_0. Altogether, we realise that the critical values of f are precisely all of the curves that connect the different n roots of unity in all possible ways by circles of radius $(n-p)/n$. This exact understanding of the parameters θ, p, c allows us to redefine these parameters in a more natural way. In particular, we can restrict θ to only apply one revolution of the inner circle and then allow c to vary so that curves are generated with P_0 located at each of the roots of unity. This gives

$$-\frac{2\pi c}{n} \leq \theta \leq 2\pi - \frac{2\pi(p+c)}{n}, \quad p = 1, \ldots, n-1, \quad c = 0, \ldots, n-1 \tag{C.24}$$

as in the statement of the theorem, which completes the proof. □

C.5 Proposition 5.2.1

Proposition. *For $SU(n)$ matrices U_1, U_2*

$$|\mathcal{O}_{12}| := \frac{1}{n}\left|\operatorname{tr}(U_1U_2) - \frac{1}{n}\operatorname{tr}(U_1)\operatorname{tr}(U_2)\right| \leq 1 \tag{C.25}$$

Proof. For square matrices A, B with entries in $\mathbb{C}$ we have the inner product

$$\langle A, B\rangle = \operatorname{tr}(A^\dagger B) \tag{C.26}$$

Then taking $A = \mathbb{1}$ and $B = U_1U_2 - \frac{1}{n}\operatorname{tr}(U_1)U_2$, we can apply the Cauchy-Schwarz inequality

$$\begin{aligned}
\frac{1}{n^2}\left|\operatorname{tr}(U_1U_2) - \frac{1}{n}\operatorname{tr}(U_1)\operatorname{tr}(U_2)\right|^2 &= \frac{1}{n^2}\left|\operatorname{tr}\left(U_1U_2 - \frac{1}{n}\operatorname{tr}(U_1)U_2\right)\right|^2 && \text{(C.27a)}\\
&= \frac{1}{n^2}\left|\langle A, B\rangle\right|^2 && \text{(C.27b)}\\
&\leq \frac{1}{n^2}\langle A, A\rangle\langle B, B\rangle && \text{(C.27c)}\\
&= \frac{1}{n}\operatorname{tr}\left(\left(U_1U_2 - \frac{1}{n}\operatorname{tr}(U_1)U_2\right)^\dagger\left(U_1U_2 - \frac{1}{n}\operatorname{tr}(U_1)U_2\right)\right) && \text{(C.27d)}\\
&= \frac{1}{n}\operatorname{tr}\left(\mathbb{1} - \frac{1}{n}\overline{\operatorname{tr}(U_1)}U_2^\dagger U_1U_2 - \frac{1}{n}\operatorname{tr}(U_1)U_2^\dagger U_1^\dagger U_2\right. && \text{(C.27e)}\\
&\quad \left. + \frac{1}{n^2}\left|\operatorname{tr}U_1\right|^2\mathbb{1}\right) && \text{(C.27f)}\\
&= 1 - \frac{1}{n^2}\left|\operatorname{tr}U_1\right|^2 && \text{(C.27g)}\\
&\leq 1 && \text{(C.27h)}
\end{aligned}$$

□

C.6 Proposition 5.2.2

Proposition. *For $SU(n)$ matrices U_1, U_2, U_3 with $n \geq 2$*

$$|\mathcal{O}_{22}| := \frac{1}{n^2-1}\left|\operatorname{tr}(U_2U_1)\operatorname{tr}(U_3) - \frac{1}{n}\operatorname{tr}(U_2U_3U_1) - \frac{1}{n}\operatorname{tr}(U_2U_1U_3) + \frac{1}{n^2}\operatorname{tr}(U_1)\operatorname{tr}(U_2U_3)\right| \tag{C.28a}$$

$$\leq 1 \tag{C.28b}$$

We provide two proofs:

Proof. **First Proof** - Because U_1, U_2, U_3 are unitary matrices, they have spectral decompositions

$$U_1 = \sum_{i=1}^{n} \alpha_i |u_i\rangle \langle u_i|, \quad U_2 = \sum_{j=1}^{n} \beta_j |v_j\rangle \langle v_j|, \quad U_3 = \sum_{k=1}^{n} \gamma_k |w_k\rangle \langle w_k| \tag{C.29}$$

where $\alpha_i, \beta_j, \gamma_k$ are the eigenvalues of U_1, U_2, U_3 respectively and $|u_i\rangle, |v_j\rangle, |w_k\rangle$ are the corresponding orthonormal eigenvectors. Then we can write

$$\mathcal{O}_{22} = \frac{1}{n^2-1}\sum_{i,j,k=1}^{n} \alpha_i\beta_j\gamma_k\left(|\langle u_i, v_j\rangle|^2 + \frac{1}{n^2}|\langle v_j, w_k\rangle|^2 - \frac{2}{n}\mathrm{Re}\big(\langle u_i, w_k\rangle \langle w_k, v_j\rangle \langle v_j, u_i\rangle\big)\right) \tag{C.30}$$

Because $\alpha_i, \beta_j, \gamma_k$ lie on the unit circle, applying the triangle inequality gives

$$|\mathcal{O}_{22}| \leq \frac{1}{n^2-1}\sum_{i,j,k=1}^{n} \left||\langle u_i, v_j\rangle|^2 + \frac{1}{n^2}|\langle v_j, w_k\rangle|^2 - \frac{2}{n}\mathrm{Re}\big(\langle u_i, w_k\rangle \langle w_k, v_j\rangle \langle v_j, u_i\rangle\big)\right| \tag{C.31}$$

The quantity

$$|\langle u_i, v_j\rangle|^2 + \frac{1}{n^2}|\langle v_j, w_k\rangle|^2 - \frac{2}{n}\mathrm{Re}\big(\langle u_i, w_k\rangle \langle w_k, v_j\rangle \langle v_j, u_i\rangle\big) \tag{C.32}$$

is always positive. To see this, notice that since $\langle v_j|$ and $|v_j\rangle$ are common to each term in the expression, we can write

$$\langle v_j| X^2 |v_j\rangle = |\langle u_i, v_j\rangle|^2 + \frac{1}{n^2}|\langle v_j, w_k\rangle|^2 - \frac{2}{n}\mathrm{Re}\big(\langle u_i, w_k\rangle \langle w_k, v_j\rangle \langle v_j, u_i\rangle\big) \tag{C.33a}$$

with

$$X := |u_j\rangle \langle u_j| - \frac{1}{n}|w_k\rangle \langle w_k| \tag{C.33b}$$

because the eigenvectors are orthonormal. Then X is explicitly Hermitian and so X^2 is positive-definite, meaning $\langle v_j| X^2 |v_j\rangle \geq 0, \ \forall i, j, k$.

Then following on from eq. (C.31), we can drop the absolute value after applying the triangle inequality:

$$|\mathcal{O}_{22}| \leq \frac{1}{n^2-1}\sum_{i,j,k=1}^{n}\left|\,|\langle u_i, v_j\rangle|^2 + \frac{1}{n^2}|\langle v_j, w_k\rangle|^2 - \frac{2}{n}\mathrm{Re}\big(\langle u_i, w_k\rangle\langle w_k, v_j\rangle\langle v_j, u_i\rangle\big)\right| \tag{C.34a}$$

$$= \frac{1}{n^2-1}\sum_{i,j,k=1}^{n}|\langle u_i, v_j\rangle|^2 + \frac{1}{n^2}|\langle v_j, w_k\rangle|^2 - \frac{2}{n}\mathrm{Re}\big(\langle u_i, w_k\rangle\langle w_k, v_j\rangle\langle v_j, u_i\rangle\big) \tag{C.34b}$$

Using the fact that the decomposition of unity is given by

$$\mathbb{1} = \sum_{i=1}^{n}|u_i\rangle\langle u_i| = \sum_{j=1}^{n}|v_j\rangle\langle v_j| = \sum_{k=1}^{n}|w_k\rangle\langle w_k| \tag{C.35}$$

we then find that

$$1 = \frac{1}{n^2-1}\sum_{i,j,k=1}^{n}|\langle u_i, v_j\rangle|^2 + \frac{1}{n^2}|\langle v_j, w_k\rangle|^2 - \frac{2}{n}\mathrm{Re}\big(\langle u_i, w_k\rangle\langle w_k, v_j\rangle\langle v_j, u_i\rangle\big) \tag{C.36}$$

and so

$$|\mathcal{O}_{22}| \leq 1 \tag{C.37}$$

□

Proof. **Second proof** - We use the Cauchy-Schwarz inequality. Let

$$A = U_2^\dagger \tag{C.38a}$$

$$B = \operatorname{tr}(U_3)U_1 - \frac{1}{n}\{U_3, U_1\} + \frac{1}{n^2}\operatorname{tr}(U_1)U_3 \tag{C.38b}$$

where $\{\,,\}$ denotes the anticommutator. Then

$$\frac{1}{(n^2-1)^2}\left|\operatorname{tr}(U_2U_1)\operatorname{tr}(U_3) - \frac{1}{n}\operatorname{tr}(U_2U_3U_1) - \frac{1}{n}\operatorname{tr}(U_2U_1U_3) + \frac{1}{n^2}\operatorname{tr}(U_1)\operatorname{tr}(U_2U_3)\right|^2 \tag{C.39a}$$

$$= \frac{1}{(n^2-1)^2}\left|\langle A, B\rangle\right|^2 \tag{C.39b}$$

$$\leq \frac{1}{(n^2-1)^2}\langle A, A\rangle\langle B, B\rangle \tag{C.39c}$$

$$= \frac{n}{(n^2-1)^2}\operatorname{tr}\left(\left(\operatorname{tr}(U_3^\dagger)U_1^\dagger - \frac{1}{n}\{U_3, U_1\}^\dagger + \frac{1}{n^2}\operatorname{tr}(U_1^\dagger)U_3^\dagger\right)\left(\operatorname{tr}(U_3)U_1\right.\right. \tag{C.39d}$$

$$\left.\left. - \frac{1}{n}\{U_3, U_1\} + \frac{1}{n^2}\operatorname{tr}(U_1)U_3\right)\right) \tag{C.39e}$$

$$= \frac{n}{(n^2-1)^2}\operatorname{tr}\left(\left(|\operatorname{tr}(U_3)|^2 + \frac{1}{n^2} + \frac{|\operatorname{tr}(U_1)|^2}{n^4}\right)\mathbb{1} - \frac{2}{n}\left(\operatorname{tr}(U_3^\dagger)U_3 + \operatorname{tr}(U_3)U_3^\dagger\right)\right. \tag{C.39f}$$

$$+ \frac{1}{n^2}\left(\operatorname{tr}(U_1)\operatorname{tr}(U_3^\dagger)U_1^\dagger U_3 + \left(\operatorname{tr}(U_1)\operatorname{tr}(U_3^\dagger)U_1^\dagger U_3\right)^\dagger\right) \tag{C.39g}$$

$$\left. - \frac{2}{n^3}\left(\operatorname{tr}(U_1)U_1^\dagger + \operatorname{tr}(U_1^\dagger)U_1\right)\right) \tag{C.39h}$$

$$= \frac{1}{(n^2-1)^2}\left(\frac{|\operatorname{tr}(U_3)|^2}{n^2}(n^4 - 4n^2) + 1 - 3\frac{|\operatorname{tr}(U_1)|^2}{n^2}\right. \tag{C.39i}$$

$$\left. + \frac{1}{n}\operatorname{tr}\left(\operatorname{tr}(U_1)\operatorname{tr}(U_3^\dagger)U_1^\dagger U_3 + \left(\operatorname{tr}(U_1)\operatorname{tr}(U_3^\dagger)U_1^\dagger U_3\right)^\dagger\right)\right) \tag{C.39j}$$

Notice that

$$\operatorname{tr}\left(\operatorname{tr}(U_1)\operatorname{tr}(U_3^\dagger)U_1^\dagger U_3 + \left(\operatorname{tr}(U_1)\operatorname{tr}(U_3^\dagger)U_1^\dagger U_3\right)^\dagger\right) \tag{C.40a}$$

$$= 2\left|\operatorname{tr}(U_1)\right|\left|\operatorname{tr}(U_3^\dagger)\right|\left|\operatorname{tr}(U_1U_3^\dagger)\right|\cos\alpha \tag{C.40b}$$

where α is the argument of $\operatorname{tr}(U_1)\operatorname{tr}(U_3^\dagger)\operatorname{tr}(U_1^\dagger U_3)$. Then because cosine is bounded by 1 we have

$$\frac{1}{n}\operatorname{tr}\left(\operatorname{tr}(U_1)\operatorname{tr}(U_3^\dagger)U_1^\dagger U_3 + \left(\operatorname{tr}(U_1)\operatorname{tr}(U_3^\dagger)U_1^\dagger U_3\right)^\dagger\right) \leq \frac{2}{n}\left|\operatorname{tr}(U_1)\right|\left|\operatorname{tr}(U_3^\dagger)\right|\left|\operatorname{tr}(U_1U_3^\dagger)\right| \tag{C.40c}$$

Then, following on from eq. (C.39j), we have

$$\frac{1}{(n^2-1)^2}\left|\langle A,B\rangle\right|^2 \leq \frac{1}{(n^2-1)^2}\Bigg(\frac{\left|\mathrm{tr}(U_3)\right|^2}{n^2}(n^4-4n^2)+1-3\frac{\left|\mathrm{tr}(U_1)\right|^2}{n^2} \tag{C.41a}$$

$$+\frac{2}{n}\Big|\,\mathrm{tr}(U_1)\Big|\Big|\,\mathrm{tr}(U_3^\dagger)\Big|\Big|\,\mathrm{tr}(U_1U_3^\dagger)\Big|\Bigg) \tag{C.41b}$$

We have established that $\frac{|\mathrm{tr}(U)|}{n} \leq 1$ for any $U \in SU(n)$ and because $n^4-4n^2 \geq 0$ for $n \geq 2$, we have

$$\leq \frac{1}{(n^2-1)^2}\left(n^4-4n^2+1+2n^2\right) \tag{C.42}$$

$$= 1 \tag{C.43}$$

□

Bibliography

[1] Robert Moerman. A gauge-invariant, symmetry-preserving truncation of JIMWLK. *Master's Dissertation*, 2017.

[2] Judith Alcock-Zeilinger and Heribert Weigert. Compact Hermitian Young projection operators. *Journal of Mathematical Physics*, 58(5):051702, 2017.

[3] Judith Alcock-Zeilinger and Heribert Weigert. Simplification rules for birdtrack operators. *Journal of Mathematical Physics*, 58(5):051701, 2017.

[4] Judith Alcock-Zeilinger and Heribert Weigert. Transition operators. *Journal of Mathematical Physics*, 58(5):051703, 2017.

[5] Leonid Vladimirovič Gribov, Evgenij M Levin, and Michail G Ryskin. Semihard processes in QCD. *Physics Reports*, 100(1-2):1–150, 1983.

[6] Alfred H Mueller. Parton saturation: an overview. In *QCD Perspectives on Hot and Dense Matter*, pages 45–72. Springer, 2002.

[7] Jamal Jalilian-Marian and Yuri V Kovchegov. Saturation physics and deuteron–gold collisions at RHIC. *Progress in Particle and Nuclear Physics*, 56(1):104–231, 2006.

[8] Edmond Iancu, Andrei Leonidov, and Larry McLerran. The color glass condensate: An introduction. In *QCD perspectives on hot and dense matter*, pages 73–145. Springer, 2002.

[9] Edmond Iancu and Raju Venugopalan. The color glass condensate and high energy scattering in QCD. *arXiv preprint hep-ph/0303204*, 2003.

[10] Heribert Weigert. Evolution at small x_{bj}: The color glass condensate. *Progress in Particle and Nuclear Physics*, 55(2):461–565, 2005.

[11] Francois Gelis, Edmond Iancu, Jamal Jalilian-Marian, and Raju Venugopalan. The color glass condensate. *Annual Review of Nuclear and Particle Science*, 60:463–489, 2010.

[12] Yuri V Kovchegov and Eugene Levin. *Quantum chromodynamics at high energy*. Cambridge University Press, 2012.

[13] Edmond Iancu, Kazunori Itakura, and Larry McLerran. Geometric scaling above the saturation scale. *Nuclear Physics A*, 708(3-4):327–352, 2002.

[14] Yuri V Kovchegov. Small-x F_2 structure function of a nucleus including multiple pomeron exchanges. *Physical Review D*, 60(3):034008, 1999.

[15] Yuri V Kovchegov. Unitarization of the BFKL pomeron on a nucleus. *Physical Review D*, 61(7):074018, 2000.

[16] Ian Balitsky. Operator expansion for high-energy scattering. *Nuclear Physics B*, 463:99–157, 1996.

[17] Ian Balitsky. Operator expansion for diffractive high-energy scattering. In *AIP Conference Proceedings*, volume 407, pages 953–957. AIP, 1997.

[18] Ian Balitsky. Factorization and high-energy effective action. *Physical Review D*, 60(1):014020, 1999.

[19] Cyrille Marquet and Heribert Weigert. New observables to test the color glass condensate beyond the large-N_c limit. *Nuclear Physics A*, 843(1-4):68–97, 2010.

[20] Yuri V Kovchegov, Janne Kuokkanen, Kari Rummukainen, and Heribert Weigert. Subleading-N_c corrections in non-linear small-x evolution. *Nuclear Physics A*, 823(1-4):47–82, 2009.

[21] Tuomas Lappi, Andrecia Ramnath, K Rummukainen, and H Weigert. JIMWLK evolution of the odderon. *Physical Review D*, 94(5):054014, 2016.

[22] Stefan Keppeler and Malin Sjödahl. Orthogonal multiplet bases in $SU(N_c)$ color space. *Journal of High Energy Physics*, 2012(9):1–50, 2012.

[23] Alexander C Edison and Stephen G Naculich. Symmetric-group decomposition of $SU(N_c)$ group-theory constraints on four-, five-, and six-point color-ordered amplitudes at all loop orders. *Journal of High Energy Physics*, 2012(9):69, 2012.

[24] E Iancu, AH Mueller, and DN Triantafyllopoulos. CGC factorization for forward particle production in proton-nucleus collisions at next-to-leading order. *arXiv preprint arXiv:1608.05293*, 2016.

[25] Heribert Weigert. Unitarity at small Bjorken x. *Nuclear Physics A*, 703(3-4):823–860, 2002.

[26] Kari Rummukainen and Heribert Weigert. Universal features of JIMWLK and BK evolution at small x. *Nuclear Physics A*, 739(1-2):183–226, 2004.

[27] Jamal Jalilian-Marian, Alex Kovner, Larry McLerran, and Heribert Weigert. Intrinsic glue distribution at very small x. *Physical Review D*, 55(9):5414, 1997.

[28] Birdtracks for $SU(N_c)$, author=Keppeler, Stefan, journal=arXiv preprint arXiv:1707.07280, year=2017.

[29] Richard Stanley. Enumerative combinatorics, vol. 1, wadsworth and brooks/cole, pacific grove, ca, 1986; second printing, 1996.

[30] MA Rashid and Saifuddin. Identity satisfied by the d-type coefficients of $SU(n)$. *Journal of Mathematical Physics*, 14(5):630–631, 1973.

[31] Bruce Sagan. *The symmetric group: representations, combinatorial algorithms, and symmetric functions*, volume 203. Springer Science & Business Media, 2013.

[32] Stefan Keppeler and Malin Sjödahl. Hermitian Young operators. *Journal of Mathematical Physics*, 55(2):021702, 2014.

[33] Wu-Ki Tung. *Group theory in physics: an introduction to symmetry principles, group representations, and special functions in classical and quantum physics*. World Scientific Publishing Company, 1985.

[34] Stephen Doty. New versions of Schur-Weyl duality. *Finite groups 2003*, pages 59–71, 2004.

[35] Predrag Cvitanović. *Group theory: birdtracks, Lie's, and exceptional groups*. Princeton University Press, 2008.

[36] AJ Macfarlane, Anthony Sudbery, and PH Weisz. On Gell-Mann's λ-matrices, d- and f-tensors, octets, and parametrizations of $SU(3)$. *Communications in Mathematical Physics*, 11(1):77–90, 1968.

[37] Predrag Cvitanović. Group theory for Feynman diagrams in non-abelian gauge theories. *Physical Review D*, 14(6):1536, 1976.

[38] David M Bishop. *Group theory and chemistry*. Courier Corporation, 1993.

[39] Edgar Bright Wilson, John Courtney Decius, and Paul C Cross. *Molecular vibrations: the theory of infrared and Raman vibrational spectra*. Courier Corporation, 1955.

[40] Mildred S Dresselhaus, Gene Dresselhaus, and Ado Jorio. *Group theory: application to the physics of condensed matter*. Springer Science & Business Media, 2007.

[41] Brian Hall. *Lie groups, Lie algebras, and representations: an elementary introduction*, volume 222. Springer, 2015.

[42] John F Cornwell. Group theory in physics. vol. 1. 1985.

[43] Jean-Pierre Serre. *Linear representations of finite groups*, volume 42. Springer Science & Business Media, 2012.

[44] William Fulton and Joe Harris. *Representation theory: a first course*, volume 129. Springer Science & Business Media, 2013.

[45] N Kaiser. Mean eigenvalues for simple, simply connected, compact Lie groups. *Journal of Physics A: Mathematical and General*, 39(49):15287, 2006.

[46] Barrie Cooper. *Almost Koszul duality and rational conformal field theory*. PhD thesis, University of Bath (United Kingdom), 2007.

[47] William Duke, Stephan Ramon Garcia, and Bob Lutz. The graphic nature of Gaussian periods. *arXiv preprint arXiv:1212.6825*, 2012.

[48] JL Brumbaugh, Madeleine Bulkow, Luis Alberto Garcia German, Stephan Ramon Garcia, Matt Michal, and Andrew P Turner. The graphic nature of the symmetric group. *Experimental Mathematics*, 22(4):421–442, 2013.

[49] Paula Burkhardt, Alice Zhuo-Yu Chan, Gabriel Currier, Stephan Ramon Garcia, Florian Luca, and Hong Suh. Visual properties of generalized Kloosterman sums. *Journal of Number Theory*, 160:237–253, 2016.

[50] Robert Bryant. Conversation on Math Overflow. https://mathoverflow.net/questions/268782/boundary-of-the-image-of-a-compact-manifold-in-the-complex-plane#comment664702_268782, 2017. [Online; accessed 8-May-2017].

[51] Greg Egan. Conversation on John Baez's blog. https://johncarlosbaez.wordpress.com/2012/09/11/rolling-circles-and-balls-part-3/#comment-90418, 2017. [Online; accessed 8-May-2017].

[52] Loring W Tu. *An introduction to manifolds*. Springer Science & Business Media, 2010.

[53] Francesco Mezzadri. How to generate random matrices from the classical compact groups. *NOTICES of the AMS, Vol. 54 (2007), 592-604; arXiv preprint math-ph/0609050*, 2006.

[54] Heribert Weigert. Private communication.

[55] CD White. An introduction to webs. *Journal of Physics G: Nuclear and Particle Physics*, 43(3):033002, 2016.

[56] Alexey A Vladimirov. Exponentiation for products of Wilson lines within the generating function approach. *Journal of High Energy Physics*, 2015(6):120, 2015.

[57] Mark Harley. On multiple gluon exchange webs. *arXiv preprint arXiv:1505.05799*, 2015.

[58] Giulio Falcioni, Einan Gardi, Mark Harley, Lorenzo Magnea, and Chris D White. Multiple gluon exchange webs. *Journal of High Energy Physics*, 2014(10):10, 2014.

[59] Sergio Blanes, Fernando Casas, JA Oteo, and José Ros. The Magnus expansion and some of its applications. *Physics Reports*, 470(5-6):151–238, 2009.

[60] N Bourbaki. Algebra. i. chapters 1–3. translated from the french. reprint of the 1989 english translation. *Elements of Mathematics. Springer-Verlag, Berlin*, 1998.

[61] Jonathan L Alperin and Rowen B Bell. Groups and representations, volume 162 of graduate texts in mathematics, 1995.

[62] John M Lee. Introduction to smooth manifolds. Number 218 in graduate texts in mathematics, 2003.

[63] Brian Sterr. Deriving the hypocycloid equations. https://www.geogebra.org/m/f3Xbwnz3. [Online; accessed 02-Feb-2018].